Democratic and Popular Republic of Algeria
Ministry of Higher Education and Scientific Research

University of Echahid Hamma Lakhdar El-Oued
FACULTY OF SCIENCES
DEPARTEMENT OF PHYSICS

THESE

Presented to obtain the degree of

SCIENCE DOCTORAT

Option: Physics of Materials

THEME

Enhancement the Transparent Conductive NiO Thin Films by F, Cu and Al Co-doping

Presented by:

Mrs. Mounira MAMMI

Publicly defended on:

In front of the Jury committee composed of:

Mr	Boubaker BENHAOUA	Professor	University of El-Oued	President
Mr	Said BENRAMACHE	Professor	University of Biskra	Supervisor
Mr	Mohammed Sadok MAHBOUB	Professor	University of El-Oued	Examiner
Mr	Abdelouahab GAHTAR	MCA	University of El-Oued	Examiner
Mrs	Nadjette BELHAMRA	MCA	University of Biskra	Examiner
Mr	Abdelghani LAKEL	MCA	University of Biskra	Examiner

2024-2025

Dedication

To .....

The support in this life and my beloved parents.

Companion of my journey, my husband.

My daughters

Brother, Sisters and My Friends

All loyal souls who aided me on the journey of my life

Mounira

Acknowledgements

First and foremost, I thank my gratitude to the Almighty Allah, whose grace empowered me to persist in this endeavor and surmount all challenges.

This work would not have been easy without the guidance and support of many individuals who, in various ways, contributed and provided valuable assistance in preparing and completing this thesis.

My sincere thanks and deep gratitude to the thesis supervisor of Mr. ***Said BENRAMACHE*** for framing this work without him will simply not exist. His scientific orientations and discussions helped me a lot.

I would also like to express profound gratitude and thanks to Dr **Aoun Yacine** for his guidance, support and encouragement throughout my research.

I would also like to thank my distinguished teacher *Prof.* ***Boubaker BEN HAOUA*** for his support and guidance every time he intended

Besides, I owe my sincere thanks to

Mr: Mohammed Sadok MAHBOUB

Mr: Abdelouahab GAHTAR

Mrs: Nadjette BELHAMRA

Mr: Abdelghani LAKEL

for their acceptance to judge this modest work.

Thank all family and friends for their continued moral support.

Mounira Mammi

Contents

Contents

List of Figures

List of Tables

GENERALE
INTRODUCTION

GENERALINTRODUCTION

The field of thin films is an ancient but very important field of study, seeing many modifications and prompting significant research efforts in recent years across diverse technological sectors to meet a growing range of requirements.

Transparent and conductive oxides (TCOs) thin films are significant materials as they possess dual attributes: transparency and electrical conductivity in the visible range [1]. Transparent Conductive Oxides are predominantly composed of metal oxides, it can be classified as either p-type or n-type semiconductors. Coatings made of n-type semiconductors, including materials like indium tin oxide and zinc oxide, play essential roles in diverse technological domains like transparent electronics and nanodevices [2-4].Moreover, thin films of a p-type semiconductor have received considerable attention in recent years, owing to their vital roles in optoelectronic devices such as changeable reflectance mirrors and other applications. Recent research has employed transition metal oxides (TMOs) derived from type p semiconductors to establish a p-n junction, in addition to other applications in the industry.

Lately, there has been an increasing interest in the study of materials (TMOs) in fundamental research, primarily due to their diverse physical applications. These applications span various fields including renewable energies, microelectronics, and nanotechnology [5]. TMOs have been employed in various technologies such as smart windows, light emitting diodes (LEDs)[6], and as materials for Li-ion battery electrodes [7]. These include metallic oxides: TiO_2, NiO, ZnO, Cr_2O3, Fe_2O_3, γ - Fe_2O_3 [8]. Lately, there has been significant focus on Nickel oxide (NiO) films and devices due to their promising attributes. These encompass UV transparent conductivity, wide band gap semiconductor characteristics with absorption edge in the near UV-visible region, and its nature as a p-type semiconductor. These properties have proven valuable in various applications such as gas sensors, UV detectors, and heterojunction LDs and LEDs [9-13]. On the other hand, Nickel Oxide (NiO) is a transition metal oxide, it has optical, electrical and magnetic properties that make it a usable material[14]. NiO is a VIII-VI semiconductor of type p [15], It forms under a crystalline salt rock structure of type NaCl [14], the mesh parameter is 4.17 Å [16].Ithas a wide band gap between 3.6 and 4.0 eV [14].

Several methods were employed for the deposition of NiO thin films, such as reactive sputtering [17], chemical vapor deposition [18], and the sol-gel technique [19]. Out of these methods, we opted for the pyrolysis spray technique due to its simplicity, cost-effectiveness,

ability to produce homogeneous large surfaces, and ease of controlling the structure of the deposited films [20].The primary aim of this study is to produce high-quality nickel oxide (NiO) thin films utilizing the spray pyrolysis technique.

The thesis consists of five chapters, structured as follows: commencing with the **general introduction, the chapter I** presents an overview of transparent conductive oxides (TCOs) and their applications across various fields. Additionally, it includes a review on the physicochemical characteristics and properties of nickel oxide (NiO) thin films, as well as their practical applications.

Chapter II introduces several experimental techniques for producing thin films. Subsequently, the experimental apparatus employed is described. This includes the pyrolysis spray technique and the preparation of sample solutions. Various characterization techniques are then discussed, including X-ray diffraction (XRD), UV-visible spectrometry, and four-point probing. The characterization of NiO samples is focused solely on nanostructure analysis and electrical properties. Deposition encompasses varying solution concentrations and examining the impact of doping and co-doping on the substrate layer.

Chapter III discusses the experimental results obtained and delves into the synthesis of our undoped NiO films of varying volumes, examining their structural, optical transparency, and electrical conductivity properties.

Chapter IV focuses on discussing the experimental findings concerning F doped NiO and Cu doped NiO and Al doped NiO and of thin films, which were deposited using varying volumes.

Chapter V presents the results obtained for F and Cu co-doped NiO and Al and F co-doped NiO and Cu and F co-doped NiO thin films at different concentrations. Finally, we will conclude this thesis with a general conclusion and perspectives.

References:

[1] Lamb, D., & Irvine, S. J. C. (2009). Near infrared transparent conducting cadmium oxide deposited by MOCVD. *Thin solid films*, *518*(4), 1222-1224, (2009).

[2] Sharma, R., Acharya, A. D., Shrivastava, S. B., Patidar, M. M., Gangrade, M., Shripathi, T., & Ganesan, V. Studies on the structure optical and electrical properties of Zn-doped NiO thin films grown by spray pyrolysis. *Optik*, *127*(11), 4661-4668, 2016.

[3] Wager, John F. "Transparent electronics." *science* 300.5623, 1245-1246, 2003.

[4] Hosono, Hideo. "Recent progress in transparent oxide semiconductors: Materials and device application." *Thin solid films* 515.15. 6000-6014. 2007.

[5] Wu, J., Wang, Q., Umar, A., Sun, S., Huang, L., Wang, J., & Gao, Y. Highly sensitive p-nitrophenol chemical sensor based on crystalline α-MnO 2 nanotubes. *New Journal of Chemistry*, *38*(9), 4420-4426, 2014.

[6]Caruge, J. M., Halpert, J. E., Bulović, V., & Bawendi, M. G. NiO as an inorganic hole-transporting layer in quantum-dot light-emitting devices. *Nano letters*, *6*(12), 2991-2994, 2006.

[7]Wang, Y., Zhang, Y. F., Liu, H. R., Yu, S. J., & Qin, Q. Z. Nanocrystalline NiO thin film anode with MgO coating for Li-ion batteries. *Electrochimica Acta*, *48*(28), 4253-4259, 2003.

[8] Wang, C., Yin, L., Zhang, L., Xiang, D., & Gao, R. Metal oxide gas sensors: sensitivity and influencing factors. *sensors*, *10*(3), 2088-2106, 2010.

[9]Zhao, Y., Wang, H., Gong, X., Wang, J., Li, H., Tang, M., & Li, X. Effect of lithium-ion doping concentration on structural and optical properties of NiO films fabricated by magnetron sputtering. *Vacuum*, *137*, 56-59, 2017.

[10] Reguig, B. A., Khelil, A., Cattin, L., Morsli, M., & Bernede, J. C. Properties of NiO thin films deposited by intermittent spray pyrolysis process. *Applied Surface Science*, *253*(9), 4330-4334, 2007.

[11] Deng, R., Yao, B., Li, Y. F., Xu, Y., Li, J. C., Li, B. H., ... & Shen, D. Z. Ultraviolet electroluminescence from n-ZnO/p-NiO heterojunction light-emitting diode. *Journal of luminescence*, *134*, 240-243, 2013.

[12] Shi, Z. F., Zhang, Y. T., Cui, X. J., Zhuang, S. W., Wu, B., Jiang, J. Y., ... & Du, G. T. Near infrared electroluminescence from n-InN/p-NiO heterojunction light-emitting diode.. *CrystEngComm*, *17*(1), 40-49, 2015.

[13] Wang, H., Zhao, Y., Wu, C., Dong, X., Zhang, B., Wu, G., ... & Du, G. Ultraviolet electroluminescence from n-ZnO/NiO/p-GaN light-emitting diode fabricated by MOCVD. *Journal of Luminescence*, *158*, 6-10, 2015.

[14] Rengaraj, A., Haldorai, Y., Kwak, C. H., Ahn, S., Jeon, K. J., Park, S. H., ... & Huh, Y. S. Electrodeposition of flower-like nickel oxide on CVD-grown graphene to develop an electrochemical non-enzymatic biosensor. *Journal of materials chemistry B*, *3*(30), 6301-6309, 2015.

[15] Hakim, A., Hossain, J., & Khan, K. A. Temperature effect on the electrical properties of undoped NiO thin films. *Renewable Energy*, *34*(12), 2625-2629, 2009.

[16] MAACHE, Mostefa. *Elaborattion de films Minces d'oxydes Semiconducteurs Par Voie sol-Gel*. PhD Thesis. Mohamed Khider University. Biskra.2014.

[17] Karpinski, A., Ferrec, A., Richard-Plouet, M., Cattin, L., Djouadi, M. A., Brohan, L., & Jouan, P. Y. Deposition of nickel oxide by direct current reactive sputtering: effect of oxygen partial pressure. *Thin Solid Films*, *520*(9), 3609-3613, 2012.

[18] Nigro, R. L., Battiato, S., Greco, G., Fiorenza, P., Roccaforte, F., & Malandrino, G. Metal organic chemical vapor deposition of nickel oxide thin films for wide band gap device technology. *Thin Solid Films*, *563*, 50-55, 2014.

[19] Soleimanpour, A. M., Hou, Y., & Jayatissa, A. H. Evolution of hydrogen gas sensing properties of sol–gel derived nickel oxide thin film. *Sensors and Actuators B: Chemical*, *182*, 125-133, 2013.

[20] Barir, R., Benhaoua, B., Benhamida, S., Rahal, A., Sahraoui, T., & Gheriani, R. (2017). Effect of precursor concentration on structural optical and electrical properties of NiO thin films prepared by spray pyrolysis. *Journal of Nanomaterials, 2017*.

ChapterI

Bibliographic study

I-1-Introduction

For a long time, conductive transparent oxides have been the focus of extensive research, because they have good transparency in the visible and high electrical conductivity. The purpose of this chapter is to first present a bibliographical study on conductive transparent oxides (TCOs), we recall the main properties of conductive transparent oxides (TCOs) and in particular those of nickel oxide, NiO properties and elaboration methods. We also describe the main properties (TCOs) obtained by different techniques and we present the selection criteria of the CVD technique (pyrolysis spray) and some applications of NiO films.

I-2-Transparent conductive oxides (TCOs):

Oxides are a chemical family of primary importance both by the quantity of compounds it contains and by the abundance of these compounds in nature. Transparent conductive oxides (TCOs) are degenerated semiconductors with wide gaps. They have the dual property of being good electrical and transparent conductors in the visible field [1].

Historically, the history of conductive transparent oxides (TCOs) began in 1907, at the discovery of cadmium oxide (CdO)in the form of a thin layer by Karl Baedeker [2]. This first observation gave rise to a new research theme which remains after a century a topical subject. Many TCOs materials then appeared, in particular: (In_2O_3, SnO_2, ZnO, Cd_2SnO_4, Sn (ITO), ZnO:Al , NiO,…….). Currently, research on conductive transparent oxides has concentrated on the study, the synthesis and improvement of the physical properties of such oxides. In addition, to achieve excellent results of TCOs, doping and heat treatment are the most demanding solutions.

I-3-Properties of conductive transparent oxides (TCOs):

Conductive transparent oxides have a set of properties that allow their use in a number of applications. TCOs have a high gap (3~4 eV) prevents them from absorbing photons with less energy than this gap [3], high mobility and low effective mass[4], Low resistivity(10^{-3} Ωcm),concentration of carriers 1020cm^{-3}[5], high electrical conductivity and low absorption in the visible [6].

Their Fermi level is all close to the conduction band (BC). They have the ability to diffuse light and transparency in the visible [7], stable against specific elements [3]. TOCs properties are strongly related to the preparation methods and its chemical composition.

I-4-Application of conductive transparent oxides:

TCOs materials are already widely industrialized and used in several applications, Figure I.1 shows some of these applications.

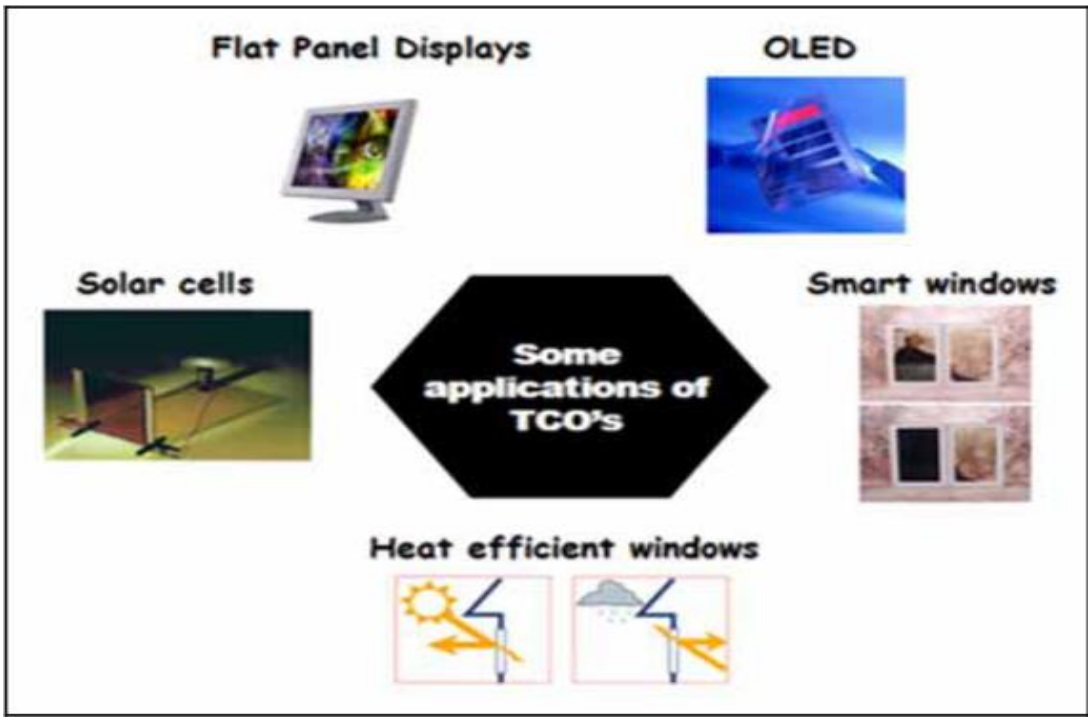

Figure 1.1: *Some TCOs Applications [8].*

Some of these applications are listed below [9,10]:

- Applications of the solar cell
- Architectural glass coatings
- Transparent heating elements
- Transparent electronic
- Optical synaptic devices with optical memory action
- Flat screens
- Photocatalysis application
- Gas sensors

I-5-Nickel oxide (NiO):

I-5-1-Definition of nickel oxide (NiO):

Nickel oxide (II) is a chemical compound of the formula NiO, it exists in nature as octahedrons. Depending on the preparation method, this oxide typically appears as a greenish-grey powder, it is obtained by pyrolysis of divalent nickel compounds such as

Ni(OH)2, Ni(NO3)2, NiCO3 or (NiCl2·6H2O) [11].Nickel oxide naturally as a bunsenite (Figure 1.2).

Figure 1.2: *Photo of a bunsenite crystal [12].*

I-5-2-Properties of nickel oxide (NiO):

Nickel oxide (NiO), belonging to the family of conductive transparent oxides (TCO), is an antiferromagnetic semiconductor. It is a material recognized by its chemical and thermal stability has a set of electrical and optical properties, used in many applications in the field of electronics and optoelectronics [13]. **Table (I-1)** shows some general properties of NiO.

Table I.1*: Some general NiO properties [14-15].*

lattice parameter (A°)	4.176
Average atomic number	18
density (g /cm³)	6 ,72
molar mass (g/mol)	74,69
average atomic mass (g)	27,35
melting point (°c)	1960
boiling point (°c)	>2000
Entropy S° ($KJ^{-1}.mol^{-1}$)	38
Solubility in water (mg/L)	1.1
Band Gap Energy (eV)	3.6-4.0

I-5-3-Crystallographic properties OF NiO:

Nickel oxide crystallizes in a cubic structure with centered faces (cfc) of the NaCl type (Rock-Salt) [16]. The lattice parameter is 0.417 nm, 18% larger than that of metallic nickel [17].

The main crystallographic characteristics under ordinary pressure conditions of nickel oxide NiO are shown in Figure I.3 (ASTM 47- 1049) and in Table I.2.

The cubic structure composed of two identical subnets A and B, where each atom in subnet A has neighbors belonging from subnet B and vice versa. The oxygen sub-network and nickel sub-network are both cfc as shown in Figure I.3.a. The plan (100) is a mixed plan, composed of 50% Ni and 50 % O and is non-polar, therefore stable (Figure I .3 (a)).

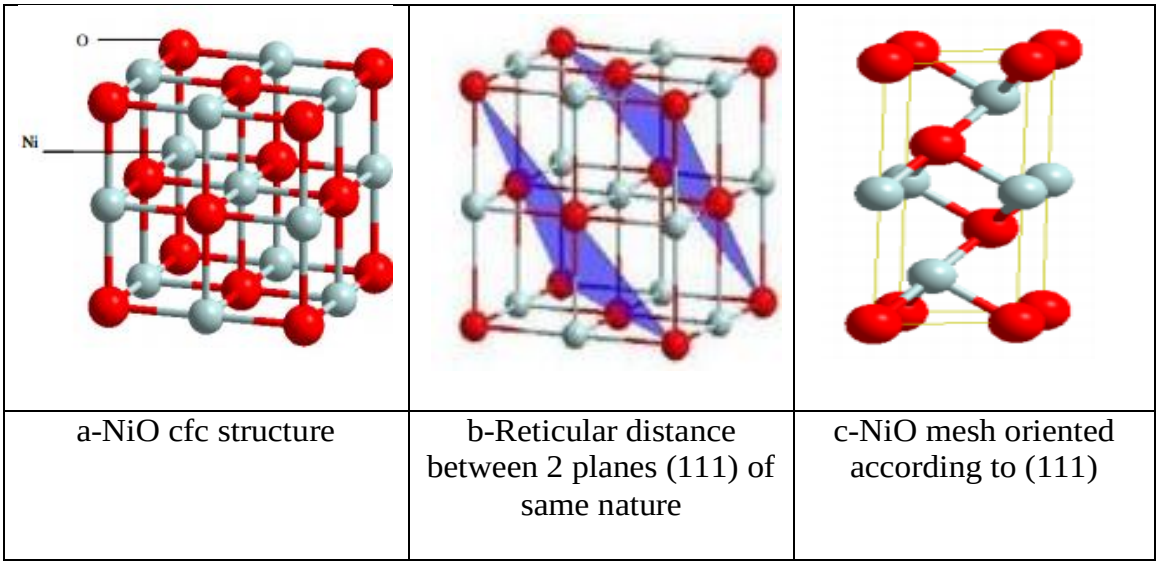

a-NiO cfc structure	b-Reticular distance between 2 planes (111) of same nature	c-NiO mesh oriented according to (111)

Figure I.3: *Nickel oxide cfc structure and surface oriented according to the plane (111) [15-17].*

The (111) planes alternate between pure Ni and pure O. The (111) face is polar and therefore unstable [15]. The NiO crystal oriented on (111) corresponds to an alternating stack of planes made up solely of anions on the one hand and cations on the other. The inter-reticular distance is 0.120 nm between two planes of different nature, and 0.241 nm, twice as much, between two planes of the same nature (Figure I.3. (b)). The cell corresponding to the face (111) has a hexagonal symmetry with the following mesh parameters: a = b = 0.29475 nm and c = 0.72119 nm (Figure I.3(c)). The vertices -tops-are occupied by oxygen atoms, two other oxygen atoms being located inside the cell. The middle of the edges-the stops-following the direction care occupied by nickel atoms, with two other nickel atoms located inside the cell. This cell contains three oxygen atoms and three nickel atoms [17-18-19].

Table I.2: *Main crystallographic characteristics of NiO.*

	Structure	***Maile***	**network**	***R***	**space group**
NiO	Cubic CFC.	a=b=c and α=β=γ=π/2	A et B cation (Ni^{+2}) anion (O^{-2})	(Ni^{+2}) =72.0 Pm (O^{-2}) =140Pm	Fm3m

I-5-4-Optical Properties of NiO:

NiO is a transparent material (40-80%) in the visible region, whose refractive index is equal to 2.33 with a large direct gap (3.6 - 4 eV) [20,21]. In the figure (Figure.I.4), it is presented the spectrum of NiO transmission [22].

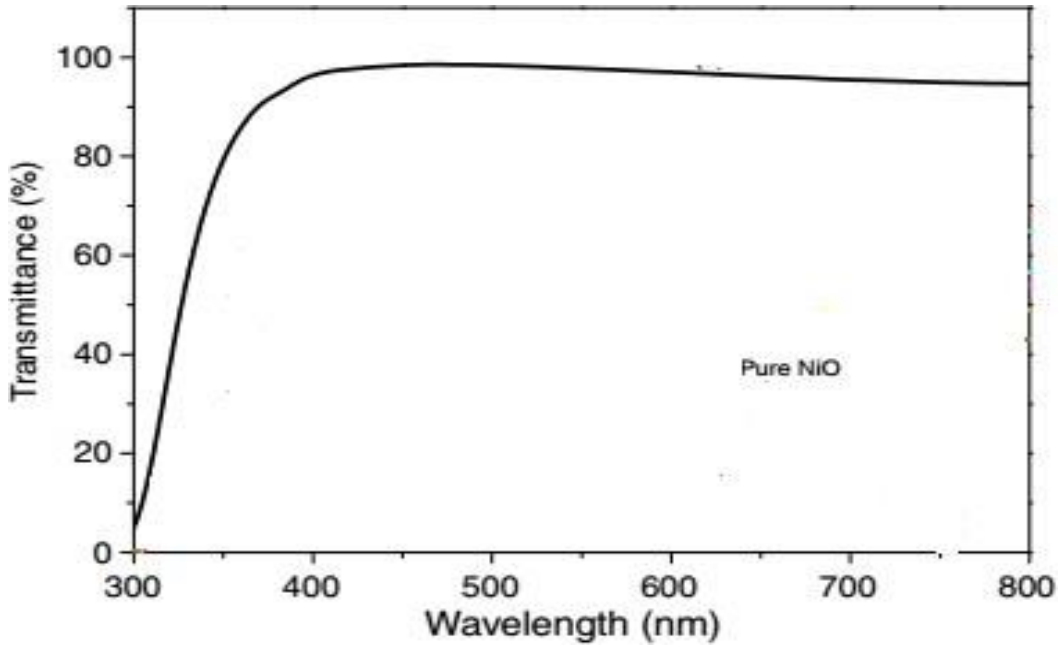

Figure I.4 : *Spectrum of transmission of NiO [22].*

In the **Table (I.3)** the parameters of the optical properties of NiO film have been illustrated obtained by CVD spray method in experimental studies.

Table I.3: *Some NiO optical property.*

solution	**T (%)-visible**	***t* (nm)**	**Eg(eV)**	**Eu(meV)**	**Réf.**
$C(NiCl_2.6H_2O)$	30-60	-	3.7-3.84	281-337	[23]
$C(Ni(NO_3)_2.6H_2O)$	57-88%	180-200	3.68-3.56	300-450	[24]
$C(Ni (CH_3CO_2)_2.4H_2O)$	80-90	800-900	3.61	-	[25]

I-5-5-electronic properties of NiO:

NiO is a semiconductor. The electronic configurations of oxygen and nickel atoms are as follows:

$O: 1s^2 2s^2 2p^4$,

$Ni: 1s^2 2s^2 2p^6 3s^2 3p^6\ 4s^2 3d^8$

NiO has been under extensive investigation for decades due to its interesting electronic structure, strongly affected by Ni electrons 3d that are located in space, but spread over a wide range of energy due to strong Coulomb repulsion between them [26,27].

Nickel oxide is among the transition metals. The magnetic property of this compound is due to the existence of band d. The band d can contain a total of 10 electron sand its width is about 5 eV. The figure (**Figure.I.5**) shows the molecular orbital diagram of the fundamental state of NiO [28].

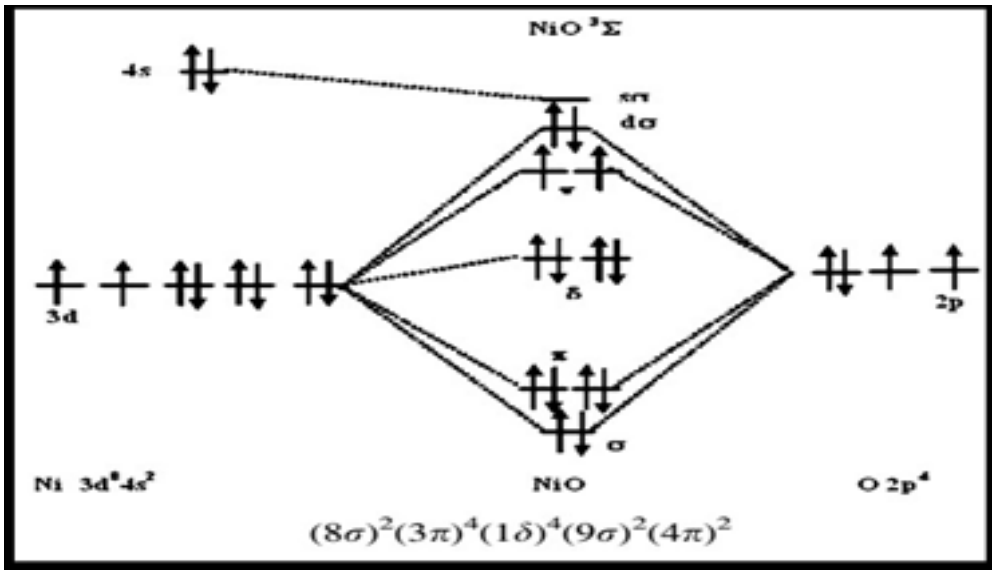

Figure I.5: *Schematic molecular diagram of the fundamental state of NiO (orbital Ni atom and O) [28].*

The energy level of the 3d electronic underlayer responsible for magnetism is slightly higher than the 4S conduction underlayer [29]. 3d orbitals are composed of two levels: t2g and eg, the orbitals of the oxide ions overlapping with the 3d orbitals of nickel form the low energy binding level, this level and the t2g level are electronically complete, the anti-binder level eg contains only two electrons.

I-5-6- Electrical properties of NiO:

Nickel oxide is a semiconductor material type p [13,30,31], having a low conductivity type p according to the method of preparation. Conductivity ranges from 10^{-2} $cm^{-1}\Omega^{-1}$ to 500K and 10^{-1} $cm^{-1}\Omega^{-1}$ to 30K. Table (I-4) shows some of the electrical properties of NiO.

Table I-4: *Shows some of the electrical properties of NiO.*

conductivity **σ** $(\Omega.Cm)^{-1}$	**0.1-1**[32]
Mobility.$\boldsymbol{\mu}$($Cm^2/V.S$)	**0.1-1**[33]
Electronic density $\boldsymbol{N_v}$ (Cm^3)	$\mathbf{10^{18}}$-$\mathbf{10^{19}}$[33]
dielectric constant	**11.9**[15]

I-5-7-The applications of NiO:

NiO has generated technological interest and growing industrial. This interest mainly concerns their properties (optical properties, magnetic, electrical and catalytic) associated with general characteristics such as mechanical hardness, thermal stability or chemical passivity. Thin films of nickel oxide were used as [34]:

1. An antiferromagnetic material.
2. p-type transparent conducting films.
3. Electrocatalysis.
4. Positive electrode in batteries.
5. Fuel cell.
6. A material for electro-chromic display devices.
7. Part of functional sensor layers in chemical sensors.
8. Solar thermal absorber.
9. Photo electrolysis.
10. Promising ion storage material in terms of cyclic stability.
11. Resistive memories.
12. Electro chromic devices.
13. Giant magneto resistive spin valve structures.

I-5-8- The process of depositing thin films of NiO:

NiO solution spraying techniques are used to deposit NiO thin films, it is prepared through a variety of methods and protocols, as shown below:

I-5-8-1- Deposition of NiO Thin Films from Nickel Chloride Solutions:

NiO thin films fabricated from nickel chloride, it can be dissolved in various solvents, including water, ethanol, and methanol solutions. When preparing a NiO solution with a water solvent, dissolve the nickel chloride dihydrate ($NiCl_2$, $2H_2O$) in water, heat the resulting solution to 50 °C, and add drops of HCl for stabilization before using it to deposit NiO thin films onto substrates. The process of decomposition of nickel chloride to nickel oxide in the presence of water was discussed by Menaka and Umadevi [35], based on the equation below [36]:

$$Ni\,Cl_2 + 2H_2O \rightarrow 2HCl + Ni\,(OH)_2$$
$$Ni\,Cl_2 + 2H_2O \rightarrow 2HCl + NiO + H_2O$$

I-5-8-2- Deposition of NiO Thin Films from Nickel Nitrate Solutions:

A NiO solution can be prepared by mixing nickel nitrate with various solvents such as water, ethanol, and methanol. In the process of making a NiO solution using a water solvent, nickel nitrate dihydrate (Ni $(NO_3)_2$. 2H2O) is mixed in the same volume as the water solvent [37]:

$$NiO(NO_3)_2 + 2NH_4OH \rightarrow Ni\,(OH)_2 + 2NH_4NO_3$$
$$2\,Ni\,(OH)_2 \rightarrow 2NiO + H_2O$$

I-5-8-3- Deposition of NiO Thin Films from Nickel Acetate Solutions:

The NiO solution is prepared using nickel acetate in various solvents such as water, ethanol and methanol. When preparing a NiO solution using a water solvent, if the nickel acetate dehydrated $Ni(CH_3COO)_2$- $4H_2O$) is added for the same size as the water solvent [38]:

$$Ni(CH_3COO)_2.4H_2O + CH_3 - OH = Ni(OH) + 2CH_3COOCH + 4H_2O$$

Table I-5*: Information of Nickel types [37-39].*

	Molecule formula	**Molar mass (g/mol)**	**Density (g/ cm³)**	**Solubility in water (mg/l)**
Nickel Chloride	($NiCl_2$, $2H_2O$)	237.69	1.92	2540×10^3(20ºC)
Nickel Acétate	$Ni(CH_3COO)_2.4H_2O$	176.78	1.798	Easily soluble in cold water, hot water
Nickel Nitrate	Ni $(NO_3)_2$.$2H_2O$	290.08	3.55	6.42×10^5at20°C

I-6-Techniques and methods of elaboration of thin films TCO:

There are many techniques of thin film deposition, which are generally divided into two main families: physical methods and chemical methods. Among the physical methods , the best known are : sputtering in all its forms [38,39,40],evaporation by joule effect [41,42,43], electron beam evaporation [44],and laser ablation[45,46].Chemical methods are used in two types of deposits vapor-phase[47]or in solution, the sol-gel method[16,48],plating[49],and reactive chemical spray technique (spray) [50,51]. Figure I.6 summarizes the ranking of all these methods. One of the advantages of these techniques is that the use of the raw material can be optimally optimized [52].

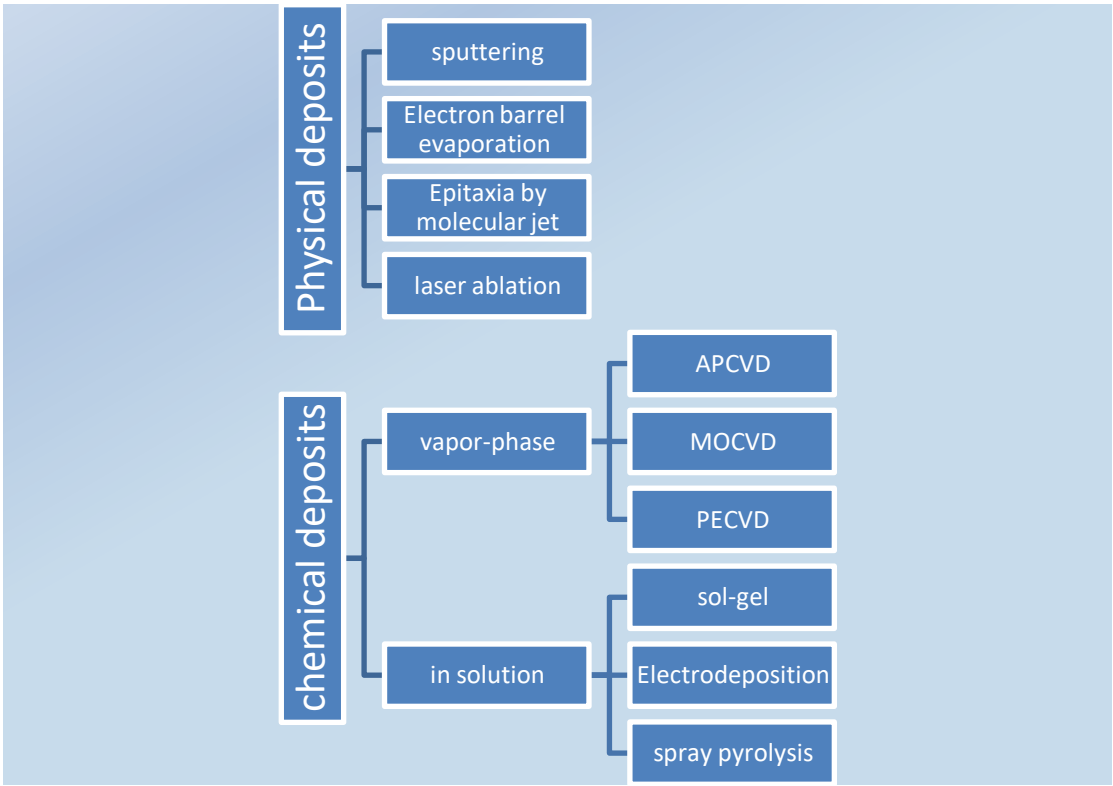

Figure I.6: *Synoptic diagram of the different thin film deposition techniques [53,54].*

I-7-Conclusion:

Through this chapter, it seems that the great importance of nickel oxide which is considered of the family of transparent and conductive oxides, and also, it has very interesting properties, it is available to be introduced to the several components, in addition, he is a good conductor, absorbent, catalyst, large capacity and stable in the field of electrochemistry. In the next chapter, the processes or methods have been applied most importantly to form its NiO thin films.

References

[1]Lamb, D, & Irvine, S. J. C. Near infrared transparent conducting cadmium oxide deposited by MOCVD. Thin solid films, *518*(4), 1222-1224, 2009.

[2]Badeker, K. Concerning the electricity conductibility and the thermoelectric energy of several heavy metal bonds. Annalen der Physik, *22*, 749, 1907.

[3]Sylvie. Fay, Zinc oxide by chemical vapor deposition as transparent electrical contact and light diffuser for solar cells, PhD thesis, University of Lausane, 2003.

[4]Coutts, T. J., Mason, T. O., Perkins, J., & Ginley, D. S. Transparent conducting oxides: status and opportunities in basic research. Proc. Electrochem. Soc, 99, 274-288, 1999.

[5]Minami, T. Transparent conducting oxide semiconductors for transparent electrodes. Semiconductor science and technology, *20*(4), S35, 2005.

[6]D.Vaufrey, Realization of surface emission OLEDs: Optimization of ITO/organic semiconductor structures, PhD thesis, University of Lyon, 2003.

[7]Minami, T. New n-type transparent conducting oxides. MRS bulletin, *25*(8), 38-44, 2000.

[8]SAADEDDIN, Iyad. Preperation and characterization of new transparent conducting oxides based on SnO_2 and In_2O_3: ceramics and thin films. PhD Thesis. Bordeaux 1. 2007.

[9]Afre, R. A., Sharma, N., Sharon, M., & Sharon, M. Transparent conducting oxide films for various applications: A review. Reviews on advanced materials science, *53*(1), 79-89, 2018.

[10] Jang, J., Kang, Y., Cha, D., Bae, J., & Lee, S. Thin-film optical devices based on transparent conducting oxides: Physical mechanisms and applications. Crystals, *9*(4), 192. 2019.

[11] Hassan, A. J. Study of optical and electrical properties of nickel oxide (NiO) thin films deposited by using a spray pyrolysis technique. Journal of Modern Physics, *5*(18), 2184. 2014.

[12] H,Labidi, development and characterization of thin metal oxide films for optoelectronic applications ,PhDthesis, Larbi Ben M'hidi University -Oum El Bouaghi. 2016.

[13] M. Menaa, Influence of annealing on the optoelectronic properties of thin layers of (ZnO)1-x(NiO)x, master thesis, Larbi Tébessi- Tébessa University, 2015.

[14] Reguig, B. A., Regragui, M., Morsli, M., Khelil, A., Addou, M., & Bernede, J. C. Effect of the precursor solution concentration on the NiO thin film properties deposited by spray pyrolysis. Solar Energy Materials and Solar Cells, 90(10), 1381-1392, 2006.

[15] AWAMAT, Samer. Adaptation d'un réacteur plasma basse pression de dépôt pour la synthèse d'oxydes soumis à de hautes températures. Application aux piles à combustible type SOFC et aux barrières thermiques. PhD Thesis. Chimie ParisTech. 2008.

[16] LE PÉVÉDIC, Séverine. Etude de la formation et de l'oxydation de couches minces d'alliages Al-Ni après dépôt d'Al sur un monocristal de Ni (111). PhD Thesis. Pierre et Marie Curie University -Paris VI. 2007.

[17] Park, Y. R., & Kim, K. J. Sol–gel preparation and optical characterization of NiO and Ni1− xZnxO thin films. Journal of Crystal Growth, 258(3-4), 380-384, 2003.

[18] A. Bouzoubaa, Atomistic modelling of the interactions between chloride ions and the surface of passivated nickel, PhD thesis, Pierre and Marie Curie University, Paris ,2008.

[19] Sekar, A., Kim, S. H., Umar, A., & Hahn, Y. B. Catalyst-free synthesis of ZnO nanowires on Si by oxidation of Zn powders. Journal of Crystal Growth, 277(1-4), 471-478, 2005.

[20] Minot, C. Water molecule dissociation at ice/MgO (1 0 0) interface. Surface science, *562*(1-3), 237-246, 2004.

[21] Rahman, M. M., Chou, S. L., Zhong, C., Wang, J. Z., Wexler, D., & Liu, H. K. Spray pyrolyzed NiO–C nanocomposite as an anode material for the lithium-ion battery with enhanced capacity retention. Solid State Ionics, 180(40), 1646-1651, 2010.

[22] Chen, S. C., Kuo, T. Y., Lin, Y. C., & Lin, H. C. Preparation and properties of p-type transparent conductive Cu-doped NiO films. Thin Solid Films, *519*(15), 4944-4947, 2011.

[23] Mrabet, C., Amor, M. B., Boukhachem, A., Amlouk, M., & Manoubi, T. Physical properties of La-doped NiO sprayed thin films for optoelectronic and sensor applications. Ceramics International, 42(5), 5963-5978, 2016.

[24] Wang, J., Yang, P., Wei, X., & Zhou, Z. Preparation of NiO two-dimensional grainy films and their high-performance gas sensors for ammonia detection. Nanoscale research letters, 10, 1-6, 2015.

[25] Desai, J. D., Min, S. K., Jung, K. D., & Joo, O. S. Spray pyrolytic synthesis of large area NiO_x thin films from aqueous nickel acetate solutions. Applied Surface Science, *253*(2006), 1781-1786, 2006.

[26] Nolting, W., Haunert, L., & Borstel, G. Temperature-dependent electronic structure and magnetic behavior of Mott insulators. Physical Review B, 46(8), 4426–4445, 1992.

[27] Bengone, O., Alouani, M., Blöchl, P., & Hugel, J. Implementation of the projector augmented-wave LDA+ U method: Application to the electronic structure of NiO. Physical Review B, *62*(24), 16392–16401, 2000.

[28] Bauschlicher, C. W., & Maitre, P. Theoretical study of the first transition row oxides and sulfides. Theoretica chimica acta, 90, 189-203, 1995.

[29] BELKHIR, Mohamed Akli. Structure de bandes à spin polarisé par la méthode des fonctions localisées : application à MnO et NiO. PhD Thesis. Paul Verlaine- University Metz. 1988.

[30] Ahmed, S. S., Hassan, E. K., & Mohamed, G. H. Investigation of optical properties of NiO0. 99Cu0. 01 thin film by thermal evaporation. International Journal, 2(2), 633-638, 2014.

[31] Studenikin, S. A., Golego, N., & Cocivera, M. Optical and electrical properties of undoped ZnO films grown by spray pyrolysis of zinc nitrate solution. Journal of Applied Physics, 83(4), 2104-2111, 1998.

[32] Reguig, B. A., Regragui, M., Morsli, M., Khelil, A., Addou, M., & Bernede, J. C. Effect of the precursor solution concentration on the NiO thin film properties deposited by spray pyrolysis. Solar Energy Materials and Solar Cells, 90(10), 1381-1392, 2006.

[33] Sato, H., Minami, T., Takata, S., & Yamada, T. Transparent conducting p-type NiO thin films prepared by magnetron sputtering. Thin solid films, 236(1-2), 27-31, 1993.

[34] A,Al-ASKari, Effect of Aqueous Solution Molarity on Structural and Optical proprieties of Nickel-Cobalt Oxide Thin Films prepared by Chemical Spray Pyrolysis Method, PhDthesis, University of Diyala,2014.

[35] Menaka, S. M., & Umadevi, G. Concentration dependent structural, morphological, spectral, optical and electrical properties of spray pyrolyzed NiO thin films. Silicon, 10(5), 2023-2029, 2018.

[36] Abbas, P. RSabah Ibrahim, and Ahmed Qasim Ubaid. Structural, optical and photoluminescence properties of nanocrystalline NiO thin films. Journal of advances in Physics 6.1, pp.1016-1023, 2014.

[37] Juybari, Hasan Azimi, Mohammad-Mehdi Bagheri-Mohagheghi, and Mehrdad Shokooh-Saremi. Nickel–lithium oxide alloy transparent conducting films deposited by spray pyrolysis technique. Journal of alloys and compounds 509.6 pp 2770-2775, 2011.

[38] Reddy, A. Mallikarjuna, A. Sivasankar Reddy, and P. Sreedhara Reddy. Thickness dependent properties of nickel oxide thin films deposited by dc reactive magnetron sputtering. Vacuum 85.10pp 949-954, 2011.

[39] Mosbah, A., Moustaghfir, A., Abed, S., Bouhssira, N., Aida, M. S., Tomasella, E., & Jacquet, M. Comparison of the structural and optical properties of zinc oxide thin films

deposited by dc and rf sputtering and spray pyrolysis. Surface and Coatings Technology, 200(1-4), 293-296, 2005.

[40] Guziewicz, M., Grochowski, J., Borysiewicz, M., Kaminska, E., Domagala, J. Z., Rzodkiewicz, W., & Piotrowska, A. Electrical and optical properties of NiO films deposited by magnetron sputtering. Optica Applicata, 41(2), pp231–240, 2011.

[41] Bouhssira, N., Abed, S., Tomasella, E., Cellier, J., Mosbah, A., Aida, M. S., & Jacquet, M. Influence of annealing temperature on the properties of ZnO thin films deposited by thermal evaporation. Applied Surface Science, 252(15), 5594-5597, 2006.

[42] S. Abed, Development and study of nonlinear optical properties of nickel, iron and bismuth doped ZnO thin films, PhD thesis, Constantine University 1, 2012.

[43] Al Asmar, R., Ferblantier, G., Sauvajol, J. L., Giani, A., Khoury, A., & Foucaran, A. Fabrication and characterisation of high quality ZnO thin films by reactive electron beam evaporation technique. Microelectronics journal, 36(8), pp694-699, 2005.

[44] Madhavi, A., Reddy, C. S., Ravindra, N. V., Lokeshand, P., & Reddy, P. S. Effect of Substrate Temperature on the Structural, Optical and Electrical Properties of Electron Beam Evaporated NiO Thin Films. International Journal of Advanced Research in Physical Science (IJARPS), 1, 16-20, 2014.

[45] S.Kemache, Development and characterization of Ni1-xZnxO thin films ,master thesis, Larbi Tébessi -Tébessa University, 2014.

[46] Scarlat, C., Mok, K. M., Zhou, S., Vinnichenko, M., Lorenz, M., Grundmann, M., & Schmidt, H. Voigt effect measurement on PLD grown NiO thin films. physica status solidi c, *7*(2), 334-337, 2010.

[47] Venkatachalam, S., Iida, Y., & Kanno, Y. Preparation and characterization of Al doped ZnO thin films by PLD. Superlattices and Microstructures, 44(1), 127-135, 2008.

[48] Natsume, Y., & Sakata, H. Zinc oxide films prepared by sol-gel spin-coating. Thin solid films, 372(1-2), 30-36, 2000.

[49] Sonavane, A. C., Inamdar, A. I., Shinde, P. S., Deshmukh, H. P., Patil, R. S., & Patil, P. S. Efficient electrochromic nickel oxide thin films by electrodeposition. Journal of Alloys and Compounds, *489*(2), 667-673, 2010.

[50] Rebien, M., Henrion, W., Bär, M., & Fischer, C. H. Optical properties of ZnO thin films: Ion layer gas reaction compared to sputter deposition. Applied Physics Letters, 80(19), 3518-3520, 2002.

[51] Hadjeris, L., Herissi, L., Benbouzid, M., Attaf, N., Assouar, M. B., Easwarakhanthan, T., & Mahdjoub, A. Structural, optical and electrical characterization of transparent and

semiconducting ZnO thin films grown by spray pyrolysis, Alger. J. Adv. Mater, 4, 9-12, 2008.

[52] S.Faÿ, Zinc oxide by chemical vapor deposition as transparent electrical contact and light diffuser for solar cells, PhD thesis, Federal Polytechnic School ,Lausanne.2003.

[53] L. Herissi, Pyrolytic spraying and characterization of semiconducting and transparent zinc oxide thin films: Improvement of the deposition system, magister thesis, Larbi Ben M'hidi- Oum ElBouaghi University, 2008.

[54] E.Defaÿ, Elaboration and characterization of piezoelectric thin films of Pb (Zr,Ti)O3 on silicon for microsystem applications, PhDthesis, National Institute of Applied Sciences-Lyon, 1999.

CHAPTER II

Method of elaboration of NiO thin films and characterizations

II-1-Introduction:

In this chapter, our focus is specifically on the technique of depositing thin films using the spray pyrolysis method. It is a relatively simple alternative that uses traditional and inexpensive means[1].Its implementation is locally feasible. we will discuss the preparation of the different solutions used for the elaboration and doping of thin films and, the different methods and techniques used in the deposit. The operating principles of the different characterization techniques we used to analyze the films we developed will also be presented in this chapter.

II-2-Spray Pyrolysis Method:

It is one of the chemical methods and we will adopt it in our work. Which was the first to utilize this method in1956, they used a selective surface to create a black copper membrane on an aluminum substrate[2].

II-2-1 General principle of the spray process:

A solution of different reactive compounds is vaporized and then projected, using an atomizer, on a heated substrate. The temperature of the substrate allows the activation of the chemical reaction between the compounds[3].The experiment can be performed in air[4],and can be prepared in an enclosure (or in a reaction chamber) under a vacuum.

II-2-2 – Advantages of the Spray:

The choice of this technique was motivated by many advantages:

- Possibility to deposit a wide choice of materials.
- Simple method of adding the precursor by means of a spray.
- The thin films prepared by this technique are of (good quality, very inexpensive and economical, fast and simple, industrializable).
- It allows to control the chemical composition of the material you want to obtain.
- Several products can be used at once, especially for doping[5].

II-3-Experimental setup used:

It is a composition made in the Technological Hall of the Department of Mechanical Engineering of the University of El-Oued. The latter is built from simple devices to which

certain modifications have been made in order to achieve homogeneous films of metal oxide. The diagram of the designed and realized deposit system is shown in **Figure II.1**.

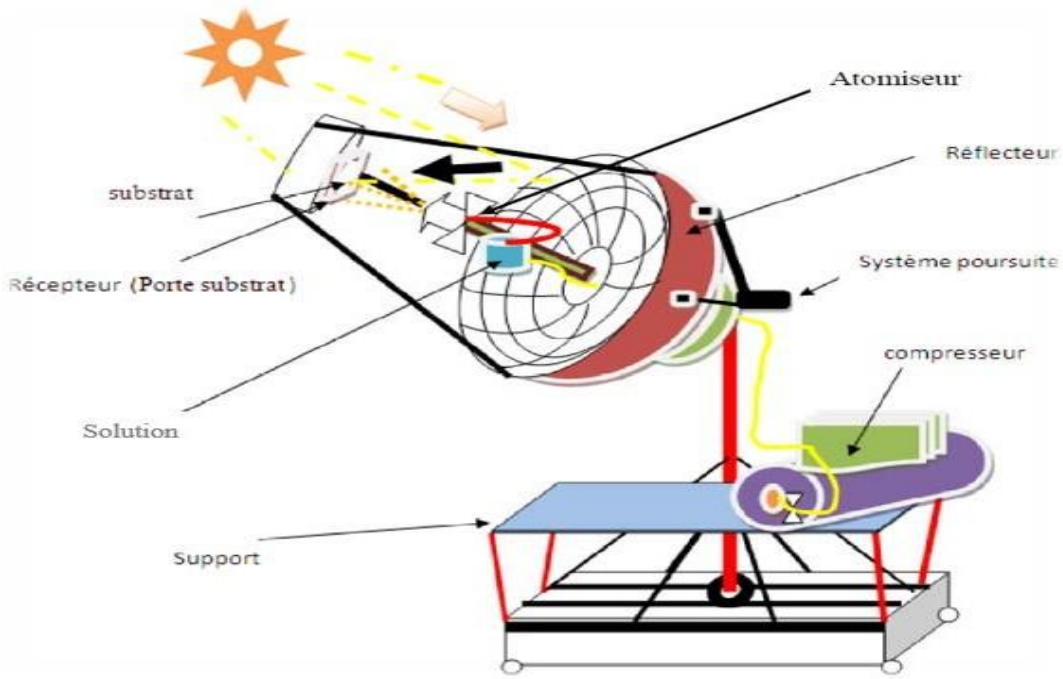

Figure II.1*: Thin film deposition device by spray technique[6].*

The main elements of this composition are:

- **A reflector:** It is a satellite receiver dish covered by a hundred small mirror surfaces that cover the inner surface of the reflector. Mirrors should have their bright side facing the sun.
- **A substrate holder:** It is a plate,15 cm long, heated by solar energy, whose temperature can be manually regulated using a millimeter.
- **Atomizer:** is an element that transforms the solution into droplets. It is placed on a height-adjustable support to control the distance between the spout and the substrate.
- **Air compressor:** It is a device that provides pressure to the atomizer in order to operate it.

In this solar composition, the reflector is facing the sun, using a controlled tracking system. It is redirected to the position of the sun from sunrise. The solar rays are reflected at the focus of the parabolic forming the sunspot which should appear in front of the plate to be heated.

***Figure II.2**: General view of the oven used.*

II-4-Temperature measuring instruments:

We used a digital millimeter (AITAV-4ME05781) with the following characteristics(**Figure II.3**):

- ✓ Model (AITAV-4ME05781).
- ✓ Power supply; one battery (9 V).
- ✓ Operating range: -20à1000°C.

***Figure II.3**: Photo of Used Digital Millimeter(AITAV-4ME05781).*

To measure the temperature reached on the oven surfaces, the millimeter probe is placed on the receiver surface (**Figure II.4**):

Figure II.4: *Position of the millimeter probe.*

II-5- Preparation:

To prepare thin layers of nickel oxide, we follow these steps:

II-5-1-Preparationofthesubstrate:

- **Choice of the deposit substrate:**

The substrate choices are important to perform characterization on the layer using glass of the substrate to study structural and optical properties. The substrates used are glass blades their dimensions(7.62x2.54)$cm^2$with thickness equal to 2 mm, cut by a diamond-tipped pen(**Figure II.5**). This choice of glass is due to two reasons:

- ✓ Adapts well for its transparency, it allows a good optical characterization of films.
- ✓ And its significant theoretical dilation coefficient giving a good adhesion of the deposited layers.

FigureII-5:*Glass substrates.*

After deposit, the sample (substrate + layer) is cooled from the deposition temperature to ambient temperature (~20°C) which causes a compressibility of the two materials constituting the sample. In this case, they have very close dilation coefficients, hence a minimization of constraints. It should be noted that the increase in substrate temperature leads to an increase in stresses. This is related to compressive stress caused by the difference between the dilation coefficients of the substrate and the deposited material(α_{glass}= 8,5x$10^{-6}K^{-1}$, α_{NiO}=7,93x$10^{-6}K^{-1}$) [7]and also for economic reasons.

❖ **Clearing :**

The quality of the deposit depends on the cleanliness and the state of the substrate. Cleaning it is therefore a very important step:all traces of grease and dust must be removed and checked by eye the surface of the substrate is free of scratches and defects. These conditions are essential for the good adhesion of the deposit on the substrate

The substrate surface cleaning process is carried out as follows:

- Substrates are cut using a diamond-tipped pen.
- Rinse with distilled water.
- Wash substrates in methanol to remove grease and impurities stuck to the surface of the substrate then they are cleaned in a distilled water bath.
- Rinse with distilled water for 10 min.
- Drying Substrates with paper, avoid touching the surface of the substrate to avoid contamination.

II-5-2-Preparation of solutions:

To elaborate of the undoped, doped and co-doped NiO thin films, a solution was prepared by the dissolution of nickel. We used nickel nitrate hexahydrate $Ni(NO_3)_2.6H_2O$(molecular weight M=290.89g/mol), as a source material, to which distilled water(V=50ml) is added to the solution to obtain a less viscous solution, and adds some drop of HCl solution to stabilize the components in the solution, using a thermalagitator. The mixture solution was stirred and heated at 45°C untila time of 4 h to transparent solution. The resulting solution is transparent green and slightly viscous(**FigureII-6**).

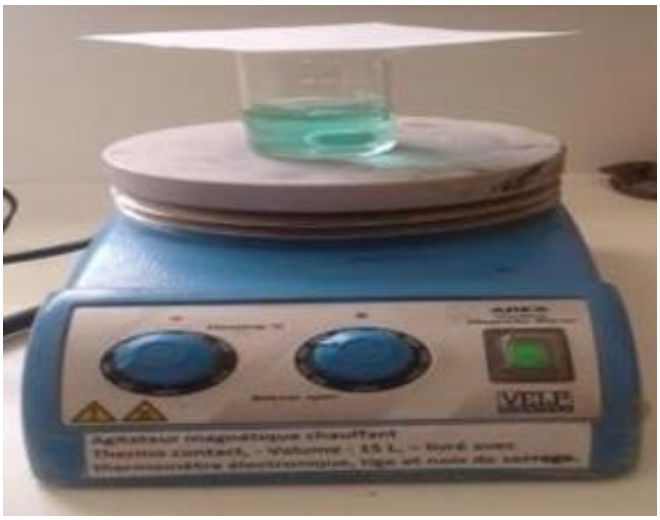

FigureII-6: *Preparation of nickel oxide.*

a-Undoped NiO:

In the **Table II.1** below, they recapitulate the experimental parameters of the work of undoped NiO.

Table II.1: *Experimental parameters of the work of undoped NiO.*

Sample	Concentration (M)	Volume (ml)	Substrate temperature (°C)
1	0.1	5	450
2		10	
3		15	
4		20	

b-Al, Cu and F doped NiO:

In **Table II.2** below, the experimental parameters of Al, Cu and Fdoped NiO.

Table II.2: *Experimental parameters of the work of Al, Cu and F doped NiO.*

Sample	C(M)	Al(%)	Cu (%)	F (%)	Volume (ml)	Substrate temperature (°C)
1	0.1	3	3	5	5	450
2					10	
3					15	
4					20	

II-5-3-Preparation of NiO thin films:

Following preparation of the solution and substrate, by employing the chemical thermal

spraying technique, we start the deposition process directly by following these procedures:

- ✓ The substrate is positioned atop the substrate holder within the focal point of the solar oven. To prevent substrates from experiencing thermal shock, the substrate holder is heated gradually from room temperature to the temperature chosen for the deposits (450°C).
- ✓ When heated, the compressor pressure is fixed, thus the flow rate of the spray solution. Very fine droplets are sprayed on the heated substrate using the air brush, activation of the chemical reaction between the compounds, the solvent evaporates due to the endothermic reaction of the two compounds forming the thin layer. The reaction results in the formation of a nickel oxide layer on the substrate surface.
- ✓ Following the completion of the deposition process, heating is halted, and the substrate is left to cool on the substrate holder until it reaches room temperature, to avoid thermal shocks that may break the glasses, then we get our sample back.

II-6-characterization techniques:

After the films were deposited, it is necessary to perform different characterizations, the undoped, doped and co-doped NiO thin films were analyzed by different characterization techniques.

II-6-1-x-ray diffraction:

This technique is a structural characterization method based on the phenomenon of X-ray diffraction on a crystalline material(**Figure II-7 and 8**), and it is fundamental and very important when evaluating thin films and to know the crystal structure of materials, as well as the arrangement of atoms within the crystals, the crystalline dimensions, and to determine certain parameters, such as the degree of crystallinity, and the preferential orientation of the grains constituting the sample, it is a simple and non-destructive sample analysis technique.

Thin films were characterized using various analytical techniques. The XRD diffractogram was obtained by a DRX Rigaku-MiniFLex600 system (and PROTO) with a Cu-Ka radiation source of λ=0.15406 nm in the range of 30°–90°. Objective is to investigate nickel oxide thin film structural characteristics (**Figure II-7 and 8**). (The characterization of the samples was performed at the **university of Biskra** and the **university of El-oued**).

Scanning area in (°) 2 Θi:30, 2 Θf:90

Step in (°): 0.002°

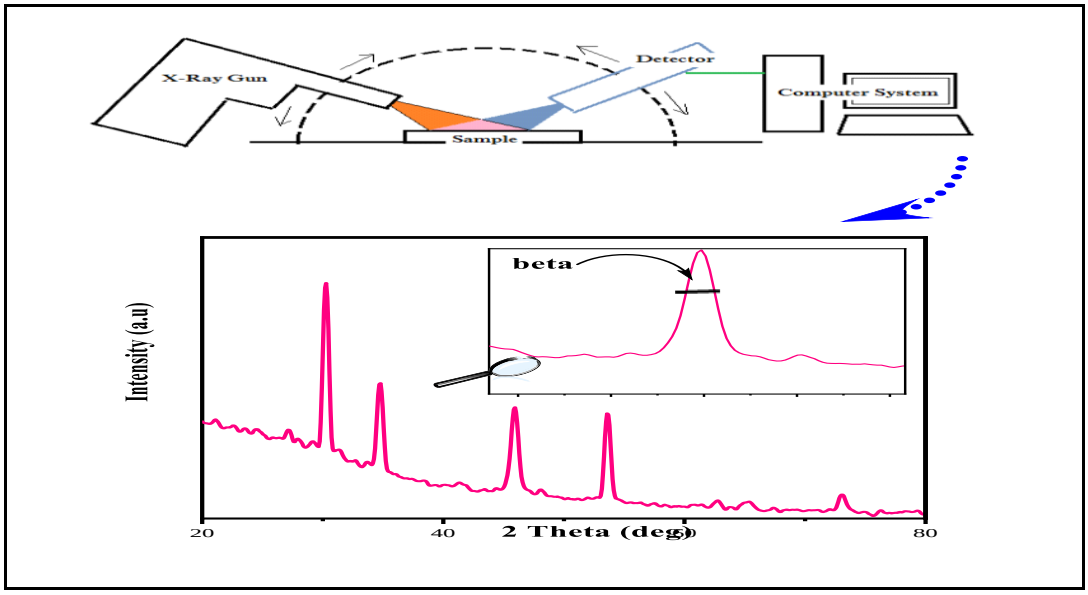

Figure II.7: *Schematic illustration of X-ray diffractometer & the exraction of the full width at half maximum (β beta) from X-ray diffraction peak.*

a-The Lattice parameters:

Equations provided by Bragg's law are used to calculate the lattice parameters for the unit cell of the phase that is present. The absence of reflection peaks indicates that the material is amorphous [8]:

$$2d_{hkl} \sin \theta = n\lambda \qquad \text{(II.1)}$$

Where:

$d_{hkl}$the spacing between the planes in the atomic lattice.

θ is the angle between the incident ray and the scattering planes.

n is an integer.

λis the wave length of the incident wave.

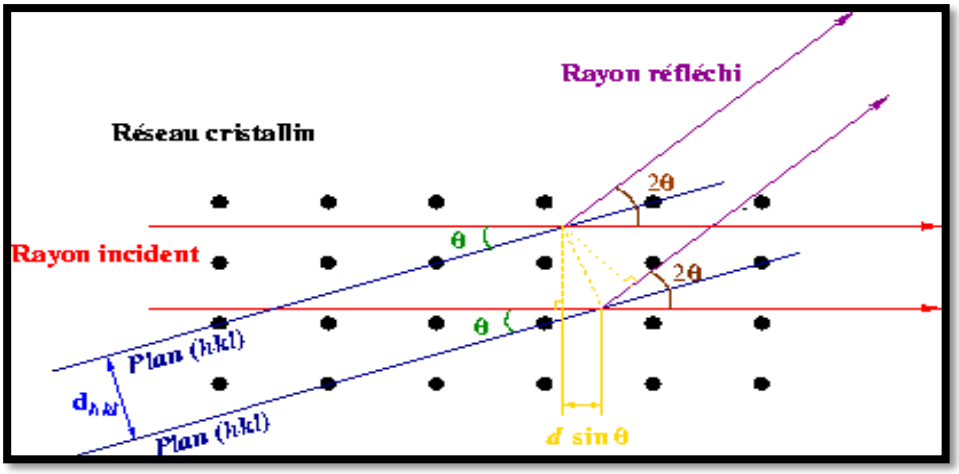

Figure II.8: *Simple diagram representing the family of crystalline planes in Bragg condition [8]*

The following formula (II.2 and 3) is used to find the cubic lattice parametera of nickel oxide thin film [9,10]:

$$\frac{1}{d_{hkl}^2} = \frac{h^2+k^2+l^2}{a^2} \qquad \text{(II.2)}$$

$$a = d_{hkl}\sqrt{h^2 + k^2 + l^2} \qquad \text{(II.3)}$$

b-Determination of the size of crystallites:

From the diffraction spectra, it is possible to calculate the approximate grain size using the Debye-Scherrer relationship[11]:

$$D = \frac{0.9\lambda}{(\beta \cos\theta)} \qquad \text{(II.4)}$$

Where: D is the size of the crystallites (nm), λ: the wavelength of the X-ray beam (Å).

β: the width at mid-height of the diffraction line, expressed in radian (Figure II.7).

θ: the diffraction angle in degrees.

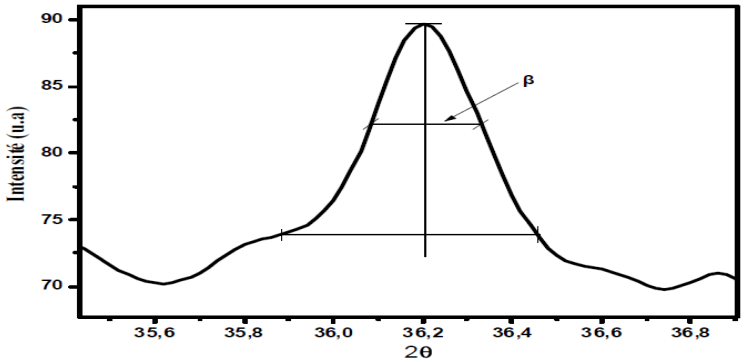

Figure II.9: *the width at mid-height of the X-ray diffraction line β [12].*

II-6-2-UV-visible spectroscopy:

The domains of spectroscopy are generally distinguished according to the wavelength interval in which the measurements are made. The following areas can be distinguished: UV-visible, UV-visible-near infrared, infrared and microwave. In our case, we used a UV-Visible spectrophotometer(SHUMATZU 1900),it is a double beam spectrometry, one for reference (glass) and the other for our sample and whose spectral range extends from UV-Visible (λ =200-900 nm).The principle of operation of this device is shown in **Figure II.10**.

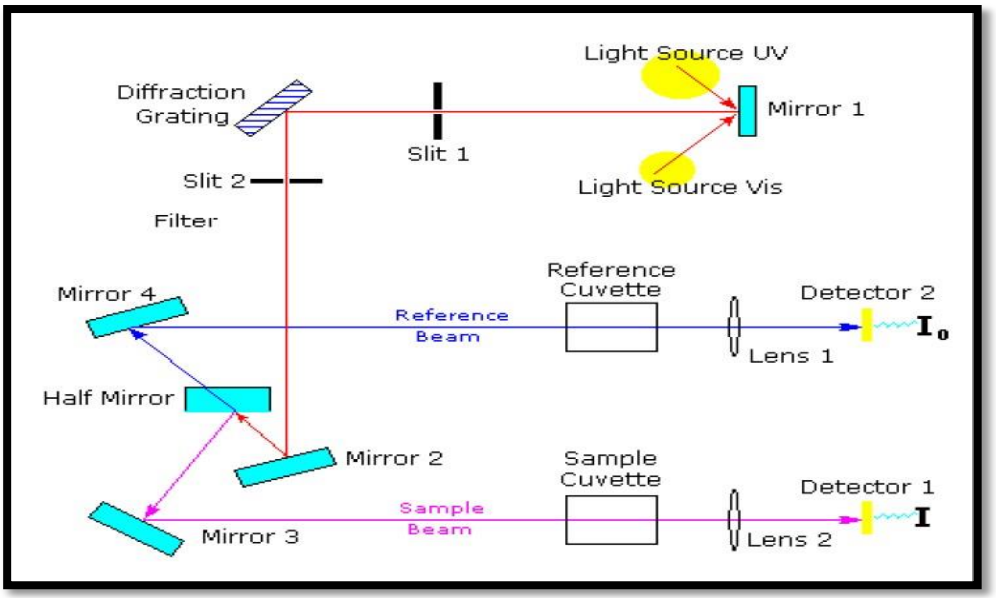

Figure II.10: *Schematic representation of the UV-Visible spectrophotometer [13].*

Figure II.11: *Experimental device of UV-visible spectroscopy used (Echahid Hamma Lakhdar University, El-Oued).*

II-6-2-1-Measurement of optical properties:

Optical methods can characterize many of the parameters, this method allows determination of the absorption coefficient, the optical gap, refractive index and film thickness, the energy of Urbach.

a-Determination of the optical gap:

NiO material has a direct gap. Therefore, the absorption coefficient as a function depending on the optical gap and energy (hυ) of photons is written in the form (Tauc equation) [14]:

$$(\alpha h\nu)^2 = A(h\nu - E_g) \qquad \text{(II.5)}$$

Where:

α:The absorption coefficient.

A: is a constant.

E_g: is the width of the bandgap (or optical gap expressed in eV).

hυ: is the energy of a photon in ev.

By tracing (α hυ) ^{2} according to hυ and extending the linear part of α ^{2}until the axis of the x-axis (that is to say for α ^{2}=0) we get the value of E_g, see figure (**Figure. II.12**).

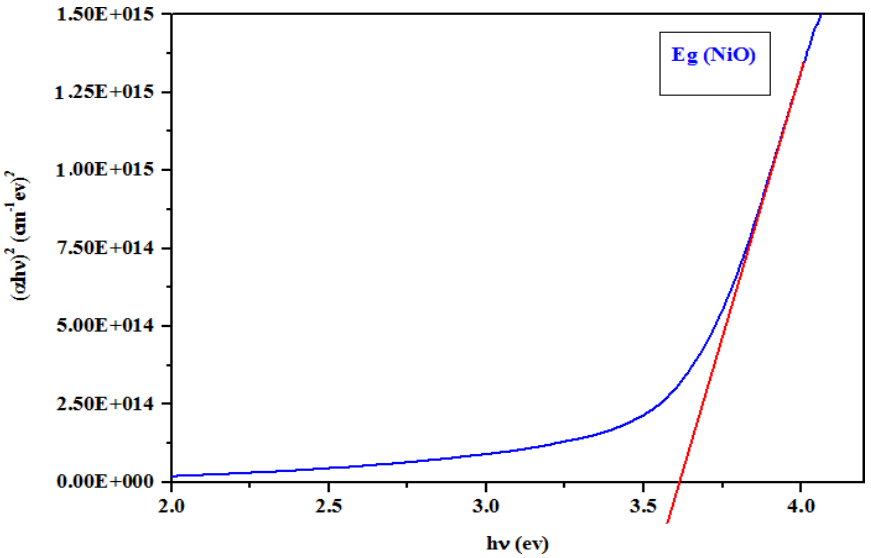

Figure. II.12: *Determination of the energy gap of a thin layer of NiO[15].*

b-Determination of the energy of Urbach:

In the pyrolysis spray deposition method, the growth of the film is by thermal

decomposition of a precipitate, at the substrate level, resulting from the vaporization of droplets. In this situation, the material that is formed contains different types of defects causing a disorder in the structure. In this case, the band edges described in the case of crystalline networks and delimited by E_v and E_c may disappear **Figure. II.13**[16].

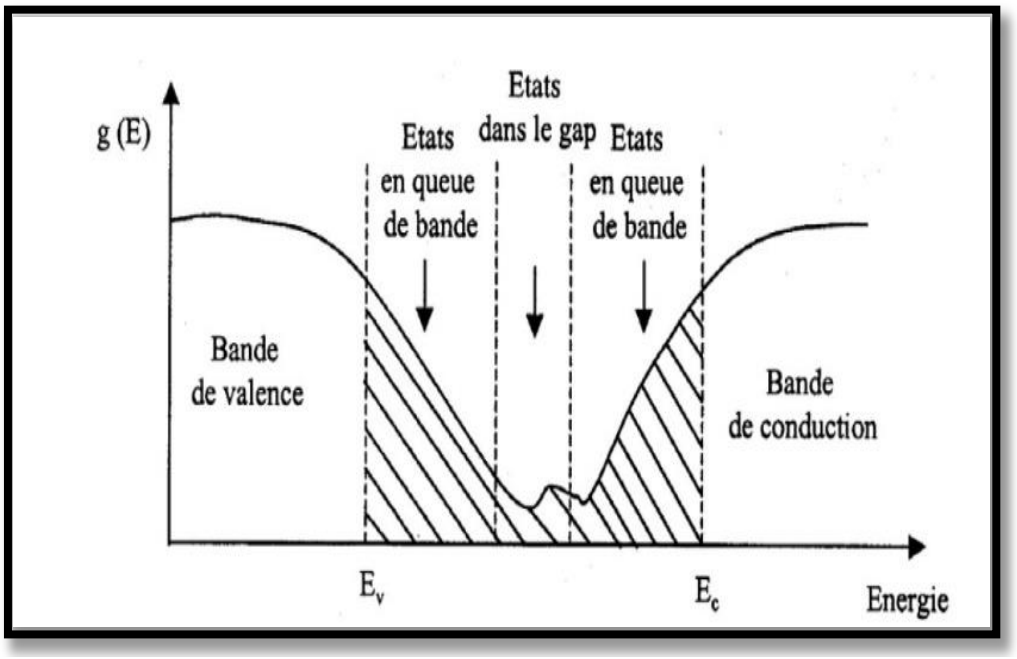

Figure. II.13: *Distribution function of energy states in bands.*

We observe what are called localized states in the band-gap which appear in bands at the borders of the valence and conduction bands. For energies higher than E_C and lower than E_V, are the extended states. When disorder becomes too great(for example with the appearance of hanging bonds or impurities in the material), the tails can encroach. Thus, it is possible to estimate the disorder existing in the layers by studying the variations of the absorption coefficient. Indeed, the absorption coefficient can be expressed by the Urbach relation[17]:

$$\alpha = \alpha_0 exp\left(\frac{h\nu}{E_U}\right) \qquad \text{(II.6)}$$

Paint lnα according to hυ **Figure. II.14**, we can access the value of $Eu=E_{00}$. By calculating the logarithmic slope, $1/E_{00}$, in this region, the disorder of films $\square_{00}$, taking the opposite of this slope, can therefore be deducted.

$$\ln \alpha = \ln \alpha_0 + \frac{h\nu}{E_{00}} \qquad \text{(II.7)}$$

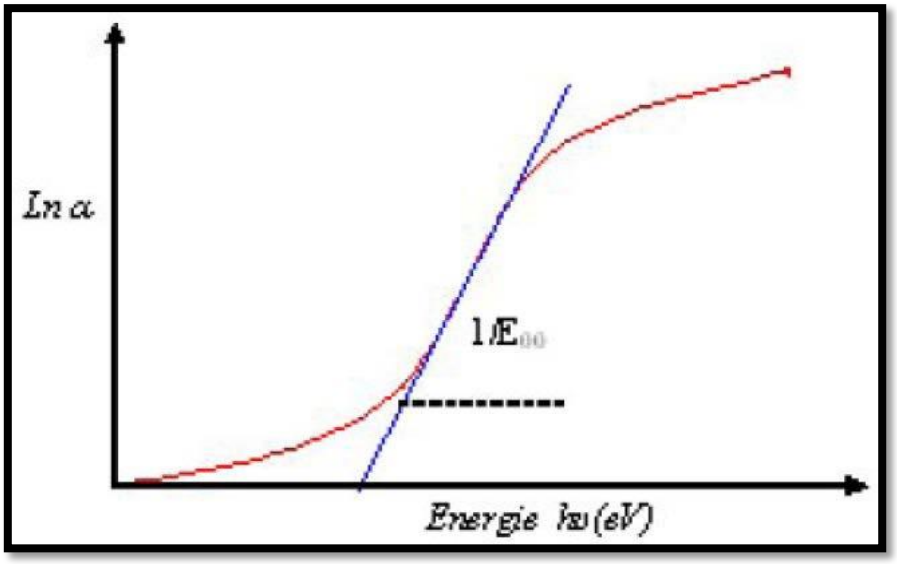

Figure. II.14: *Example illustrating the determination of the Urbach parameter from the variation of lnα according to hυ [18].*

II-6-3-Four-point probe technique:

To know directly the surface resistance R_S, we used a four-point probe device. The probe consists of four contacts aligned and evenly spaced the figure(**Figure. II.16**). A source provides a current I flowing through the external borders. The voltage U is measured at the terminals of the two inner points.

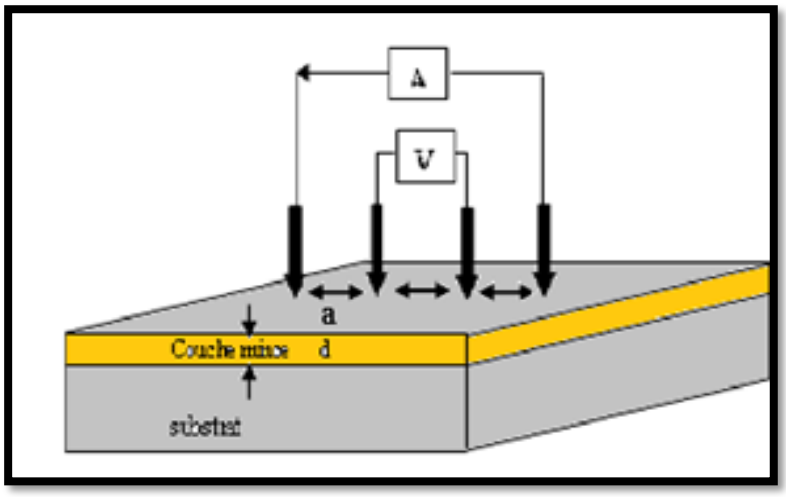

Figure. II.15: *Diagram of a four-point device [19].*

In our work, we applied an electrical voltage U = 5mV between the internal probes, and we measured the current I passing through the external probes. The sheet resistance of the thin layers is given by the formula[20]:

$$R_s = \frac{\pi}{\ln 2}\frac{U}{I} = \frac{\rho}{d} \quad \text{(II.8)}$$

If the film thickness is known, we can easily calculate electrical resistivity using relationship:

$$\rho = R_s * d \quad \text{(II.9)}$$

Where: d is the film thickness.

Figure. II.16: *Experimental setup of the four-point technique.*

II-7- problems encountered:

Here are the most important problems we encountered during our work:

- The problem of reading the temperature because its value changes rapidly under the influence of wind speed.
- The problem of mounting the probe of the multimeter and the spraying system (atomizer) in front of glass substrate holder.
- The problem of spraying solution on substrates in a homogeneous way.

II-8-Conclusion:

In this chapter, we have just made a description of the spray technique, we also set the experimental conditions, and we described the different characterization techniques used to analyze.

References:

[1]B.A.Reguig,L.Kheli,L.Catin,M.Morsli,J.C.Bernéde,TheOptical,Electricalandsurface difference, Applied Surface Science,2534330-4334,2007.

[2]Zaouche,C.THE ROLE OF Ni AND Zn ON DILUTED MAGNETIC SEMICONDUCTOR Ni1-x Znx O THIN FILMS, PhDthesis, University of Mohamed Kheider Biskra, 2021.

[3]Lenggoro, I. W., Kang, Y. C., Komiya, T., Okuyama, K., &Tohge, N. Formation of submicron copper sulfide particles using spray pyrolysis method. Japanese journal of applied physics, 37(3A), 288-290, 1998.

[4]D. Vaufrey, Realization of OLED with Emission by the surface: Optimization of ITO/ organic semiconductor structures, PhDthesis, UMRCNRS. 2003.

[5]B. Habiba. The effect of substrate temperature and molarity on the properties of zinc sulfide thin films deposited by ultrasonic spray, memoir of the magister, Mohamed Khider -Biskra University, 2013.

[6]Y.Aoun, Design and development of a solar furnace for the preparation of metal oxides – characterization of the oxides , PhDthesis, Mohamed Khider-Biskra University,2016.

[7]L. Herissi, Development and characterization of metal oxide thin films for optoelectronic applications, PhDthesis, Larbi Ben M'hidi University -Oum El Bouaghi (Algeria),2016.

[8]Okuyama, K., &Lenggoro, I. W. Preparation of nanoparticles via spray route. Chemical engineering science, *58*(3-6), 537-547, 2003.

[9]Bakr, N. A., Khodair, Z. T., &Shano, A. M. Effect of aqueous solution molarity on structural and optical properties of Ni0. 92Co0. 08O thin films prepared by chemical spray pyrolysis method. Int. J. Thin. Fil. Sci. Tec, *4*(2), 111-119, 2015.

[10]Qiao, Z. Fabrication and study of ITO thin films prepared by magnetron sputtering PhD Thesis, Duisburg, Essen, Univ. Diss., 2003.

[11]Moualkia Hassiba, Elaboration and Characterization of Cadmium Sulphide(CdS) Thin Films, PhDthesis, Mentori Constantine University, 2010.

[12]R. Azouani, Development of new photocatalytic nanomaterials under visible radiation, PhDthesis, University of Paris13, 2009.

[13]A. Hafdallah, Doping study of ZnO thin films developed by ultrasonic spray, memoir of the magister, Constantine University 1, 2007.

[14] S.Chelouche,Properties of ZnO:Al optical windows for thin film solar cells based on CIGS, memoir of the magister, Ferhat Abbas-Sétif University -Algeria,2012.

[15] Barr, R., Benhaoua, B., Benhamida, S., Rahal, A., Sahraoui, T., &Gheriani, R. Effect of precursor concentration on structural optical and electrical properties of NiO thin films prepared by spray pyrolysis. Journal of Nanomaterials, 2017(1), 5204639, 2017.

[16] S. Kemache, Elaboration and characterization of thin films of Ni1-xZnxO, master thesis, Tébessa University .2014.

[17] Aksoy, S., Caglar, Y., Ilican, S., &Caglar, M. J. O. A. Effect of Sn dopants on the optical and electrical properties of ZnO films. Optica Applicata, *40*(1), 7-14,2010.

[18] F. Bouabida, Variation of the structural and optical properties of thin ZnO layers under the effect of deposition time, master thesis, Larbi Tébessi University. Tébessa, 2013.

[19] A. Rahal, Development of conductive lenses by deposition of ZnO on ordinary glasses, Magister thesis, Achahid Hamma Lakhdar University -El-Oued, (2013).

[20] J.Osuwa,G. Onyejiuwa, Structural and electrical properties of annealed nickel oxide(NiO)thin films prepared by chemical bath deposition, JOvonic Res,**9**(2013)9-15.

ChapterIII

NiO Thin Films

III-1- Introduction:

NiO is a semiconductor material that is p-type and has an optical band gap that can vary from 3.6 to 4 eV[1].NiO's chemical stability and durability make it one of the most important oxide materials it has low toxicity, high optical density, affordability, and excellent thermal stability[2].The primary objective of this project is to try to create a semiconductor made of NiO thin films that have a highly crystalline structure with well optical and electrical characteristics.

In this work, thin films with nanostructure NiO were examined. Which are developed using the spray pyrolysis method, the deposition temperature for NiO on a glass substrate was 450 °C during heating with different NiO solution volumes of 5, 10, 15 and 20 ml. we present the results obtained, we will try to study the structural properties, optical and electrical thin films of undoped NiO.

III-2-Results and discussion:

III-2-1-structural properties:

X-ray diffractions of undoped NiO films are illustrated in the figure (**FigureIII.1**), these spectra are processed by X'Pert High Score software. NiO thin films were produced with different NiO solution volumes of 5, 10, 15 and 20 ml using the spray technique. All films have crystallized structures according to direction (111), Except for 5ml has amorphous structure. These layers belong to the cubic system with centered face (FCC) which is called cubic NaCl type[3].

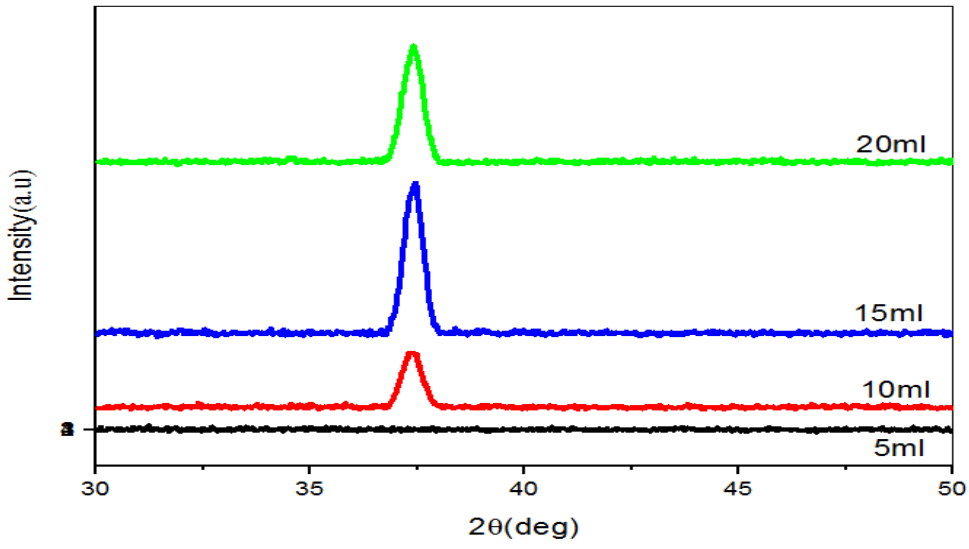

Figure III-1: *The results of X-ray diffraction spectra of undoped NiO thin films at different NiO solution volumes.*

X-ray diffraction (XRD) diagrams of undoped NiO thin films developed by pyrolysis spray (chemical spraying),were observed for various volumes(5-20 ml) and in the range 2θ (30-50°) (see Figure (**Figure.III.1**)).

The structure of the thin film deposited at 5 ml is amorphous, suggesting the low crystallinity of the film. This might be attributed to the incomplete formation of the NiO film at this volume. We also note that, from the DRX diagrams, a single peak is observed at 2θ=37,4°. This is attributed to the presence of the diffraction peak (111) clearly indicating that the NiO phase exists in NaCl type (cfc) and agrees with Joint Committee on Powder Diffraction Standards (J.C.P.D.S - No: 47- 1049) [4].

The obtain NiO thin film has a nanocrystalline structure because the spectra's of NiO thin films having one peak with higher in the sharper indicating, except the spectrum corresponding to 5ml. We found a good result for the film that were set with 15 and 20ml due to the increase in FWHM of the peaks.

To acquire more structural information, the various structural parameters have been calculated, such as lattice parameter a, d_{hkl} the inter-reticular distance, and crystallite size D(the size of the crystallites) [5],main strain ε [6], and the density of dislocation δ[7] thin films of NiO .

In the case of a cubic structure, main strain ε in NiO thin films can estimate via the formula[8]:

$$\varepsilon = \frac{a-a_0}{a_0} * 100\% \qquad \text{(III.1)}$$

Where: a anda_0 are NiO thin film lattice parameter and the standard lattice parameter of the material(a0=4.1769 A°) according to the standard card (JCPDS, number 47-1049).

The density of dislocation δ, was calculated using the following relationship [7]:

$$\delta = \frac{1}{D^2} \qquad \text{(III.2)}$$

The following table summarizes the variations of the different structural parameters of the developed NiO thin films.

TableIII -1: *the structural parameters of the undoped NiO thin films.*

	***2θ*(deg)**	***a*(Å)**	***β*(deg)**	***D*(nm)**	***ε*(%)**	***δ*.10^{15}(lines/m^2)**
5ml	-	-	-	-	-	-
10 ml	37.36807	4.1682	0.54223	15.49026	-0.00282	4.168
15 ml	37.40107	4.16130	0.52371	16.04687	-0.00373	3.883
20 ml	37.38874	4.16303	0.55652	15.08650	-0.00332	4.394

The figure (III-2) are shown the variation of the crystallite size and the main strain of undoped NiO thin films at different volumes. As can be observed, with the increase in volumes, the change in crystallite size exhibits an inverse correlation with the main strain (refer to **Table III -1**), this can be explained by the FWHM's variation. Where, the maximum crystallite size, obtained at 15 ml, is 16.05 nm, this can be explained by the homogeneous surface and coalescence, corresponding to the minimum value of lain strain (see Table III -1).

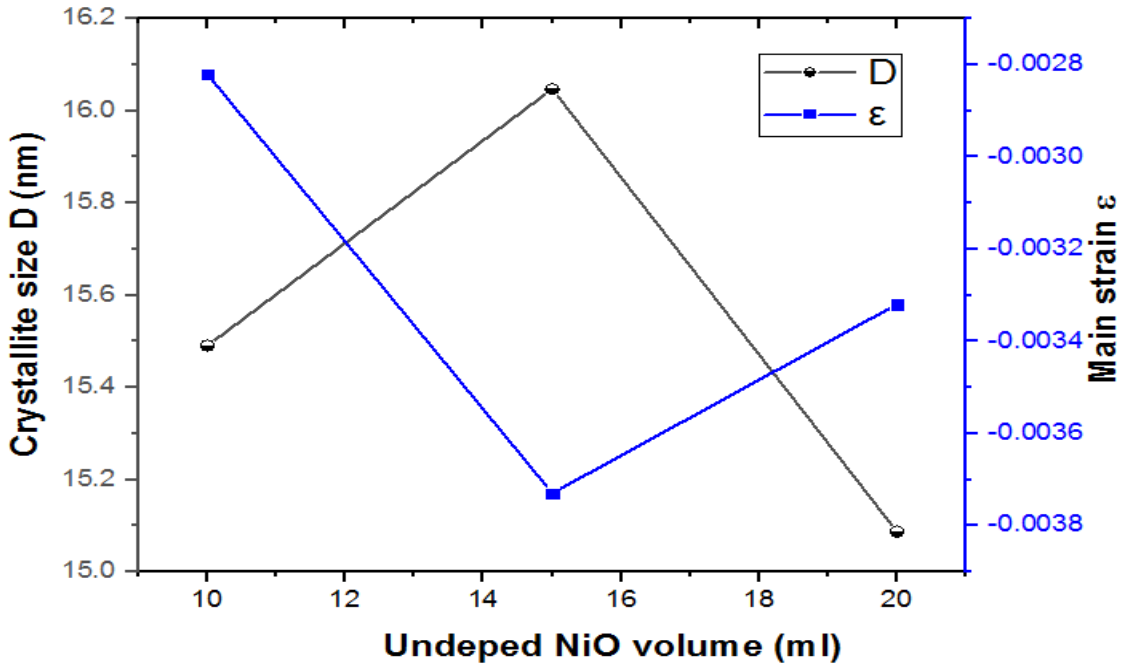

Figure III-2: *The variation of crystallite size D and main strain ε of undoped NiO thin films at different NiO volumes.*

III-2-2-Optical properties:

III-2-2-1 Transmittance:

The optical characteristics of NiO thin films, deposited at various volumes, were examined by assessing their transmittance across a wavelength range of 300 to 900 nm, as illustrated in **Figure (III-3)**. Height transparency of NiO thin films prepared in the visible

region with an average transmission of approximately 65%,Various literature suggests that films can achieve high transparency, typically ranging from 40% to 60%, when compared to their original natural state[9,10].The absorption edge region was detected as transmission decreased, indicating a transition between the valence and conduction bands[11], occurring within the wavelength range of 320–370 nm.

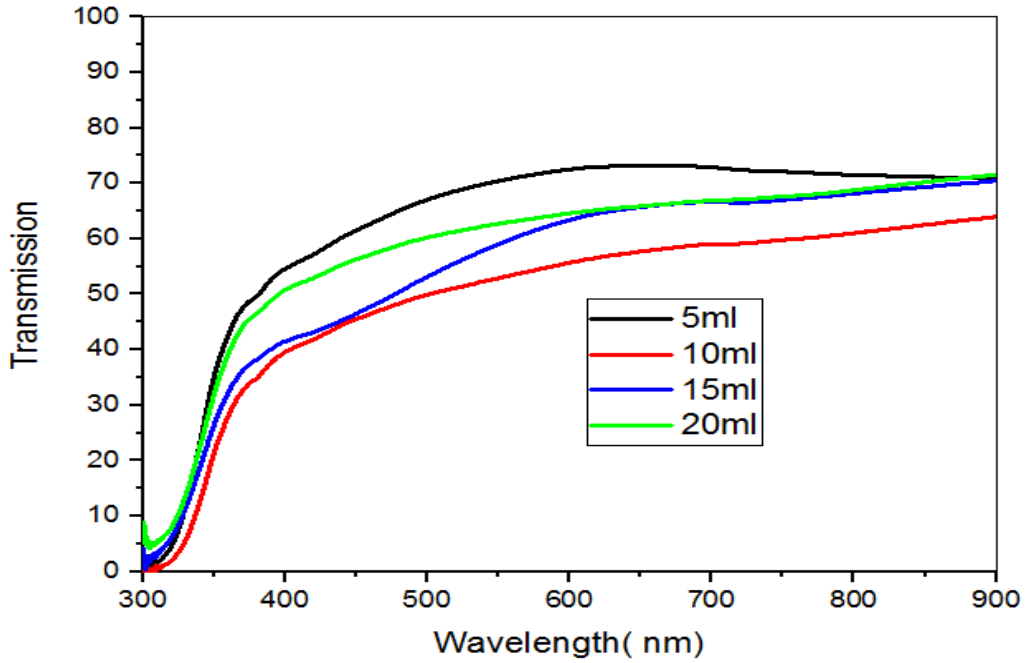

Figure III-3: *the transmittance of the thin films prepared at various volumes of NiO.*

Table III -2: *Presents the average transmittance and Film thickness of undoped NiO thin films prepared.*

Samples	NiO,05 ml	NiO, 10 ml	NiO, 15ml	NiO, 20 ml
Average Transmittance (%) 400-800 nm	69.1	53.9	68.1	63
Film thickness (nm)	163.1	214.1	262.2	334.8

III-2-2-2-Optical gap energy:

When calculating optical values such as the absorption coefficient (α), energy gap (E_g), and disorder (Urbach energy) (E_u), these parameters are defined as optical properties characterizing the crystalline structure of thin films [12].

Using the equation in chapter(II .Eq.4) to determine the energy of the optical gap is based on the Tauc law model [13].By tracing$(\alpha h\upsilon)^2$ as a function of hυ and that we extend the linear part of α^2up to the x-axis (that is for $\alpha^2 = 0$), we get the value of E_g in the

literature [14,15].

Figure (III.4) shows that of estimate optical gap (E_g) NiO thin films not doped prepared at 450°C with different volumes.

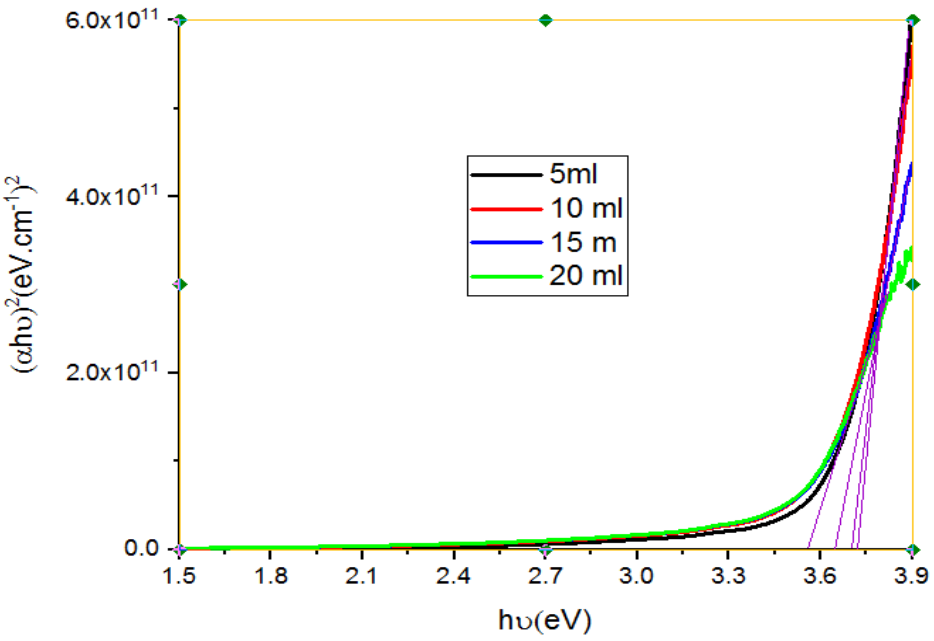

FigureIII-4: *determination the optical gap of undoped NiO layers prepared.*

Optical bandgap values for undoped NiO films in different volumes(5-10-15and 20ml) were estimated at E_g(3,59to 3,76eV) indicating in the table(III-3).For the undoped NiO film, it is evident that the bandgap values vary gradually with increasing volumes. This alteration in band energy could be linked due to the influence of diverse factors like preparation state, film thickness, grain size, and the presence of impurities within the films [16,17].

III-2-2-3The energy of Urbach:

We can determine Urbach energy, the absorption coefficient can be expressed by the equation(see Chapter II.Eq.5)[18],E_U (=E_{00}) measures the extension of the Urbach tail and is an indirect measure of the structural disorder Srikant et al[19]by drawing ln(A) as a function of hυ, we can obtain the value of E_u= E_{00}.

By calculating the logarithmic slope 1/E_{00}, in this region, disorder of the film, taking the conversely of this slope. They interpreted the Urbach energy [20] as the band width of states located within the width of the prohibited band E_g. The figure (III-5), shows the variation of **LnA** as a function of photon energy **hυ**, describes the regions where different

types of optical absorption phenomena. We are interested in the fundamental absorption(E_v and E_c band) and Urbach energy we draw the tangent in Figure(III-5).

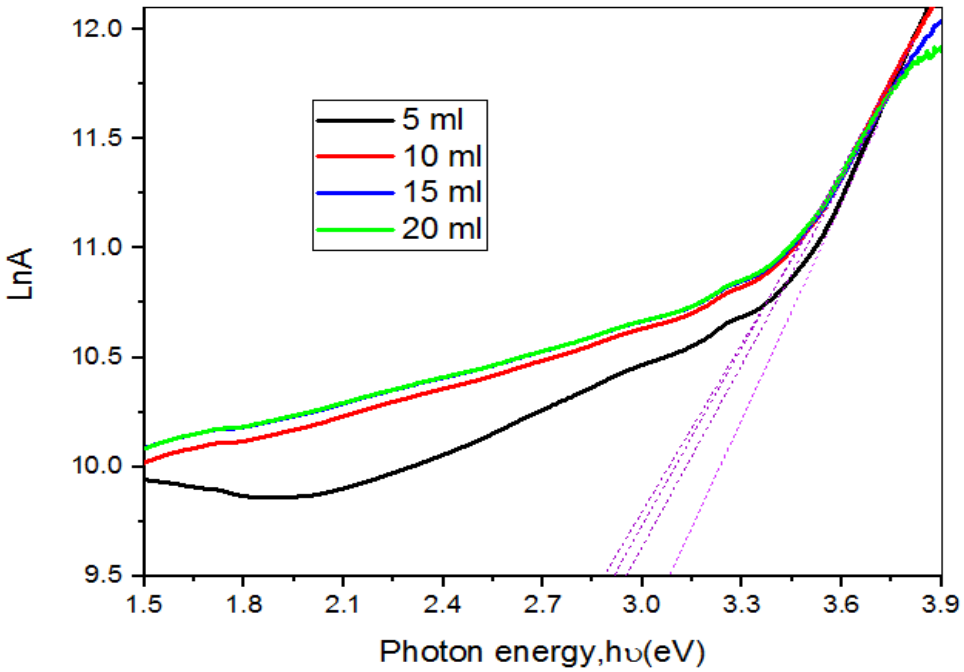

Figure III-5: *The variation of LnA as a function of hυ of undoped NiO thin films prepared.*

In the **Figure(III-6)** we note that, all samples of unposed NiO thin films prepared at 450°C the experimental values of the gap band are reversed to the experimental values of the Urbach energy[21].

As evident in the table below (Table III.3),the energy band interval is between 3.59-3.76eV.The decrease in the optical band gap can be attributed to changes in grain size and the increased of structural disorder in the films, as observed through Urbach energy analysis.

Table III.3*: Shows the values of optical gap (**E_g**), thickness(**t**) and energy of Urbach(**E_u**) NiO thin films prepared at 450°C.*

	***t*(nm)**	***Eg*(eV)**	**E_u(meV)**
5ml	163.17	3.76	310
10 ml	214.12	3.71	362
15 ml	262.24	3.66	390
20 ml	334.77	3.59	405

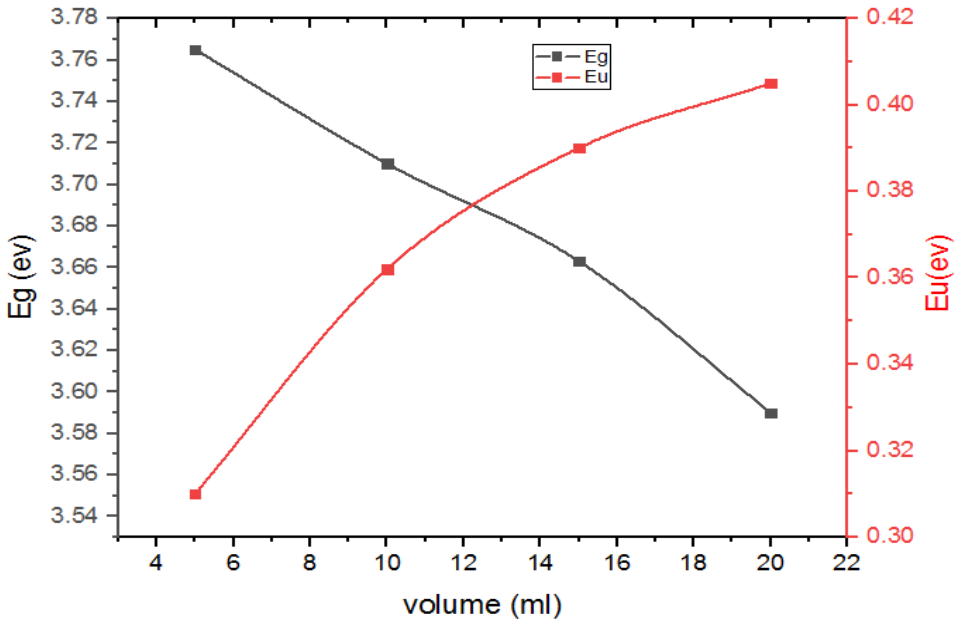

***Figure III-6**: Variation of the optical gap and Urbach energy as a function of volume of the undoped NiO layers.*

III-2-3-Electrical properties:

To identify the electrical properties of the elaborated NiO thin films with different volumes, using the four-point method and allowed to trace electrical conductivity as a function of volume.

The Figure (III-7) below shows the variation of electrical conductivity NiO thin films as a function of volume. As it can be observed, with increasing volume, the electrical conductivity increases from 5 to 20 ml, this increase in conductivity can be interpreted as the increase in the number of charge carriers (electrons) [10], resulting in a semiconductor that is p-type. The NiO thin film elaborated with 20 ml has a maximum electrical conductivity was $6.527*10^{-6}$ $(\Omega.cm)^{-1}$.

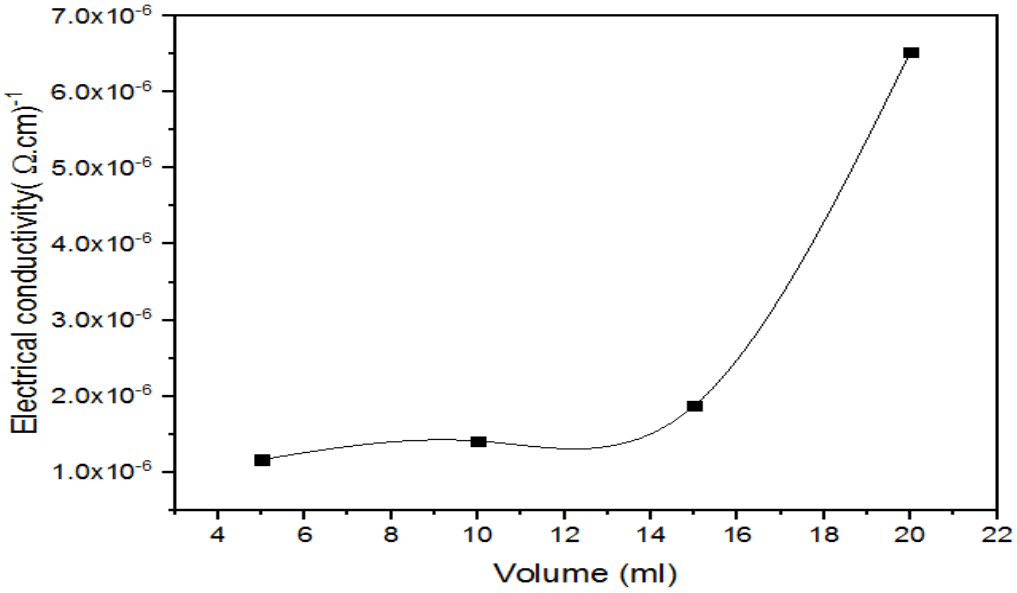

FigureIII-7*: Variation of conductivity of NiO thin films as a function of volume.*

III-3-Conclusions:

The NiO thin films were prepared using spray pyrolysis method on glass substrate at 450 °C with different volume. Thin films of nanostructures NiO were examined for their structural, optical, and electrical properties. It was observed that NiO thin films had a nanocrystalline cubic structure with a strong (111) preference orientation, it was observed that only one phase in all the films prepared. The largest crystallite size (16.05 nm) was recorded for the film deposited with 15 ml. In all NiO thin films prepared, the average transmittance was approximately 65%. The band gap energy of NiO thin films varies between 3.59 and 3.76 eV, the minimum value was found at 20 ml. The NiO thin film elaborated with 20 ml has a maximum electrical conductivity was $6.527*10^{-6}$ $(\Omega.cm)^{-1}$.

References:

[1]Manouchehri, I., Mehrparvar, D., Moradian, R., Gholami, K., &Osati, T. Investigation of structural and optical properties of copper doped NiO thin films deposited by RF magnetron reactive sputtering. *Optik*, *127*(19), 8124-8129, 2016.

[2]Diha, A., Benramache, S., &Benhaoua, B. Transparent nanostructured Co doped NiO thin films deposited by sol–gel technique. *Optik*, *172*, 832-839, 2018.

[3]Sasaki, S., Fujino, K., &Takéuchi, Y. X-ray determination of electron-density distributions in oxides, MgO, MnO, CoO, and NiO, and atomic scattering factors of their constituent atoms. *Proceedings of the Japan Academy, Series B*, *55*(2), 43-48, 1979.

[4]Wang, J., Yang, P., Wei, X., & Zhou, Z. Preparation of NiO two-dimensional grainy films and their high-performance gas sensors for ammonia detection. *Nanoscale research letters*, *10*, 1-6, 2015.

[5]Lagashetty, A., Havanoor, V., Basavaraja, S., Balaji, S. D., & Venkataraman, A. Microwave-assisted route for synthesis of nanosized metal oxides. *Science and Technology of Advanced Materials*, *8*(6), 484. 2007.

[6]Wang, Y., Zhu, J., Yang, X., Lu, L., & Wang, X. Preparation of NiO nanoparticles and their catalytic activity in the thermal decomposition of ammonium perchlorate. *Thermochimica Acta*, *437*(1-2), 106-109. 2005.

[7]Padiyan, D. P., Marikani, A. U., & Murali, K. R. Influence of thickness and substrate temperature on electrical and photoelectrical properties of vacuum-deposited CdSe thin films. *Materials Chemistry and Physics*, *78*(1), 51-58. 2003.

[8]Ukoba, K. O., Eloka-Eboka, A. C., &Inambao, F. L. Review of nanostructured NiO thin film deposition using the spray pyrolysis technique. *Renewable and Sustainable Energy Reviews*, *82*, 2900-2915, 2018.

[9]Iftimie, S., Mallet, R., Merigeon, J., Ion, L., Girtan, M., &Antohe, S. On the structural, morphological and optical properties of ITO, ZnO, ZnO: Al and NiO thin films obtained by thermal oxidation. *Digest Journal of Nanomaterials and Biostructures*, *10*(1), 221-229, 2015.

[10] Benramache, S., &Benhaoua, B. Influence of substrate temperature and Cobalt concentration on structural and optical properties of ZnO thin films prepared by Ultrasonic spray technique. *Superlattices and Microstructures*, *52*(4), 807-815, 2012.

[11] Tian, J., Deng, H., Sun, L., Kong, H., Yang, P., & Chu, J. Effects of Co doping on structure and optical properties of TiO2 thin films prepared by sol–gel method. *Thin Solid Films*, *520*(16), 5179-5183. (2012).

[12] Tauc, J., Grigorovici, R., &Vancu, A. Optical properties and electronic structure of amorphous germanium. *physica status solidi (b)*, *15*(2), 627-637, 1966.

[13] Casey Jr, H. C., Sell, D. D., & Wecht, K. W. Concentration dependence of the absorption coefficient for n− and p− type GaAs between 1.3 and 1.6 eV. *Journal of Applied Physics*, *46*(1), 250-257. 1975.

[14] Juybari, H. A., Bagheri-Mohagheghi, M. M., & Shokooh-Saremi, M. Nickel–lithium oxide alloy transparent conducting films deposited by spray pyrolysis technique. *Journal of alloys and compounds*, *509*(6), 2770-2775. (2011).

[15] Amor, M. B., Boukhachem, A., Boubaker, K., & Amlouk, M. Structural, optical and electrical studies on Mg-doped NiO thin films for sensitivity applications. *Materials science in semiconductor processing*, *27*, 994-1006, 2014.

[16] Oliva, A. I., Solıs-Canto, O., Castro-Rodrıguez, R., & Quintana, P. Formation of the band gap energy on CdS thin films growth by two different techniques. *Thin solid films*, *391*(1), 28-35, 2001.

[17] Rao, S. L. S., Ramadevudu, G., Shareefuddin, M., Hameed, A., Chary, M. N., & Rao, M. L. Optical properties of alkaline earth borate glasses. *International Journal of Engineering, Science and Technology*, *4*(4), 25-35, 2012.

[18] Urbach, F. The long-wavelength edge of photographic sensitivity and of the electronic absorption of solids. *Physical review*, *92*(5), 1324. 1953.

[19] Srikant, V., & Clarke, D. R. Optical absorption edge of ZnO thin films: the effect of substrate. *Journal of applied physics*, *81*(9), 6357-6364. 1997.

[20] Fang, G., Li, D., & Yao, B. L. Fabrication and vacuum annealing of transparent conductive AZO thin films prepared by DC magnetron sputtering. *Vacuum*, *68*(4), 363-372, 2002.

[21] Rao, S. L. S., Ramadevudu, G., Shareefuddin, M., Hameed, A., Chary, M. N., & Rao, M. L. Optical properties of alkaline earth borate glasses. *International Journal of Engineering, Science and Technology*, *4*(4), 25-35, 2012.

Chapter IV

Synthesis of nanostructured of:

- ✓F doped NiO
- ✓Al doped NiO
- ✓Cu doped NiO

IV-1-Introduction:

Metal oxide semiconductors play a crucial role in advancing industrial applications because of their diverse inherent properties, photocatalytic capabilities, including UV light absorption, photocatalytic capabilities, magnetic and dielectric properties, as well as high chemical stability [1–2].

Incorporating dopants into materials stands out as one of the foremost methods for improving material properties [3].Recently, NiO has shifted its attention towards doping with various transition metals (TMs) including Cu[4], Na[5], Zn[6], V[7], Mn[8], Al, Ga, In[9], Li[10], Ag[11], Mg[12], Co[13], and Mo[14], with nickel, aiming to enhance electrical conductivity.

In this chapter, a description and analysis of measurements and discussion of results will be provided for F doped NiO thin films, Al doped NiO thin films and Cu doped NiO thin films. We will try to study the structural, optical and electrical properties of these thin films.

IV-2-F doped NiO thin films:

IV-2-1 structural properties:

FigureIV-1 illustrates the XRD spectra of F-doped NiO thin films prepared at different NiO:F solution volumes of 5, 10,15 and 20 ml .As an initial result, we have observed that all the films displayed a diffraction peak at$2\theta = 37$ related to the (111) plane of the NiO phase, which corresponds to a single crystal cubic structure. The XRD spectra obtained approximately corresponded with the joint committee's powder diffraction system (JCPDS, No. 47-1049) [15].It can be observed that the thin film of F doped NiO deposited with 20 ml exhibits a good crystal structure as indicated by the highest and strong peak, this confirms that increasing the deposition volume can improve the crystalline quality of F-doped NiO thin films.

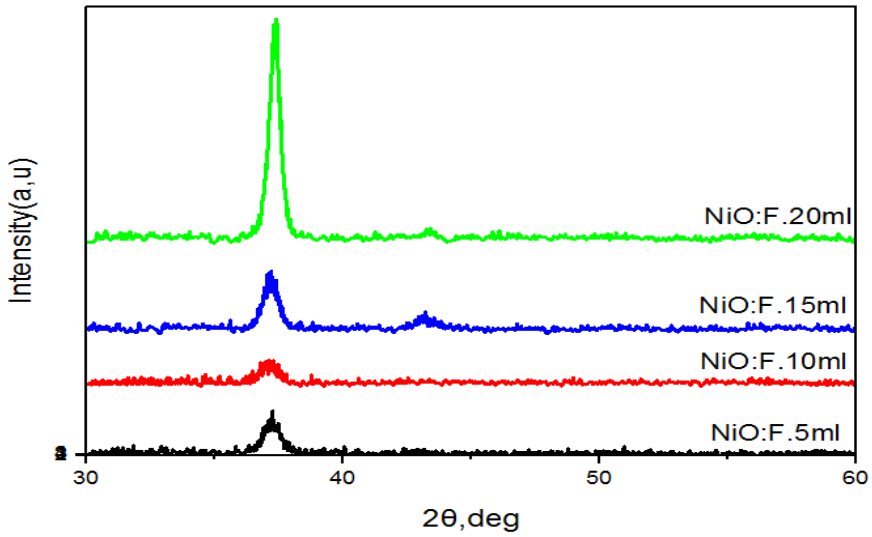

***Figure IV-1**: X-ray diffraction spectra of F-doped NiO thin films at different NiO: F volumes.*

The crystallite size (111) and main strain of the F-doped NiO thin films, were calculated using the following equations [13-15]:

$$D = \frac{0.9\lambda}{\beta \cos\theta} \qquad \text{(IV- 1)}$$

$$\varepsilon = \frac{\beta}{4 \tan\theta} \qquad \text{(IV- 2)}$$

Where:

D is the crystallite size.

λ is the X-ray wavelength (λ = 1.5406 A°).

β is the full width at half-maximum (FWHM).

θ is the angle of diffraction peak.

ε is the main strain.

***Table IV-1:**Shows the crystal structure of F doped NiO thin films of F doped NiO thin films as a function of NiO:F volume.*

Samples	Diffraction angle 2Θ (°)	FWHM β (°)	Crystallite size D (nm)	Lattice parameter a (nm)	Main strain ε
NiO: F, 5 ml	37,21	0,80	12.47	0,442662	0,00459
NiO:F, 10 ml	37,09	0,91	10.94	0,44205	0,00525
NiO:F, 15 ml	37,15	0,69	14.45	0,44032	0,00397
NiO:F, 20 ml	37,32	0,52	19.21	0,43982	0,00298

Figure IV-2illustrates the variation of the crystallite size and the main strain of F doped NiO thin films at different NiO: F volumes. As can be observed, as the volumes increases, the

crystallite size varies inversely with the main strain(see **Table IV-1**), we can explain it by the variation of the FWHM. Where, the highest crystallite size, measuring 19.21 nm, was achieved with a deposition volume of 20 ml, this is can be explained by the homogeneous in the surface and coalescence, this corresponds to the minimum value of strain(see Table IV-1).

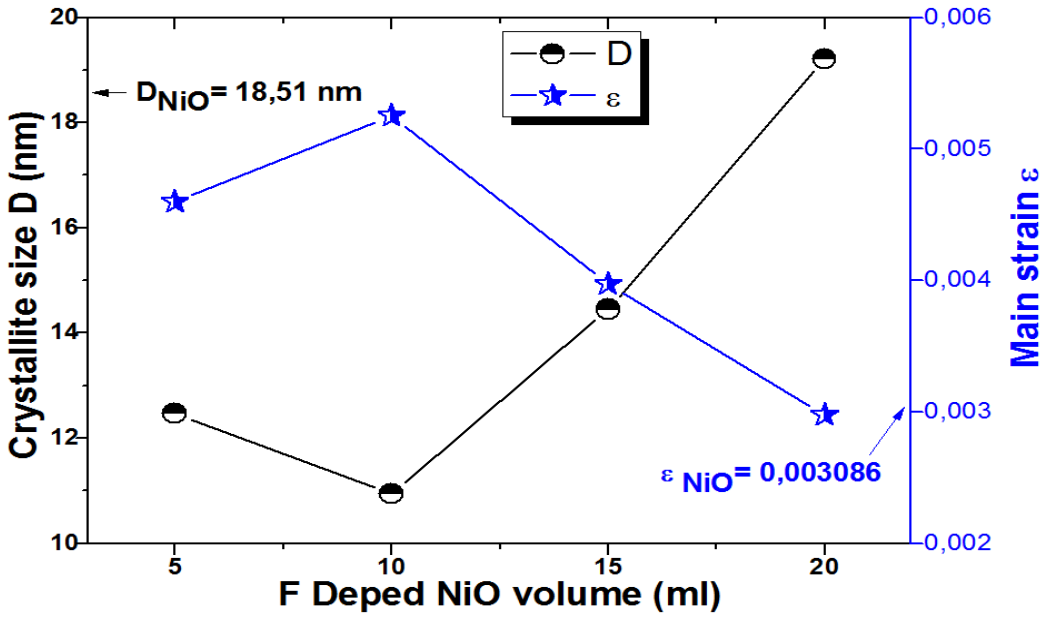

Figure IV-2: *The crystallite size D(111) and main strain ε of F doped NiO thin films at different NiO: F volumes.*

IV-2-2-Optical properties:

The optical properties of F doped NiO thin films were represented by the transmission spectra in the range of 300 to 900 nm of wavelength. **Figure IV-3** illustrates the variation in transmission of the deposited thin films at different volumes of NiO: F. As the NiO: F volume increased, the transmission decreased due to an increase in film thickness. Despite this, the prepared F doped NiO thin films exhibit good transmission approximately 80 % in the visible region due to the fluorine doping (see **Table IV-2**). The transmittance of 20 ml sample (78%) is higher than that of the 15 ml (73.8%) due to the improved crystallinity of the film. The region between 300 and 400 nm is characterized by strong absorption, heir the decrease in transmission of F-doped NiO is attributed to the excitation and migration of electrons from the conduction band to the valence band.

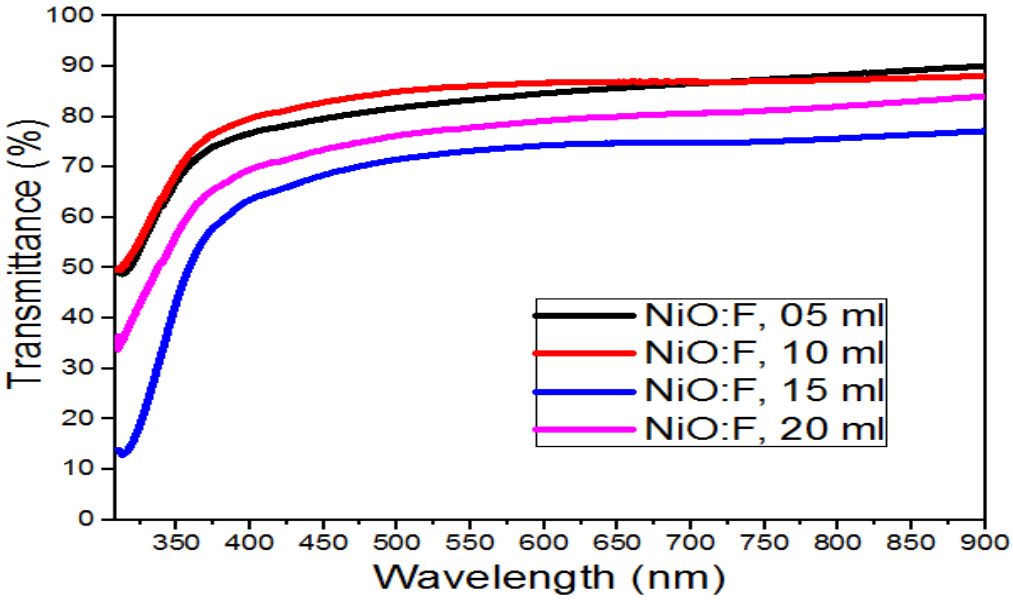

***Figure IV-3**: The transmission spectra of F doped NiO thin films at different NiO:F volumes*

***Table IV-2:**Presents the average transmittance and Film thickness of F doped NiO thin films prepared.*

Samples	NiO:F,05 ml	NiO:F, 10 ml	NiO:F, 15ml	NiO: F, 20 ml
Average Transmittance (%) 400-800 nm	83.9	85.6	73.8	78.0
Film thickness (nm)	110	112	134	140

IV-2-2-1Optical gap energy:

The optical band gap energy of the thin films of F doped NiO was determined from transmission spectra, which it was applied the following equations [15-17].

$$A = \alpha d = -\ln T \qquad \text{(IV- 3)}$$

$$(Ahv)^2 = B(hv - E_g) \qquad \text{(IV -4)}$$

Where: E_g the optical band gap energy; Ais the absorbance, d is the film thickness; T is the transmission spectra of thin films; α is the absorption coefficient values; B is a constant and hv is the photon energy.

It was determined by extrapolating the curve of $(Ahv)^2$ vs hv at A = 0 [18], as indicated in **Figure IV-4**, which shows the drawn of the $(Ahv)^2$as a function of $hv$of F doped NiO thin films.

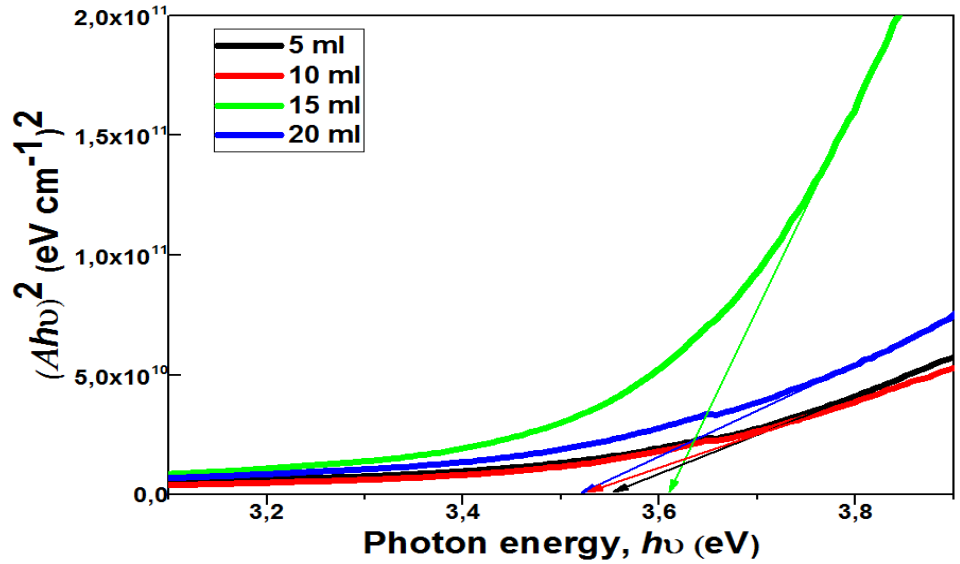

Figure IV-4: *The typical variation of values* $(Ahv)^2$ *as a function of photon energy hv of F doped NiO thin films prepared at different NiO: F volumes.*

IV-2-2 -2-The Disorder (Urbach energy):

The Urbach energy of F doped NiO thin films has been determined by the following equation [18,19]:

$$A = A_0\, exp(\frac{h\upsilon}{E_u}) \qquad \text{(IV- 5)}$$

Where: A_0 is a constant, and E_u is the Urbach energy.

Figure IV-5depictsthe variation of the drawn ofLnAas a function of the photon energy $h\upsilon$, where the Urbach energy was determined as the inverse of the slope of the curve.

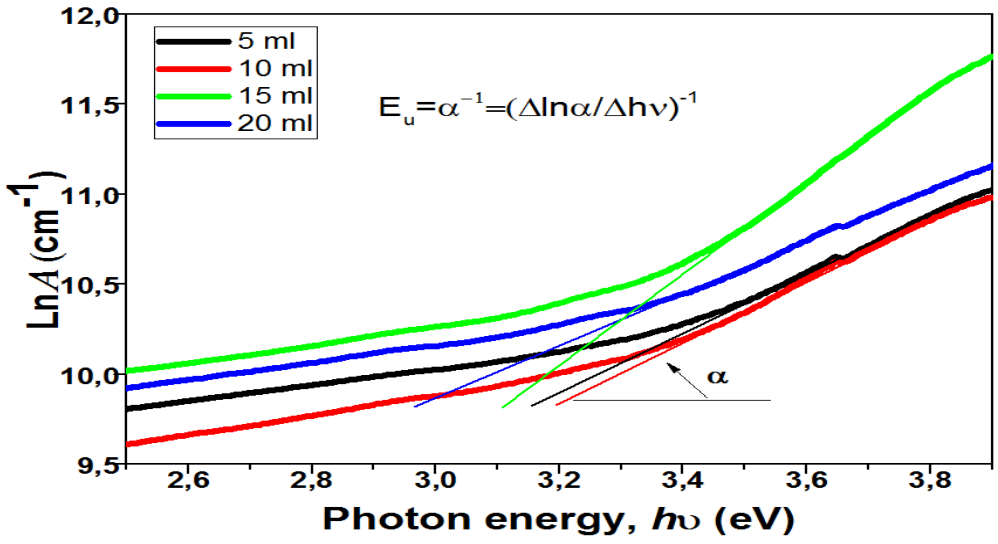

Figure IV-5: *The typical variation of values LnA as a function of photon energy hv of F doped NiO thin films prepared at different NiO:F volumes.*

FigureIV- 6 illustrates the variation of the band gap energy and the Urbach energy of newly deposited F doped NiO thin films prepared at different volumes. As observed, with increasing volumes, the variation of the optical energy shows an inverse relationship with the Urbach energy(see **Table IV-3**). The film deposited with 20 ml exhibits the lowest optical energy and highest Urbach energy, this is can be explained by the increased mobility of F in the NiO:F, and the corporation between F and O and thus there is an increase in the substitutional site.

Table IV-3*Shows the variation of optical band gap energy and Urbach energy of F doped NiO thin films as a function of NiO:F volume.*

Samples	Optical gap energy$\mathbf{E_g}$(eV)	Urbach energy$\mathbf{E_u}$ (eV)
NiO:F, 05 ml	**3,54**	**0,609**
NiO:F, 10 ml	**3,52**	**0,595**
NiO:F, 15 ml	**3,61**	**0,394**
NiO:F, 20 ml	**3,51**	**0,689**

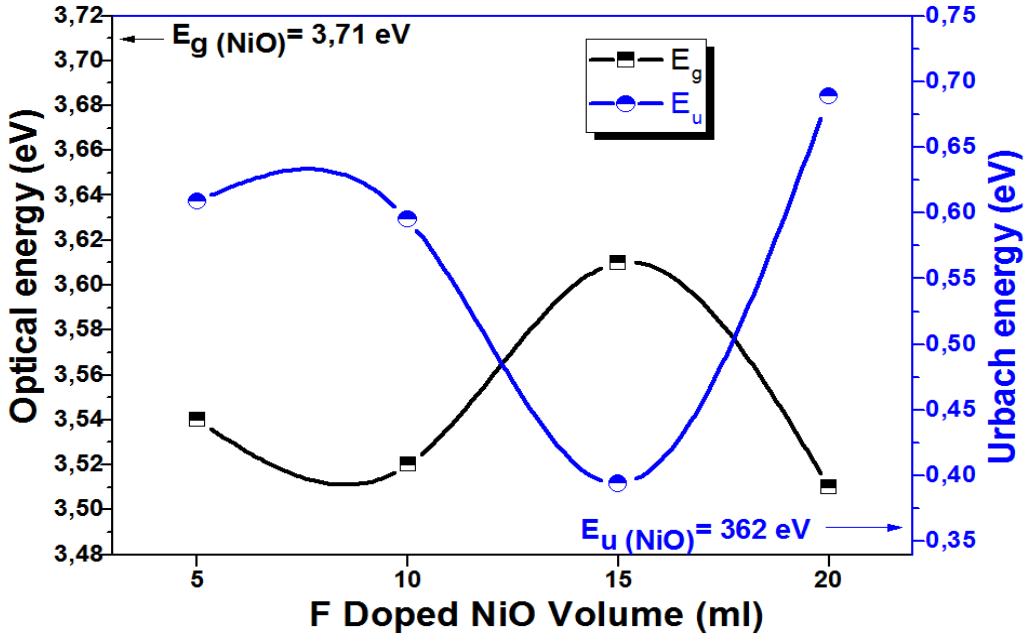

Figure IV-6: *The variation of Optical band gapE_g and Urbach energy $E_u$of F doped NiO thin films at different NiO:F volumes.*

IV-2-3Electrical properties:

We used four- point probe technique for determining the electrical conductivity of F doped NiO thin films, this technique is based on the measured voltage, current and sheet resistance expressed by:

$$R_{sh} = \left(\frac{\pi}{ln\,2} * \frac{V}{I}\right) \qquad \text{(IV -5)}$$

$$\sigma = \frac{1}{\rho} = \frac{1}{dR_{sh}} \qquad \text{(IV-6)}$$

Where: R_{sh} is the sheet resistance, d is the film thickness, σ is the conductivity, ρ is the resistivity; V is the applied voltage =5mV; and I is the measurement current (see **Table IV-4**). As can be seen, as observed, with increasing volume, the electrical resistivity of F doped NiO thin films rises (see **Table IV-4**), this increase can be attributed to a decrease in the number of electrons and mobility, leading to a p-type semiconductor. The F-doped NiO thin film with 5 ml exhibits the lowest electrical resistivity 231 Ω·cm (see **Table IV-4**).

Table IV-4: *Presents the variation of measured current and voltage and the sheet resistance of F doped NiO thin films as a function of the NiO:F volume.*

Samples	Measured Current $\boldsymbol{I}$ (nA)	Measured voltage $\boldsymbol{V}$ (mV)	Sheet resistance $\boldsymbol{R_{sh}}$ (Ω)	Electrical resistivity $\boldsymbol{\rho}$ (Ω.cm)
NiO:F, 05 ml	10.80	5	$2.1x10^7$	231 Ω.cm
NiO:F, 10 ml	0.13		$1.7x10^9$	$1.9x10^3$ Ω.cm
NiO:F, 15 ml	0.080		$2.8x10^9$	$3.8x10^3$ Ω.cm
NiO:F, 20 ml	0.087		$2.6x10^9$	$3.6x10^3$ Ω.cm

IV-3-Al doped NiO thin films:

IV-3-1structural properties:

Figure IV-7 illustrates the XRD spectra of NiO thin films prepared with different volumes of NiO:Al solution. We observed that each of the films exhibited a diffraction peak at 2θ = 37, this suggests the presence of the (111) plane within the NiO phase, characterized by its single crystal cubic structure. The XRD spectra obtained approximately matched those of the Joint Committee on Powder Diffraction Standards(JCPDS, No. 47-1049)[15].It is apparent that the thin film of Al-doped NiO, deposited with 15 ml, exhibits a well-defined crystal structure, as indicated by a prominent and robust peak.

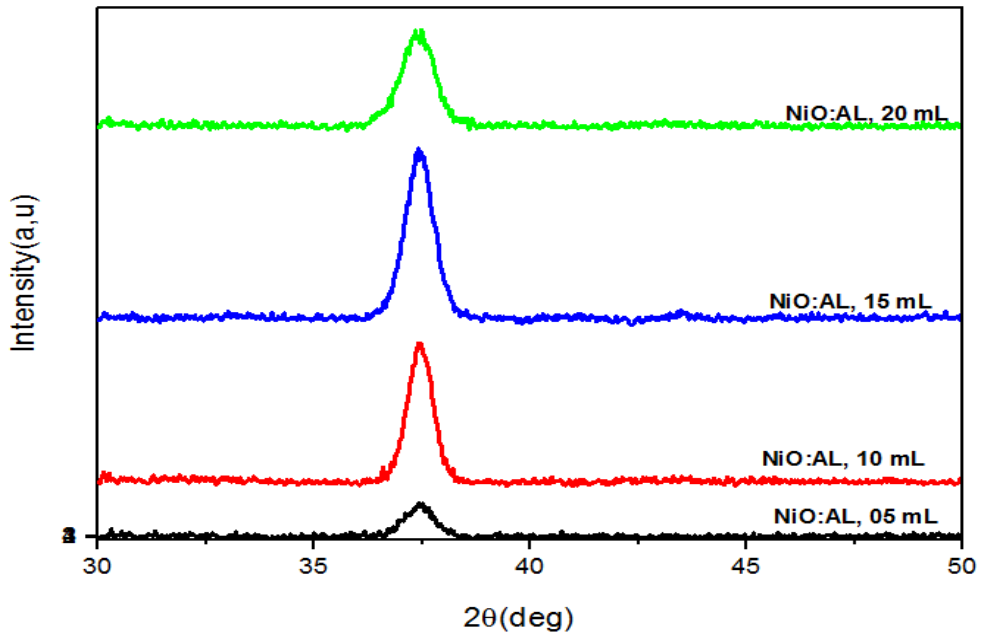

FigureIV-7: *X-ray diffraction spectra of Al-doped NiO thin films at different NiO: Al volumes.*

For obtaining further structural information, various structural parameters such as the lattice parameter$a$, the crystallite sizes, main strain ε of Al doped NiO thin films as a function of NiO:Al volume (see **Table IV-5**).

Table IV-5*: Shows the crystal structure of Al doped NiO thin films of Al doped NiO thin films as a function of NiO: Al volume.*

Samples	Diffraction angle 2θ (°)	FWHM β (°)	Crystallite size D (nm)	Lattice parameter$a$ (nm)	Main strainε
NiO: Al, 05 ml	37,42	0,68	12.42	0.41593	0.00388
NiO: Al, 10 ml	37,45	0,59	14.24	0,41560	0,0037
NiO : Al, 15 ml	37,44	0,65	15.09	0,41571	0,00336
NiO : Al, 20 ml	37,42	0,73	13.43	0,41593	0,00416

Figure IV-8 presents the variation of the crystallite size and the main strain of Al doped NiO thin films at different NiO: Al volumes. We notice that with an increase in volume, there is a reverse fit between crystallite size and main strain $\boldsymbol{\varepsilon}$,this can be explained by the variation (FWHM).we observe that, the maximum crystallite size of 15.09 nm was observed for the 15 ml sample, this corresponds to the minimum value of lattice strain.

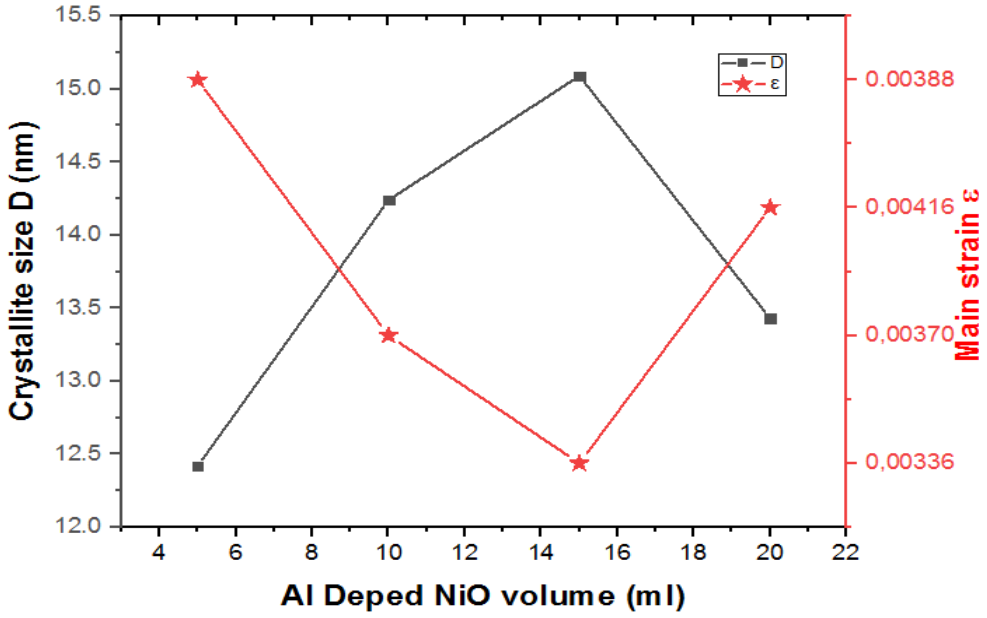

***Figure IV-8**:The variation of crystallite size and main strain ε of Al doped NiO thin filmsat different volumes.*

IV-3-2-Optical properties:

Figure IV.9 shows the optical transmittance spectra recorded in the wavelength range from 300 to 900 nm. For all Al-doped NiO thin films prepared at different volumes, the spectra exhibit two regions: The first region, with a wavelength of less than 450 nm, shows a rapid decrease in transparency for all samples, indicating fundamental absorption at the outset due to the transition between the valence band and the conduction band. The second region with a wavelength greater than 450 nm, showing an average transmission between 54 and 75%.

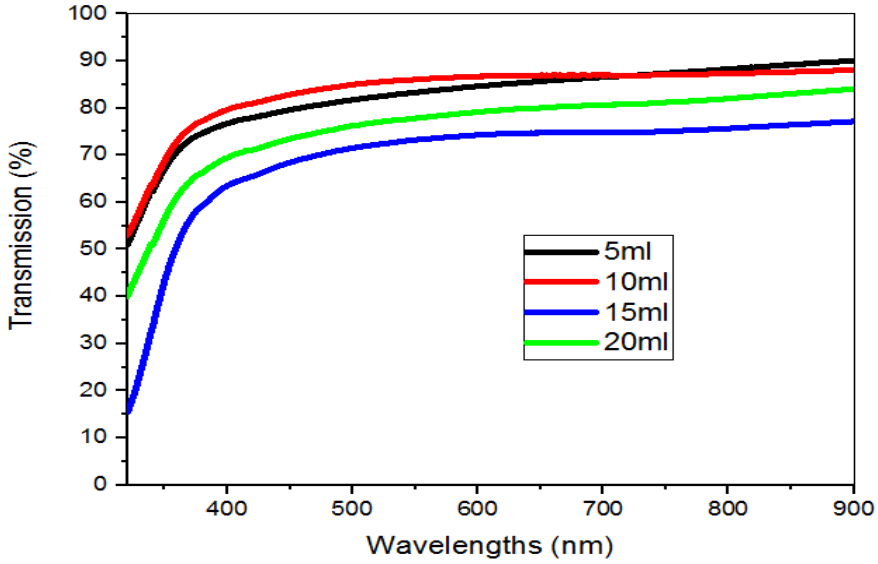

***Figure IV-9**:Transmission spectra of Al doped NiO thin films prepared at different NiO:Al volumes.*

Table IV-6:*Presents the average transmittance and Film thickness of Al doped NiO thin films prepared at different NiO:Al volumes.*

Samples	NiO: Al, 5 ml	NiO: Al,10 ml	NiO: Al,15ml	NiO: Al, 20 ml
Average Transmittance (%) 400-800 nm	66.4	75.1	53.9	63.0
Film thickness (nm)	142	168	178	213

IV-3-2 -1-Optical gap energy:

Figure IV-10 illustrates the plot of values$(Ahv)^2$a function of photon energyhv of Al doped NiO thin films deposited at different NiO: Al volumes, used for determining the optical band gap energy.

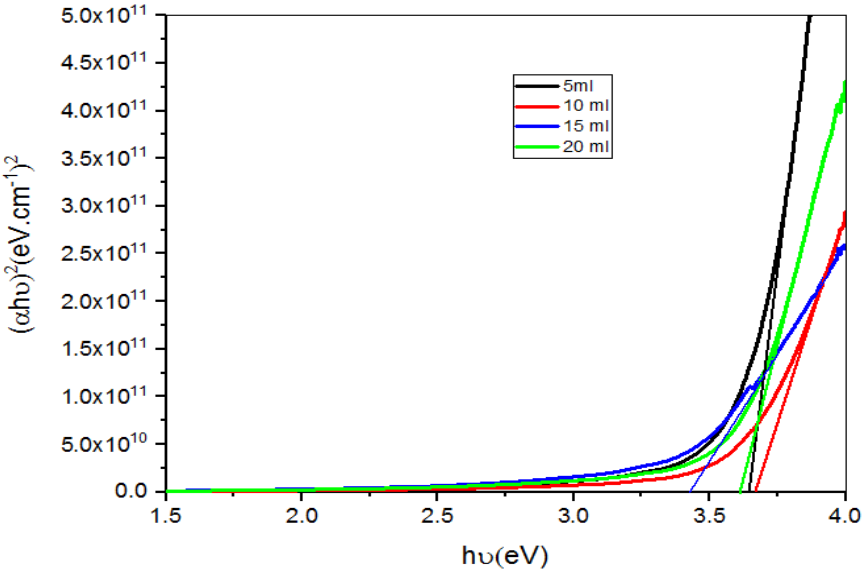

Figure IV-10*: The variation of values* $(Ahv)^2$ *as a function of photon energy hv of Al doped NiO thin films prepared.*

IV-3-2-2-Urbach energy:

Figure IV-11 depicts the variation of LnA as a function of the photon energy hv, where the Urbach energy was determined by taking the inverse of the slope of the curve.

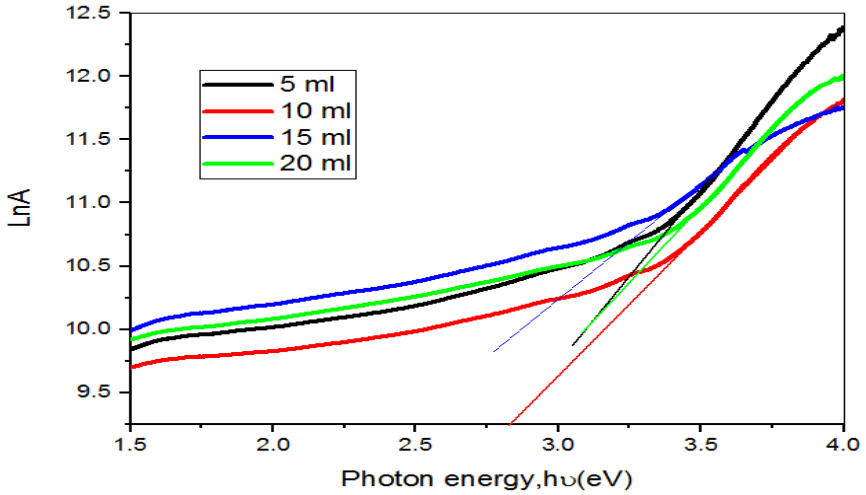

***Figure IV-11**: The variation of value sLnA as a function of photon energy hv of Al doped NiO thin films prepared.*

Figure IV-12 presents the variation of the band gap energy and the Urbach energy of Al-doped NiO thin films at different volumes**.** Generally, we notice that the two previous parameters are varied inversely according to volume. The film deposited with 15 ml shows the minimum optical energy and maximum Urbach energy, as indicated in **Table IV-7**.

***Table IV-7:** Shows the variation of optical band gap energy and Urbach energy of Al doped NiO thin films prepared at different NiO:Al volumes.*

Samples	**Optical gap energy E_g (eV)**	**Urbach energy E_u (eV)**
NiO :Al, 05 ml	3.66	0.632
NiO: Al, 10 ml	3.7	0.438
NiO: Al, 15 ml	3.5	0.644
NiO: Al, 20 ml	3.63	0.424

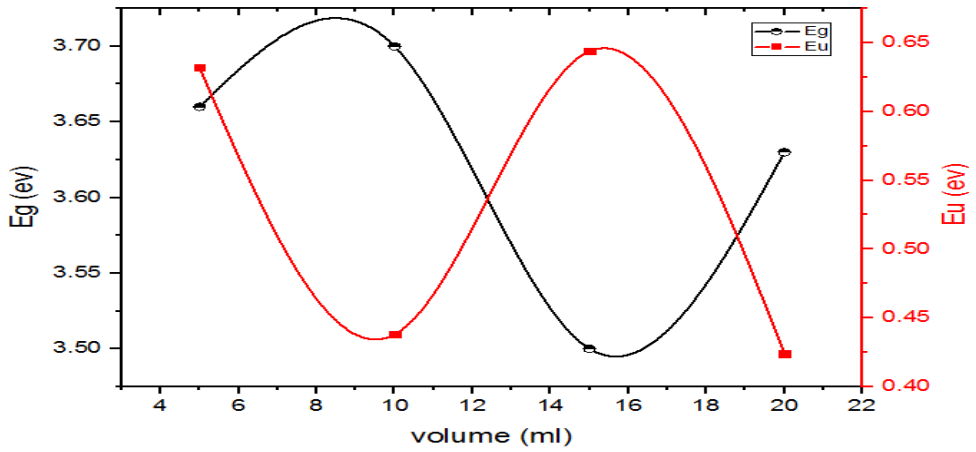

***Figure IV-12:** The variation of optical band gapE_g and Urbach energy $E_u$of Al doped NiO thin films as function of NiO: Al volumes.*

IV-3-3-Electrical properties:

The four-point probe technique was employed to determine the electrical conductivity of Al doped NiO thin films, it is based on the measured current, voltage and sheet resistance expressed by:

$$R_{sh} = \left(\frac{\pi}{ln\,2} * \frac{V}{I}\right) \qquad \text{(IV-7)}$$

$$\sigma = \frac{1}{\rho} = \frac{1}{dR_{sh}} \qquad \text{(IV-8)}$$

Where: R_{sh} is the sheet resistance; d is the film thickness; σ is the conductivity; ρ is the resistivity; $V$is the applied voltage =5mV and I is the measurement current (see **Table IV-8**).As the volume increases, it becomes evident that the electrical resistivity also increases, this increase can be attributed to a reduction in the number of electrons and their mobility. The Al doped NiO thin film with 15 ml has a minimum the electrical resistivity of $6.9x10^4\Omega$.cm (see **Table IV-8**).

Table IV-8: *Presents the variation of measured current and voltage and the sheet resistance of Al doped NiO thin films at different NiO: Al volumes.*

Samples	MeasuredCurrent$I$ (nA)	Measured voltage V(V)	Sheet resistance R_{sh} (Ω)	Electrical resistivity ρ (Ω.cm)
NiO: Al, 05 ml	0.5	5	$4.5\ x10^{10}$	$6.4\ x10^5$
NiO: Al, 10 ml	0.2		$1.1x10^{11}$	$1.8\ x10^6$
NiO: Al, 15 ml	5.8		$3.9\ x10^9$	$6.9\ x10^4$
NiO: Al, 20 ml	0.715		$3.2x10^{10}$	$6.8\ x10^5$

IV-4-Cu doped NiO thin films:

IV-4-1 structural properties:

Figure IV.14represents X-ray diffractions of Cu doped NiO films at different NiO: Cu volumes. We observe that all films are a single crystal and cubic structure (cfc) NaCl type[20].The XRD spectra obtained corresponded with the joint committee's powder diffraction system (JCPDS, No. 47-1049).

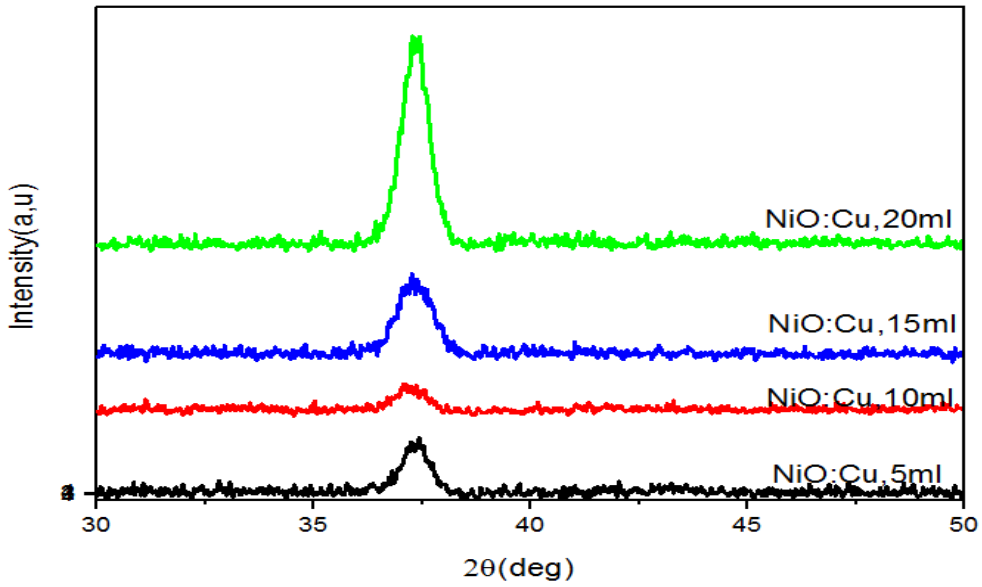

FigureIV-13: *X-ray diffraction spectra of Cu-doped NiO thin films at different NiO: Cu volumes.*

Table IV-9*:Shows the crystal structure of Cu doped NiO thin films as a function of NiO: Cu volume.*

Samples	Diffraction angle 2θ (°)	FWHM β (°)	Crystallite size D (nm)	Lattice parameter a (nm)	Main strain ε
NiO: Cu, 05 ml	37,34	0,67	12.51	0,4168	0,00383
NiO: Cu, 10 ml	37,27	0,96	8.81	0,4176	0,00545
NiO: Cu, 15 ml	37,14	0,67	12.50	0,4189	0,00386
NiO: Cu, 20 ml	37,43	0,53	15.91	0,4159	0,00301

Figure IV-14 indicates the variation of the main strain and the crystallite size of Cu doped NiO thin films prepared at different volumes. As evident from the data presented in **Table IV-9**, as the volume increases, the variation in crystallite size is inversely proportional to the main strain, this can be elucidated by the variation of FWHM.

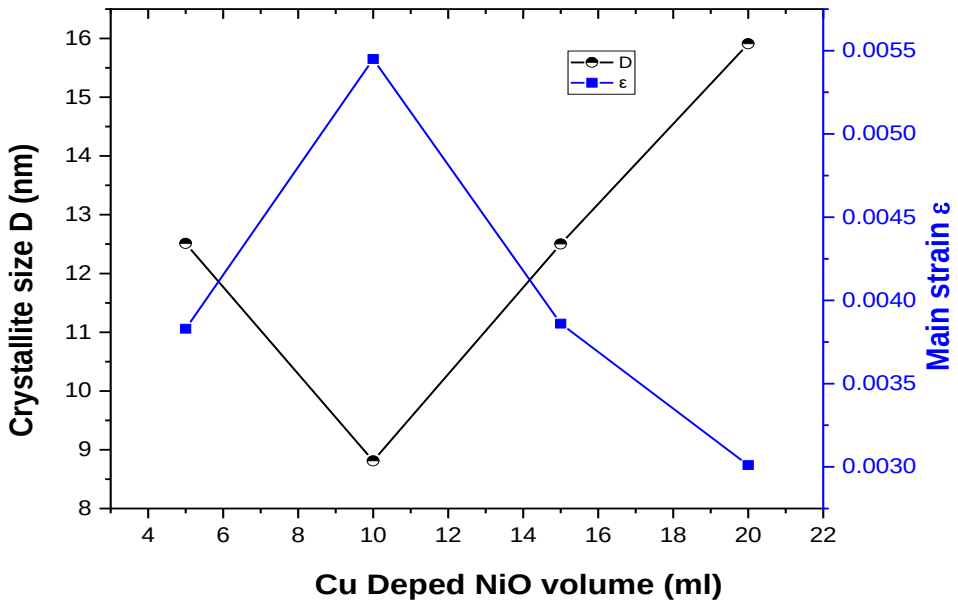

Figure IV-14: *The variation of crystallite size and main strain ε of Cu doped NiO thin films as function of NiO: Cu volumes.*

IV-4-2-Optical properties:

Figure IV-15shows the transmittance of Cu-doped NiO thin films at different NiO: Cu volumes. It is evident that the transmittance for all samples increases rapidly as the wavelength increases from 300 to 350 nm, and then slowly increases at higher wavelengths. We can observe height transmittance about 65% to 75% in the visible region.

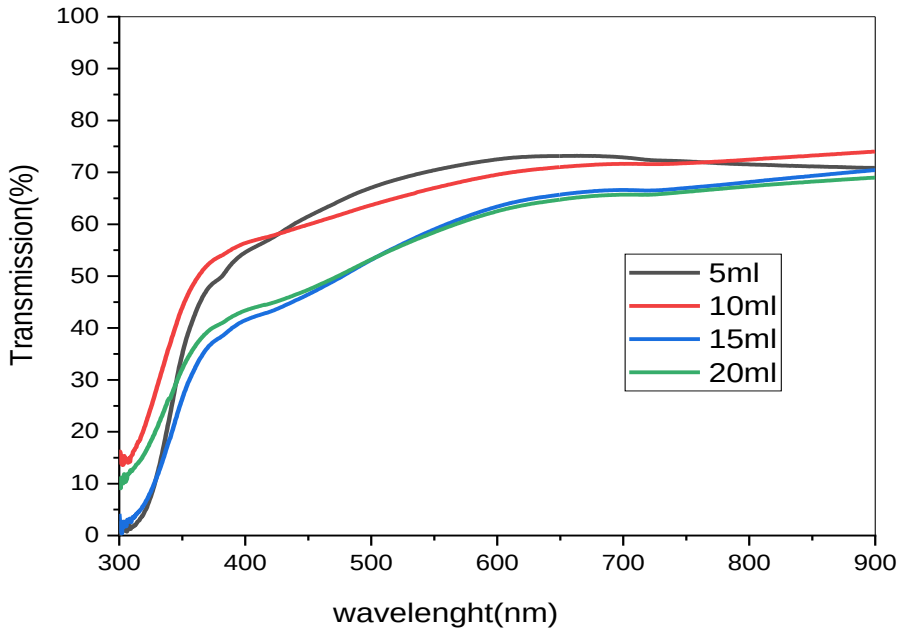

Figure IV-15: *The transmission spectra of Cu-doped NiO thin films as function of NiO: Cu volumes.*

Table IV-10:*Shows the average transmittance and Film thickness of Cu doped NiO thin films at different NiO:Cu volumes.*

Samples	NiO:Cu,5ml	NiO:Cu,10ml	NiO:Cu,15ml	NiO:Cu,20ml
Average Transmittance (%) 400-800 nm	69.1	67.4	59.5	59.2
Film thickness (nm)	113	164	191	192

IV-4-2 -1Optical gap energy:

Figure IV-16 shows the drawn of values $(Ahv)^2$ as a function of photon energy hv of Cu doped NiO thin films prepared at different NiO: Cu volumes, used for determining the optical band gap energy.

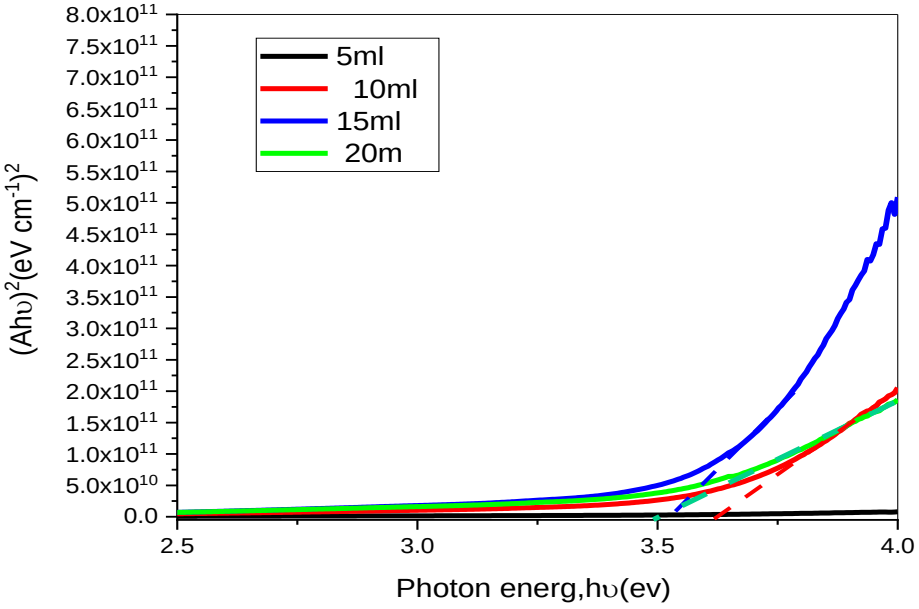

Figure IV-16*: The variation of values* $(Ahv)^2$ *as a function of photon energy hv of Cu doped NiO thin Films* at different NiO:Cu volumes.

IV-4-2-2-Urbach energy:

Figure IV-17illustrates the variation of LnA as a function of the photon energy hv of Cu doped NiO thin films, Where the Urbach energy was determined by taking the inverse of the slope of the curve.

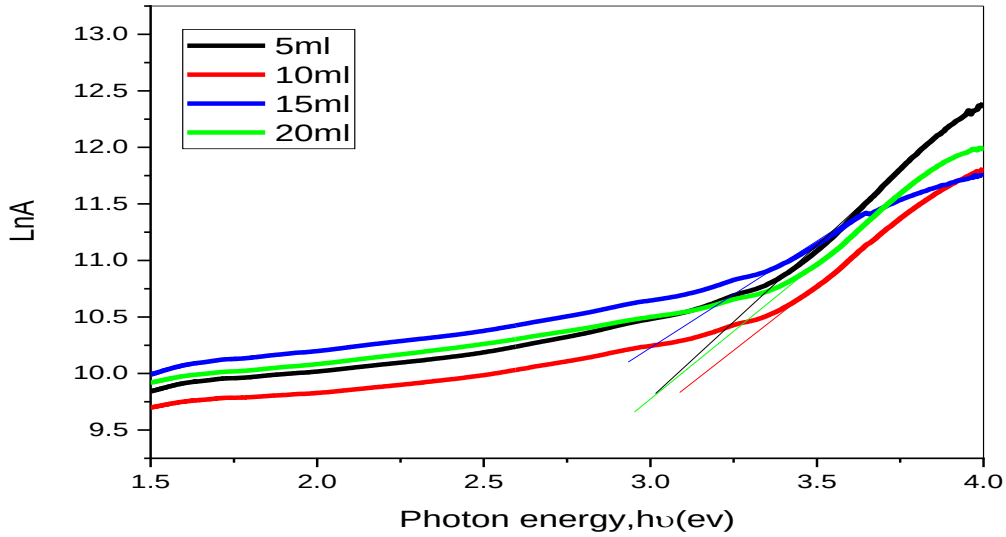

***Figure IV-17**: The variation of values LnA as a function of photon energy hν of Cu doped NiO thin films.*

FigureIV-18gives the variation of the band gap energy and the Urbach energy of Cu doped NiO thin films at different volumes. The variation of optical energy is inversely related to Urbach energy, as indicated in **Table IV-11**.

***Table IV-11**: Presents the variation of optical band gap energy and Urbach energy of Cu doped NiO thin films at different NiO:Cu volumes.*

Samples	Optical gap energy Eg (eV)	Urbach energy Eu (eV)
NiO: Cu, 05 ml	3.49	0.535
NiO: Cu, 10 ml	3.54	0.414
NiO: Cu, 15 ml	3.64	0.358
NiO: Cu, 20 ml	3.57	0.452

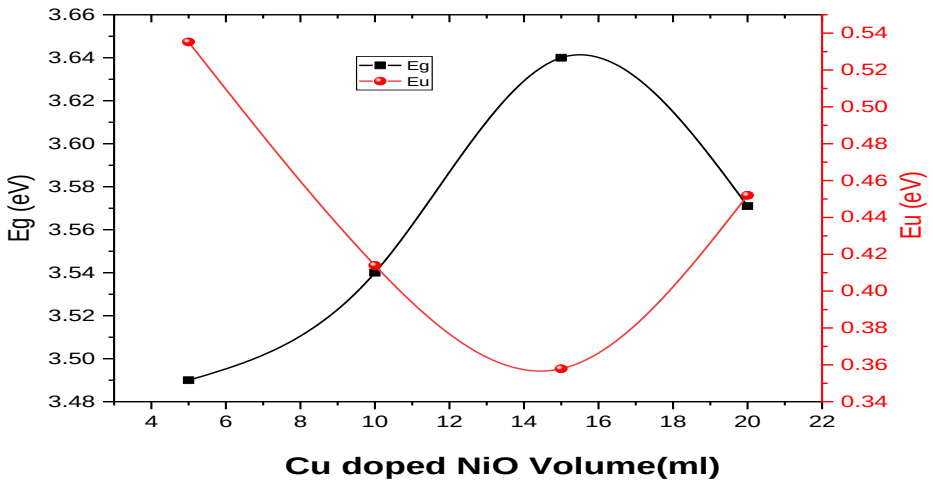

***Figure IV-18:** The variation of optical band gapE_g and Urbach energy $E_u$of Cu doped NiO thin films as function of NiO: Cu volume.*

IV-4-3-Electrical properties:

The four-point probe technique was employed to determine the electrical conductivity of Cu doped NiO thin films, it is based on the measured current, voltage and sheet resistance. The following equations were used in the calculation:

$$R_{sh} = \left(\frac{\pi}{ln\,2} * \frac{V}{I}\right) \qquad \text{(IV-9)}$$

$$\sigma = \frac{1}{\rho} = \frac{1}{dR_{sh}} \qquad \text{(IV-10)}$$

Where:$R_{sh}$is the electrical resistivity; d is the film thickness; σ is the conductivity; ρ is the resistivity; $V$is the applied voltage =5mV, and I is the measurement current (see **Table IV-12**). The Cu doped NiO thin film with 10 ml has a minimum the electrical resistivity of 46Ω.cm (see **Table IV-12**).

Table IV-12:*Presents the variation of measured current and voltage and the sheet resistance of Cu doped NiO thin films prepared.*

Samples	Measured Current I (nA)	Measured voltage V (mV)	Sheet resistance R_{sh} (Ω)	Electrical resistivity ρ (Ω.cm)
NiO: Cu, 05 ml	0.164	5	1.4×10^8	1.6×10^3
NiO: Cu, 10 ml	8.05		2.8×10^6	442.7
NiO: Cu, 15 ml	0.155		1.5×10^8	2.9×10^3
NiO: Cu, 20 ml	0.16		1.4×10^8	2.7×10^3

TableIV-13presents a comparative analysis of the structural, optical, and electrical characteristics of both F-doped NiO and Al-doped NiO and Cu -doped NiO thin films. As can be observed, we achieve a lower crystallite size, good transmittance, and favorable electrical properties.

TableIV-13:*The comparative study of the structural, optical and electrical properties of F doped NiO and Al-doped NiO and Cu -doped NiO thin films*

Thin films	Experimens	Film thickness (nm)	Crystallite size G (nm)	Transmittance (%)	Optical Band Gap Eg (eV)	Sheet resistance or electrical resistivity	Ref.
NiO NiO: 1F% NiO: 5F% NiO: 10F%	- Spray deposition - ST=400 °C - 0.1M - 0.3 mL/s		25 35 21.9 13.5	75 75+1 75+2 75+2	3.67 3.72 3,71 3.72	18 Ωcm 2 Ωcm 14 Ωcm 18 Ωcm	[21]
NiO NiO: 1Li% NiO: 2Li% NiO: 3Li% NiO: 4Li% NiO: 5Li%	- Spray deposition - ST= 500 °C -0.1M -13 mL	197 236 221 374 435 421	41 59 31 45 44 36	59 32 48 37 50 47	3.865 3.744 3.697 3.738 3.714 3.716	- $2.403x10^{9}\Omega$ $1.195x10^{7}\Omega$ $7.984x10^{6}\Omega$ $1.386x10^{7}\Omega$ $1.694x10^{7}\Omega$	[22]
NiO NiO: 1Cu% NiO: 2Cu% NiO: 3Cu% NiO: 4Cu% NiO: 5Cu%	- Spray deposition - ST= 410 °C -0.2 M	-	64 37 51 38 51 57	about 50	3.572 3.519 3.536 3.461 3.473 3.467	2712 Ωcm 589 Ωcm 490 Ωcm 1106 Ωcm 545 Ωcm 669 Ωcm	[23]
NiO, 10ml NiO:F, 5ml NiO:F, 10ml NiO:F, 15ml NiO:F, 20ml	- Spray deposition - ST=450 °C - 0.1M - F/Ni = 5%	160 110 112 134 140	18.51 12.47 10.94 14.45 19.21	53.6 83.9 85.6 73.8 78.0	3.71 3,54 3,52 3,61 3,51	$1.5x10^{5}\Omega.cm$ 231 Ω.cm $1.9x10^{3}\Omega.cm$ $3.8x10^{3}\Omega.cm$ $3.6x10^{3}\Omega.cm$	This Work
NiO:Al, 05ml NiO: Al,10ml NiO: Al, 15ml NiO: Al 20ml	Spray deposition - ST=450 °C - 0.1M -Al /Ni = 3%	142 168 178 213	12.42 14.24 15.09 13.43	66.4 75.1 53.9 63.0	3.66 3.7 3.5 3.63	$6.4x10^{5}\Omega.cm$ $1.8x10^{6}\Omega.cm$ $7x10^{4}\Omega.cm$ $6.8x10^{5}\Omega.cm$	This Work
NiO:Cu 05ml NiO:Cu,10ml NiO:Cu,15ml NiO:Cu,20ml	Spray deposition - ST=450 °C - 0.1M - Cu /Ni = 3%	113 164 191 192	12.51 8.81 12.50 15.90	69.1 67.4 59.5 59.2	3.49 3.54 3.64 3.57	$1.6 x10^{3}$ 442.7 $2.9 x10^{3}$ $2.7 x10^{3}$	This Work

IV-5-Conclusion:

Finally, the structural, optical and electrical properties of F doped NiO and Al doped NiO and Cu doped NiO thin films were investigated. The thin films of F(Al, Cu)doped NiO were deposited using the spray technique at substrate temperature of 450 °C with different NiO:F(Al, Cu) solution volumes of 5, 10, 15 and 20 ml. All the synthesized NiO thin films exhibit a

monocrystalline nature with a cubic structure, the (111) diffraction peak is the preferred orientation.

For F doped NiO thin films, the largest crystallite size is19.21 nm, was achieved with 20 ml. The optical properties indicate that all the prepared F-doped NiO thin films exhibit good transmittance, approximately 80%, in the visible region. The F-doped NiO thin films deposited using 20 ml show a minimum optical bandgap energy of 3.51 eV and the highest Urbach energy value of 0.689 eV. However, the thin film prepared with 5 ml exhibits a minimum electrical resistivity of 231 Ω·cm, making it suitable for gas sensing applications.

Al doped NiO thin films, the largest crystallite size, which is 15.09 nm, was achieved using a volume of 15 ml. The optical analysis reveals that all the Al -doped NiO thin films prepared exhibit well transparency, reaching 60% in the visible region. The Al-doped NiO thin films deposited using15 ml exhibit a minimum optical bandgap energy of 3.5 eV, with the highest Urbach energy value recorded at 0.644eV. The thin film, which was prepared using 15 ml, exhibits a minimum electrical resistivity of $6.9x10^4$ Ω.cm.

Cu doped NiO thin films, the maximum crystallite size is 15.91 nm obtained for 20 ml. All of the Cu-doped NiO thin films prepared demonstrate good transmittance, approximately 70% within the visible region. The Cu-doped NiO thin films prepared using 20 ml demonstrate a minimum optical bandgap energy of 3.49 eV, with the highest Urbach energy value recorded at 0.535 eV. The thin film deposited using 10 ml shows a minimum electrical resistivity of 442.7 Ω.cm.

References:

[1]Doğan, N., Bingölbali, A., & Arda, L. Preparation, structure and magnetic characterization of Ni doped ZnO nano-particles. *Journal of Magnetism and Magnetic Materials*, *373*, 226-230, 2015.

[2]Wang, J., Ju, Y., Huang, Y., Zheng, J., & Zheng, Z. Study of the influence of porous structure on the permeability of rock using Lattice Boltzmann method. *Procedia engineering*, *102*, 1835-1841, 2015.

[3]Shareef Ahmed .A, Structural optical and electrical properties of some metal oxide nano materials, PhDthesis, Aligarh Muslim University, 2013.

[4]Wang, S. H., Jian, S. R., Chen, G. J., Cheng, H. Z., &Juang, J. Y. Annealing-driven microstructural evolution and its effects on the surface and nanomechanical properties of Cu-doped NiO thin films. *Coatings*, *9*(2), 107, 2019.

[5]Aoun, Y., Marrakchi, M., Benramache, S., Benhaoua, B., Lakel, S., &Cheraf, A. Preparation and characterizations of monocrystalline Na doped NiO thin films. *Materials Research*, *21*, e20170681, 2018.

[6]Zaouche, C., Gahtar, A., Benramache, S., Derouiche, Y., Kharroubi, M., Belbel, A., ... &Dahbi, L. The determination of urbach energy and optical gap energy by many methods for Zn doped NiO thin films fabricant semiconductor by spray pyrolysis. *Digest Journal of Nanomaterials & Biostructures (DJNB)*, *17*(4), 2022.

[7]Panneerselvam, V., Chinnakutti, K. K., Thankaraj Salammal, S., Soman, A. K., Parasuraman, K., Vishwakarma, V., &Kanagasabai, V. Role of copper/vanadium on the optoelectronic properties of reactive RF magnetron sputtered NiO thin films. *Applied Nanoscience*, *8*, 1299-1312, 2018.

[8]Aswathy, N. R., Varghese, J., Nair, S. R., & Kumar, R. V. Structural, optical, and magnetic properties of Mn-doped NiO thin films prepared by sol-gel spin coating. *Materials Chemistry and Physics*, *282*, 125916, 2022.

[9]Raj, I. L. P., Valanarasu, S., Asuntha, A., Rimal Isaac, R. S., Shkir, M., Algarni, H., &AlFaify, S. Development of a highly sensitive UV sensor using Al, Ga, and In-doped NiO thin films via nebulizer spray pyrolysis method for photodetector applications. *Journal of Materials Science: Materials in Electronics*, *33*(15), 11753-11767, 2022.

[10]Chu, X., Leng, J., Liu, J., Shi, Z., Li, W., Zhuang, S., ... & Yin, J. Effect of annealing conditions on the structural, electrical and optical properties of Li-doped NiO thin films. *Journal of Materials Science: Materials in Electronics*, *27*, 6408-6412, 2016.

[11]Abdel-wahab, M. S., El Emam, H. K., & El Rouby, W. M. Sputtered Ag-doped NiO thin films: structural, optical, and electrocatalytic activity toward methanol oxidation. *Journal of Materials Science: Materials in Electronics*, *34*(22), 1637, 2023.

[12] Zhao, Y., Yan, J., Huang, Y., Lian, J., Qiu, J., Bao, J., ... & Chen, K. Interfacial self-assembly of monolayer Mg-doped NiO honeycomb structured thin film with enhanced performance for gas sensing. *Journal of Materials Science: Materials in Electronics, 29*, 11498-11508, 2018.

[13] Kate, R. S., Bulakhe, S. C., &Deokate, R. J. Co doping effect on structural and optical properties of nickel oxide (NiO) thin films via spray pyrolysis. *Optical and Quantum Electronics*, *51*(10), 319, 2019.

[14] Abdelhalium, H. H., Abdel-wahab, M. S., Tamm, M. T., & Tawfik, W. Z. Highly efficient ultraviolet photodetector based on molybdenum-doped nanostructured NiO/ITO thin film. *Applied Physics A*, *129*(6), 459, 2023.

[15] Wang, J., Yang, P., Wei, X., & Zhou, Z. Preparation of NiO two-dimensional grainy films and their high-performance gas sensors for ammonia detection. *Nanoscale research letters*, *10*, 1-6, 2015.

[16] Diha, A., Benramache, S., & Fellah, L. The crystalline structure, optical and conductivity properties of fluorine doped ZnO nanoparticles. *Journal of nano-and electronic physics*, (11, no. 3), 03002-1, 2019.

[17] Kumar, A., & Sahay, P. P. Lithium doping in spray-pyrolyzed NiO thin films: results on their microstructural, optical and electrochromic properties. *Applied Physics A*, *127*, 1-17, 2021.

[18] Gahtar, A., Benramache, S., Ammari, A., Boukhachem, A., &Ziouche, A. Effect of molar concentration on the physical properties of NiS thin film prepared by spray pyrolysis method for supercapacitors. *Inorganic and Nano-Metal Chemistry*, *52*(1), 112-121, 2022.

[19] Alver, U., Yaykaşlı, H., Kerli, S., &Tanrıverdi, A. Synthesis and characterization of boron-doped NiO thin films produced by spray pyrolysis. *International Journal of Minerals, Metallurgy, and Materials*, *20*, 1097-1101, 2013.

[20] Aydin, H., Mansour, S. A., Aydin, C., Al-Ghamdi, A. A., Al-Hartomy, O. A., El-Tantawy, F., &Yakuphanoglu, F. Optical properties of nanostructure boron doped NiO thin films. *Journal of sol-gel science and technology*, *64*, 728-733, 2012.

[21] Sasaki, S., Fujino, K., & Takéuchi, Y. X-ray determination of electron-density distributions in oxides, MgO, MnO, CoO, and NiO, and atomic scattering factors of their constituent atoms. *Proceedings of the Japan Academy, Series B*, *55*(2), 43-48, 1979.

[22] Kerli, S., &Alver, U. Effect of F-doping on structural, electrical, and optical properties of NiO thin films. *Crystallography Reports*, *59*, 1103-1106, 2014.

[23] Joseph, D. P., Saravanan, M., Muthuraaman, B., Renugambal, P., Sambasivam, S., Raja, S. P., &Venkateswaran, C. Spray deposition and characterization of nanostructured Li doped

NiO thin films for application in dye-sensitized solar cells. *Nanotechnology*, *19*(48), 485707, 2008.

[24] Aftab, M., Butt, M. Z., Ali, D., Bashir, F., & Khan, T. M. Optical and electrical properties of NiO and Cu-doped NiO thin films synthesized by spray pyrolysis. *Optical Materials*, *119*, 111369, 2021.

Chapter V

Synthesis of nanostructured of:

- ✓ F and Cu co-doped NiO
- ✓ Al and F co-doped NiO
- ✓ Cu and F co-doped NiO

V-1-Introduction:

In this work, we deposited F and Cu co-doped NiO and Al and F co-doped NiO and Cu and F co-doped NiO thin films at different concentrations on glass substrate employing spray pyrolysis technique, and we examined their structural properties, optical and electrical properties.

V-2-F and Cu co-doped NiO thin films:

F and Cu co-doped NiO thin films were prepared according the following Table V.1.

Table V.1 *illustrates the experimental conditions for the preparation of F and Cu co-doped NiO thin films.*

Sample	C(mol/l)	F(%)	Cu(%)	V(ml)	T(°C)
1	0.1	5	1	10	450
2			3		
3			5		

V-2-1 structural properties:

Figure V.1 depicts the XRD spectra of F and Cu co-doped NiO thin films prepared at various concentrations of Cu (1-3-5%).Our preliminary findings suggest that all the films exhibited a diffraction peak at $2\theta = 37$corresponding to the (111) plane of the NiO phase, which possesses a single crystal cubic structure(CFC) NaCl type[1].The XRD spectra obtained corresponded with the joint committee's powder diffraction system (JCPDS, No. 47-1049)[2].Spectra show decrease in the intensity of the (111) peak as the level of Cu doping increases.

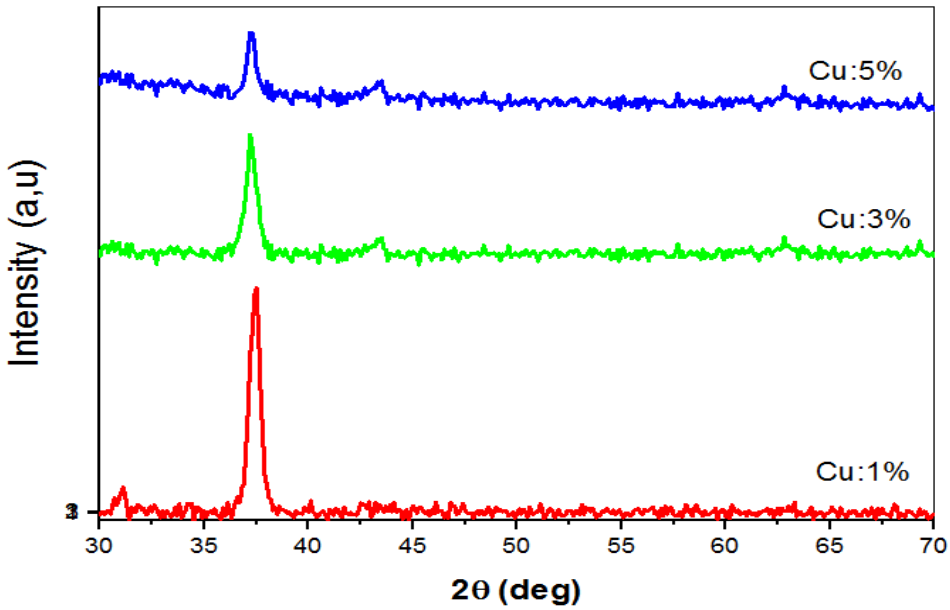

Figure V-1*: X-ray diffraction spectra of F and Cu co-doped NiO thin films at different concentrations of Cu.*

They are calculated the structural parameters of thin films of NiO, using the equation of the lattice constant of NiO (a) of cubic structure (cfc) [3], the size of crystallites (D) at peak (111) in the wavelength λ= (1.54056 Å) and the mean stress ε use the Scherrer relationship [4].The structural parameters of *F and Cu co-doped* NiO films are evaluated and given in **Table V.2.**

We note an increase in the lattice constant of the crystalline NiO film (**see Table** (**V.2**) below) the doping effect. This behavior could be explained by the variance in the ionic radii of Cu^{2+} (0.96 Å) and Ni^{2+} (0.69 Å) when they substitute into the NiO lattice, leading to the expansion of the NiO crystal, results are reported by other researchers [5, 6].

Table V-2*Shows the crystal structure of F and Cu co-doped NiO thin films as a function of concentration of Cu.*

Samples	**Diffraction angle 2Θ (°)**	**FWHM β (°)**	**Crystallite size D (nm)**	**Lattice parameter a (nm)**	**Main strain ε**
Cu(1%),	37.43	0.47	17.84	4.1581	0.00269
Cu(3%),	37.25	0.49	17.11	4.1776	0.00279
Cu(5%),	37.22	0.59	14.44	4.1808	0.00336

Figure V-2 illustrates the variation in crystallite size and main strain of F and Cu co-doped NiO thin films at various concentrations of Cu. As observed, with increasing volumes,

there is an inverse relationship between the variation in crystallite size and main strain, as indicated in **Table V-2**. The maximum crystallite size of 17.84 nm is achieved for Cu (1%), corresponding to the minimum value of main strain, as shown in **Table V-2**.

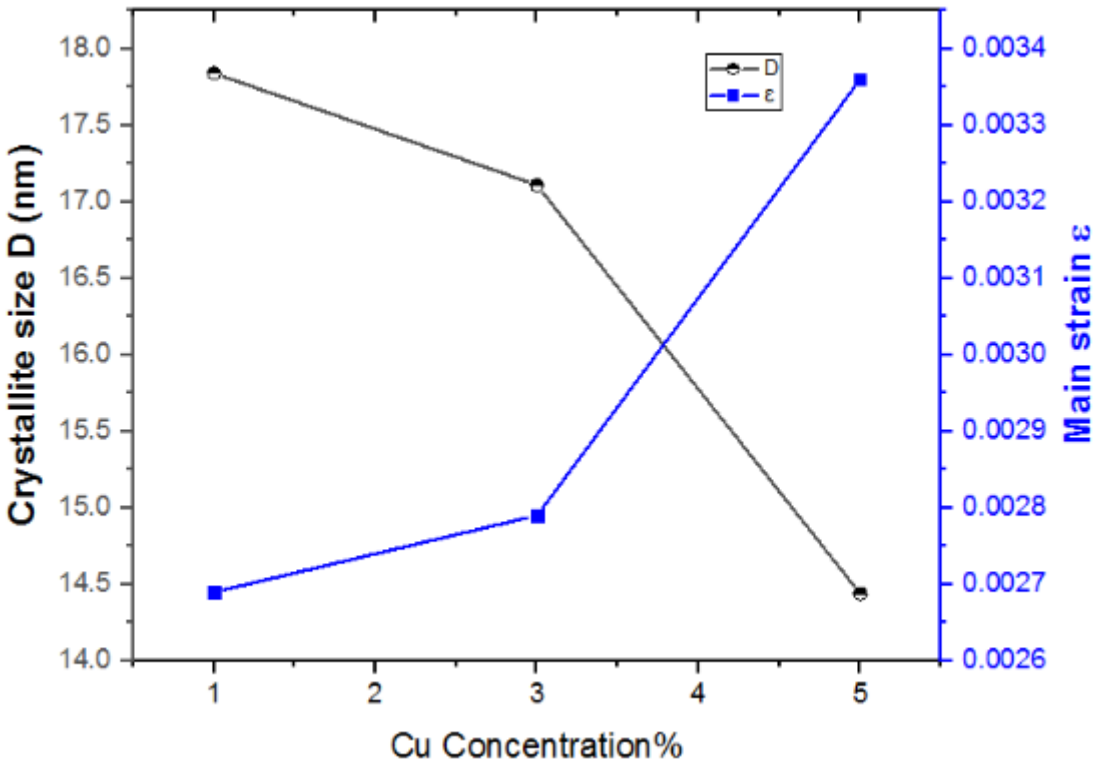

Figure V-2: *The crystallite size D and main strain ε of F and Cu co-doped NiO thin films at different concentration of Cu.*

V-2-2-Optical properties:

V-2-2-1Transmittance spectra:

Figure V.3 illustrates the transmittance for F and Cu co-doped NiO thin films at different doping concentrations in the range wavelength of 300 to 900 nm. From this figure, it can be observed that all the prepared films exhibit good transparency in the visible region, with an average transmission value of about 80%.Strong absorption has been noted in the range of 300-360nm, indicating the fundamental absorption edge of NiO, which arises from the transition between its valence band and conduction band. The results depicted in **Figure V.3** indicate that the NiO thin films generated are suitable for transparent electronics owing to their minimal absorbance in the visible region[7, 8].

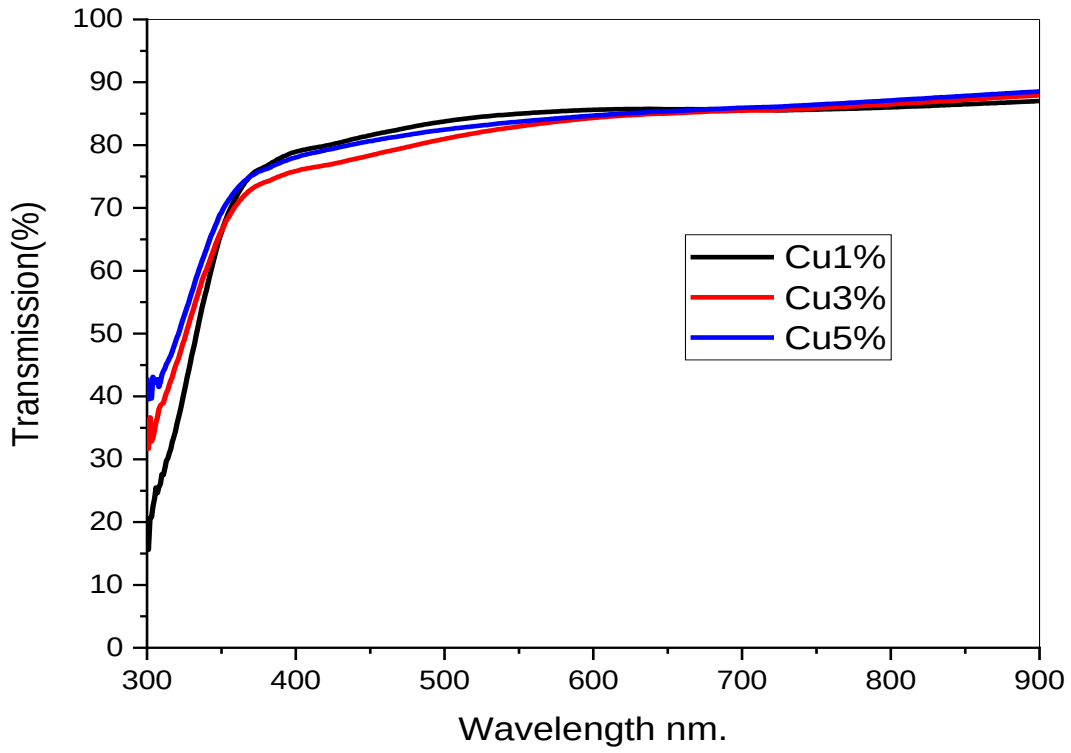

Figure V.3: *Transmittance spectra of F and Cu co-doped NiO thin films at different doping concentrations.*

Table V.3*displays the average transmittance and Film thickness of F and Cu co-doped NiO thin films as a function of doping concentrations.*

Samples	Average Transmittance (%) 400-800 nm	Film thickness (nm)
NiO: 1% Cu	84.4	115
NiO: 3% Cu	83	117
NiO: 5% Cu	84	183

V-2-2-2-Optical Gap energy:

The optical band gap Eg, was determined by extrapolating the linear segment of the plot $(Ah\upsilon)^2$ as a function of ($h\upsilon$) to A = 0 [4], as illustrated in **Figure V.4** using the following equation[9,10]:

$$A=\alpha d=-\ln T \qquad \text{(V.1)}$$

$$(Ah\upsilon)^2=C(h\upsilon-E_g) \qquad \text{(V.2)}$$

Where: A is the absorbance, d represents the thickness of the film, T denotes the transmission of thin films, α is the absorption coefficient values, C stands for a constant, $h\upsilon$ represents the photon energy, and E_g the band gap energy of the semiconductor.

The optical gap (E_g) by identifying the point where the linear segment intersects the hυ axis, as illustrated in **Figure V.4**,by utilizing this approach, the band gap values of the thin films are range from 3.59 and 3.7eV, demonstrating favorable concurrence with NiO's E_g value (ranging from 3.6 to 4 eV) [11].

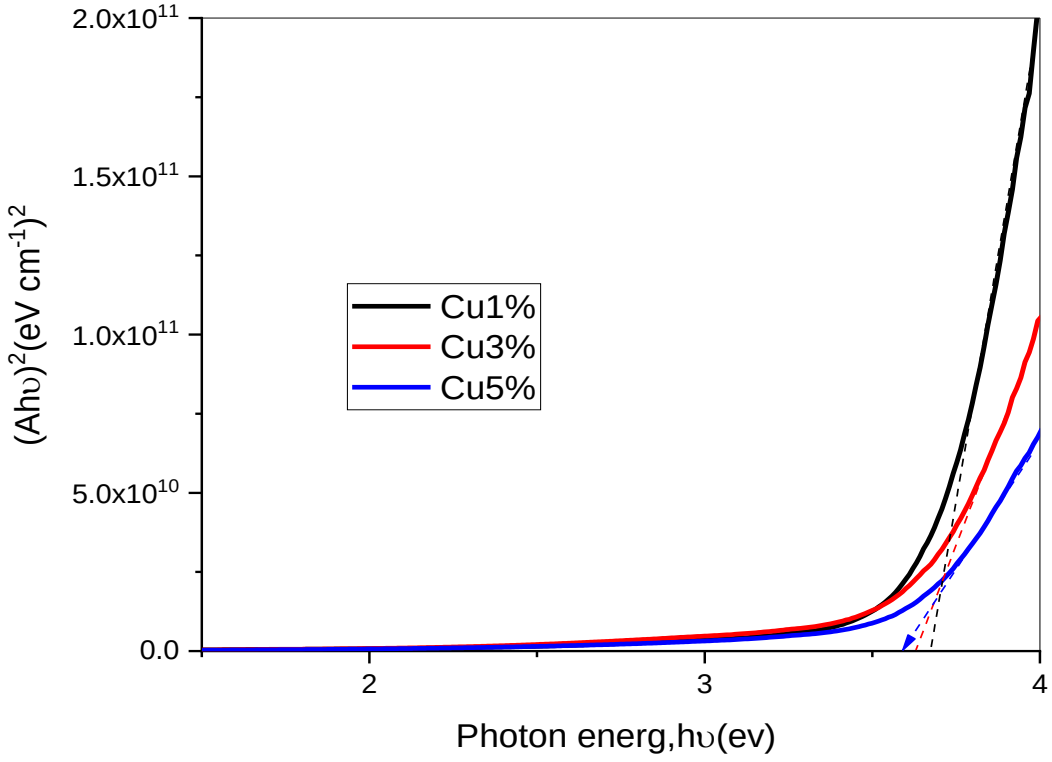

Figure V.4: *The variation of $(Ahv)^2$as a function of hυ for F and Cu co-doped NiO thin films at different doping concentrations.*

V-2-2-3-Urbach energy (The Disorder):

The Urbach energy (E_u) is indicative of the disorder present in the film network, as indicated by the following expression[12]:

$$A = A_0 exp\left(\frac{h\vartheta}{E_u}\right) \qquad (V.3)$$

Where: A_0 constant, hυ is the photon energy, and E_u is the Urbach energy.

Figure (V.5) depicts the plot of LnA as a function of photon energy hυ using to determine the Urbach energy. These curves have been acquired for F and Cu co-doped NiO thin films at different doping concentrations.

From the curve, Urbach energy values(Eu) increase by increasing in doping concentrations, with the lowest value of E_u= 395 meV(see ***TableV.4***).

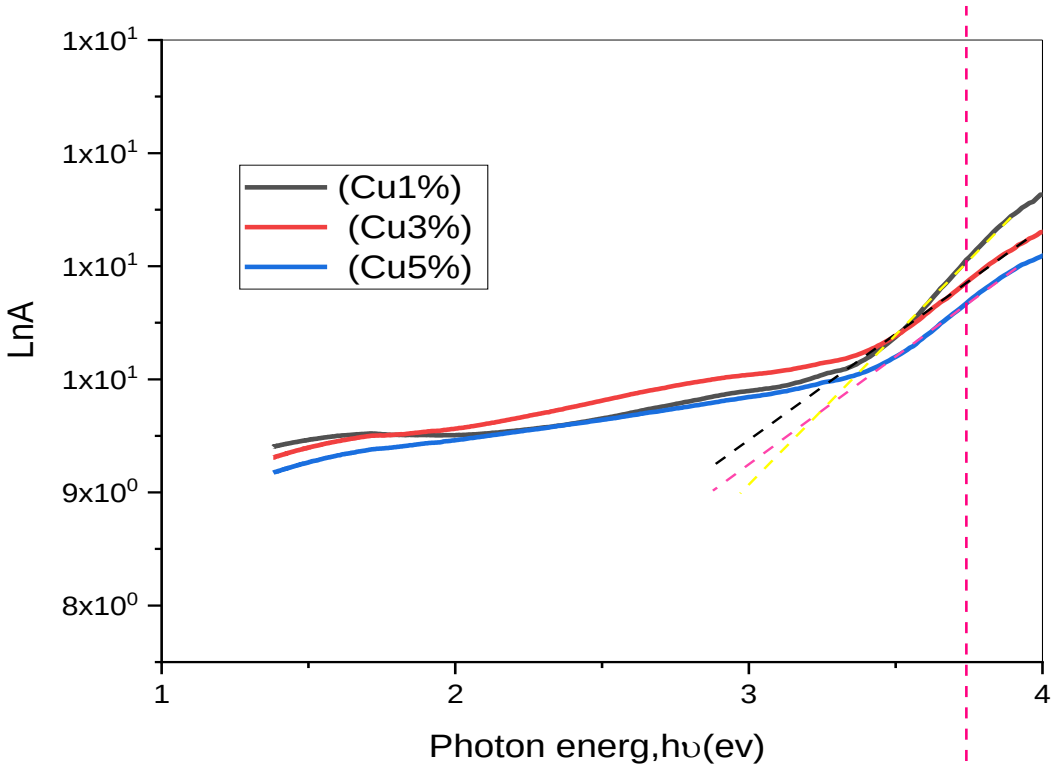

Figure V.5: *Variations of LnA as a function of* hυ *of F and Cu co-doped NiO thin films at different doping concentrations.*

Figure V.6 presents the variation of the band gap energy and the Urbach energy of F and Cu co-doped NiO thin films at different doping concentrations. As observed, with increasing doping concentrations, there is an inverse relationship between the variation of the optical energy and the Urbach energy, as indicated in **Table V.4.** the decreases in the optical band gap energy can be attributed to the increase in electrical conductivity of NiO thin films with F and Cu co doped.

TableV.4*Shows the variation of optical band gap energy and Urbach energy of F and Cu co-doped NiO thin films at different doping concentrations.*

Samples	Optical gap energy E_g (eV)	Urbach energy E_u (eV)
NiO: 1% Cu	3,7	0.395
NiO: 3% Cu	3,67	0.518
NiO: 5% Cu	3,59	0.533

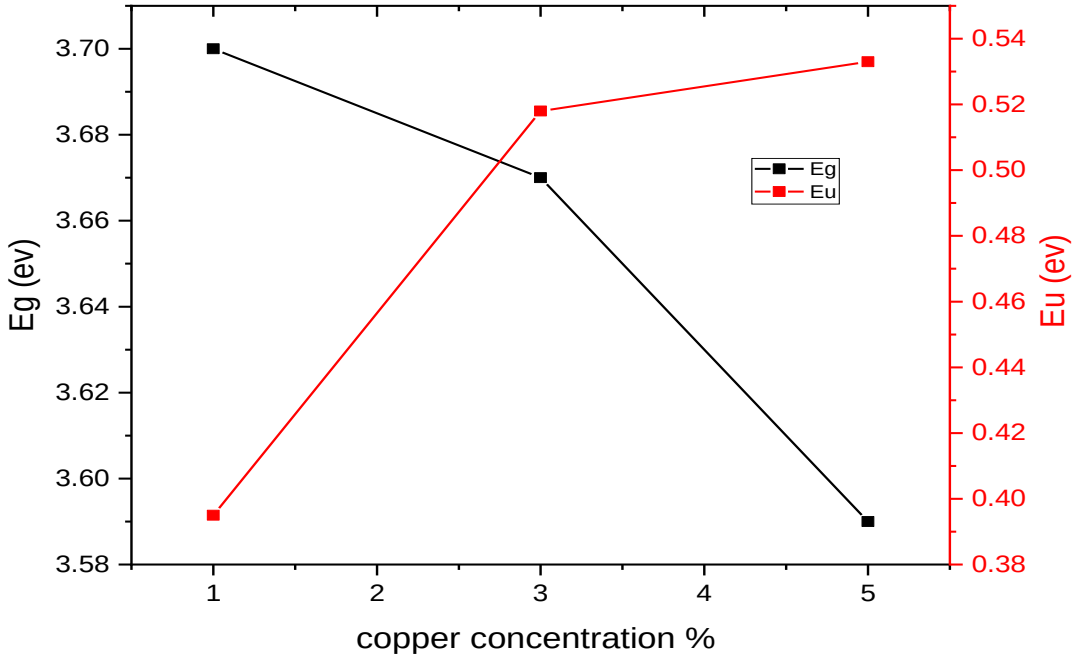

***Figure V.6**: The variation of the band gap energy and the Urbach energy of F and Cu co-doped NiO thin films at different doping concentrations.*

V-2-3-Electrical properties:

The electrical conductivity of F and Cu co-doped NiO thin films was determined by four-point probe technique, the resistivity is calculated in the following relationship:

$$\rho = dR_s \qquad \text{(V.4)}$$

$$\sigma = \frac{1}{\rho} = \frac{1}{dR_{sh}} \qquad \text{(V.5)}$$

Where: ρ is the resistivity, d is the film thickness, R_{sh} is the electrical resistivity, σ is the conductivity.

Table V.5presents the variation of the sheet resistance of F and Cu co-doped NiO thin films at different doping concentrations. As can be seen, as the concentration increases, the electrical resistivity decrease (see **Table V.5**),this decrease can be which may be due to the substitution of Ni^{+2} by Cu^{+2}, creating more acceptor levels. Therefore, the greater electrical conduction as the Cu doping level increases[13,14].Where, the F and Cu co-doped NiO thin film with 5%Cu has a minimum the electrical resistivity of 19.7 Ω.cm (see **Table V.5**).

Table V.5:*Shows the variation of the sheet resistance* and electrical resistivity *of F and Cu co-doped NiO thin films at different doping concentrations.*

Samples	Sheet resistance R_{sh} (Ω)	Electrical resistivity ρ (Ω.cm)
NiO: 1% Cu	208 x10^6	2.4 x 10^3
NiO: 3% Cu	174 x10^6	2 x 10^3
NiO: 5% Cu	1.08x10^6	19.7

V-3-Al and F co-doped NiO thin films:

Al and F co-doped NiO thin films were prepared according the following Table V.6.

TableV.6 *Shows the experimental conditions of prepared of Al and F co-doped NiO thin films.*

Sample	C(mol/l)	Al (%)	F (%)	V(ml)	T(°C)
1	0.1	3	1	10	450
2			3		
3			5		

V-3-1-Optical properties:

V-3-1-1-Transmittance spectra:

The optical transmission spectra of Al and F co-doped NiO thin films at different doping concentrations prepared by spray pyrolysis technique, in the wavelength range between 300 and 900 nm, are depicted in **Figure V.7**.Wecanobservethatthe samples exhibit good transmittance (T %), where the average transmission in the visible range about 80% .

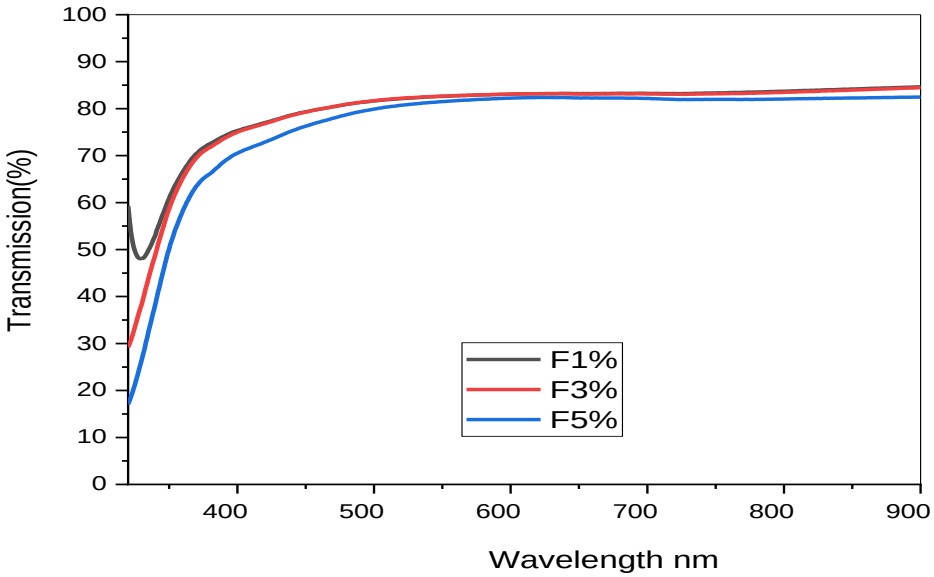

Figure V.7:*Transmittanc spectra of Al and F co-doped NiO thin films at different doping concentrations*

Table V. 7*:Shows the average transmittance and Film thickness of Al and F co-doped NiO thin films as a function of doping concentrations.*

Samples	Average Transmittance (%) 400-800 nm	Film thickness (nm)
NiO: 1%F	82	122
NiO: 3%F	81.9	123
NiO: 5%F	80.3	129

V-3-1-2- Optical Gap energy:

The optical band gap energy (E_g) of the films can be determined from the transmission spectra by applying the Tauc law equation[15].For directly allowed transitions, the optical band can be derived from plotting $(\alpha h\upsilon)^2$ as a function of hυ, and then extrapolating the linear portion of the graph with the energy axis, as shown in **Figure V.8**.The E_g values obtained are listed in **Table V.8**. As evident from the table, the optical band gap of NiO thin films varies between 3.43 and 3.66 eV as the doping concentration changes from 1 to 5%. Variations in the optical gap energy are closely tied to the existence of energy levels within the material's band gap, indicating potential alterations in its electronic configuration.

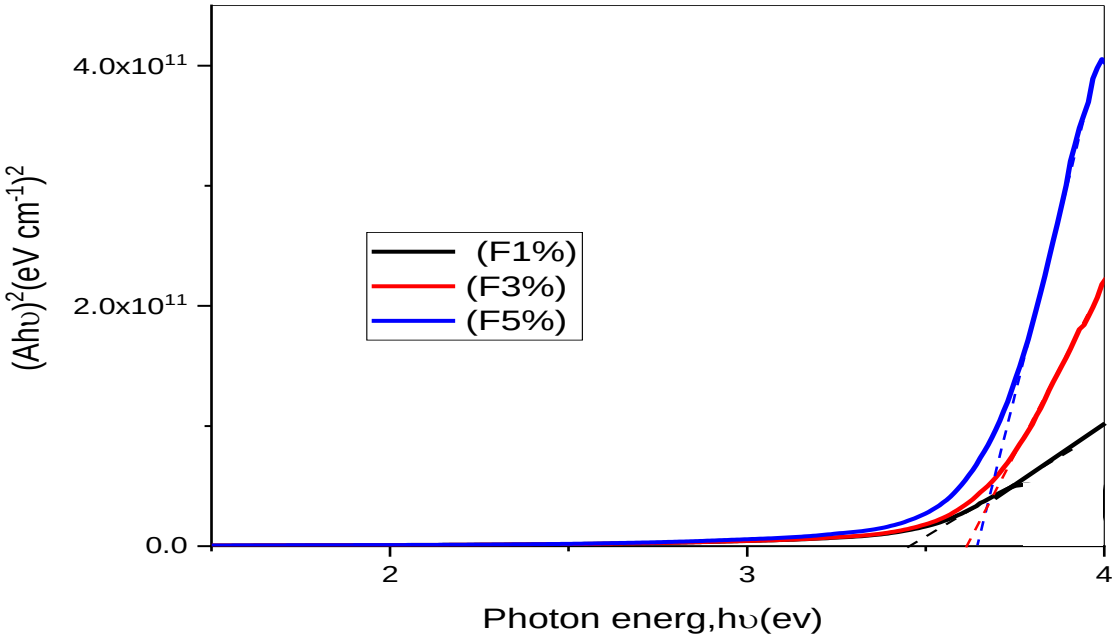

Figure V.8:*The variation of $(Ahv)^2$ as a function of hv for Al and F co-doped thin films at different doping concentrations.*

V-3-1-3-The Disorder (Urbach energy):

We used the relationship (V.3) to find Urbach energy values. The **Figure V.9** illustrates LnA as a function of photon energy hυ to determine the Urbach energy, its values are presented in the **Table V.8**

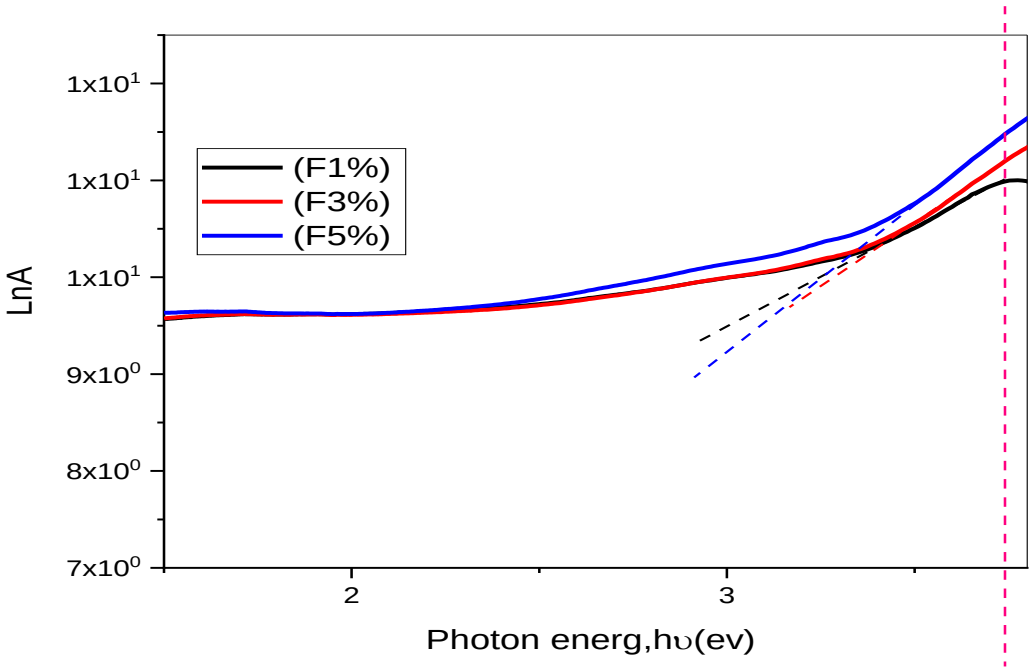

Figure V.9:*The variation of LnA as a function of hυ for Al and F co-doped thin films at different doping concentrations.*

Figure V.10 shows the variation of the band gap energy and the Urbach energy of Al and F co-doped thin films at different doping concentrations. From this figure we observe, as concentrations the increases, the variation of the optical energy is inversely with the Urbach energy (see **TableV.8**) the increases in the optical band gap energy can be attributed to the decrease in electrical conductivity of NiO thin films with Al and F co doped.

Table V.8*: Displays the variation in optical band gap energy and Urbach energy of Al and F co-doped NiO thin films across different doping concentrations.*

Samples	Optical gap energy E_g (eV)	Urbach energy E_U (eV)
NiO:1%F	3.43	0.52
NiO:3%F	3.6	0.392
NiO:5%F	3.66	0.344

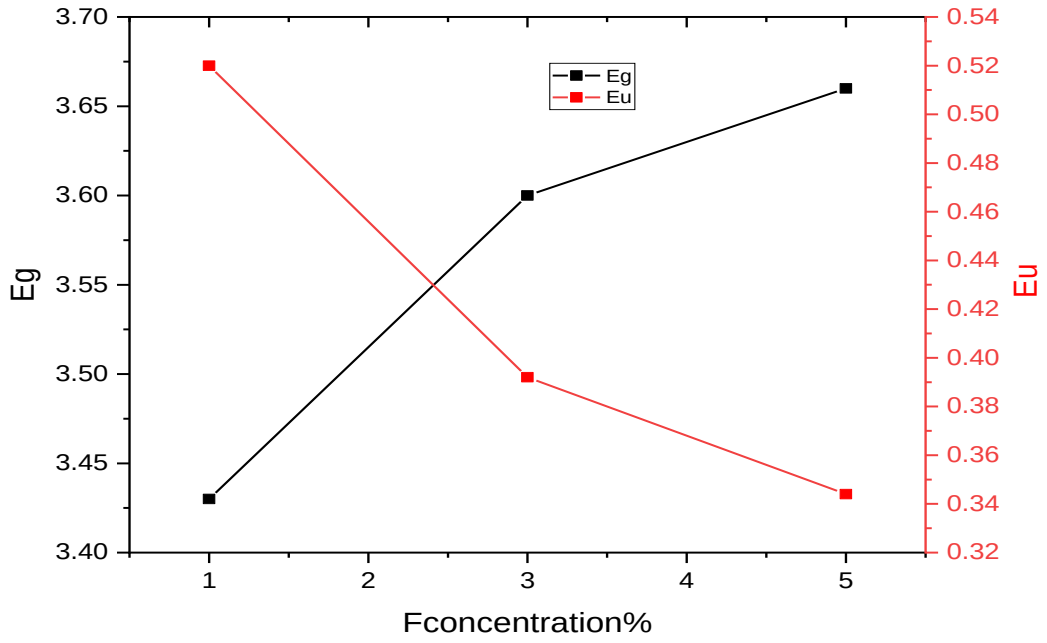

FigureV.10*: the variation of the band gap energy and the Urbach energy ofAl and F co-doped thin films at different doping concentrations.*

V-3-2-Electrical properties:

We use four- point probe technique for to determine the electrical conductivity of Al and F co-doped thin films at different doping concentrations, using the relationship(V.4) and(V.5) to calculate electrical resistivity of these thin films.

Table V-9 *Shows the variation of sheet resistance and Electrical resistivity of Al and F co-doped thin films at different doping concentrations.*

Samples	Sheet resistance R_{sh} (Ω)	Electrical resistivity ρ (Ω.cm)
NiO: 1F%	-	-
NiO: 3F%	-	-
NiO: 5F%	1.84 x10^{8}	2.37 x10^{3}

V-4-Cu and F co-doped NiO thin films:

Table V-10 *presents the experimental conditions of prepared of Cu and F co-doped NiO thin films.*

Sample	C(mol/l)	Cu(%)	F (%)	V(ml)	T(°C)
1	0.1	3	1	10	450
2			3		
3			5		

V-4-1-Optical properties:

V-4-1-1-Transmittance spectra:

Figure V.11 displays the optical transmittance spectra of Cu and F co-doped NiO thin films at different doping concentrations, which were sprayed, across the wavelength range of 300 to 900 nm. From this graph, the transmission of all samples clearly increases in wavelength range 320 to 390 nm, it increases gradually at higher wavelengths, and the optical transmittance of these films decreases as the concentration increases. The spectra exhibit high transmittance, ranging from approximately 67% to 84%, in the visible region.

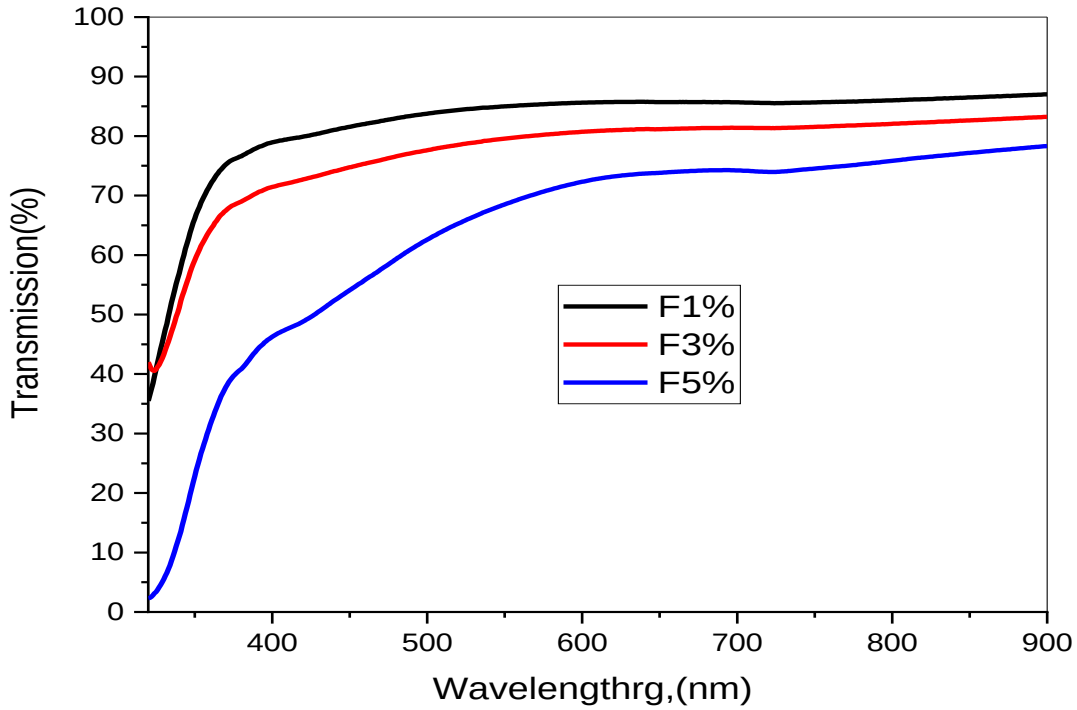

FigureV.11*:Optical transmittance spectra of Cu and F co-doped NiO thin films at different doping concentrations.*

Table V.11*:* presents *the average transmittance and Film thickness of Cu and F co-doped NiO thin films as a function of doping concentrations.*

Samples	Average Transmittance (%) 400-800 nm	Film thickness (nm)
NiO: 1F%	84.4	115
NiO: 3F%	79.2	130
NiO: 5F%	67.6	163

V-4-1-2-Optical Gap energy:

The optical band gap E_g was determined by extending the linear segment of the plot $(Ah\upsilon)^2$

as a function of (hυ) to A = 0, refer to **Figure V.12** and using the equation(V.1)and(V.2).

Figure V.12 illustrates the variation of $(Ah\upsilon)^2$ as a function of hυ for Cu and F co-doped thin films at various doping concentrations. The E_g values obtained of Cu and F co-doped thin films are listed in **Table V.12.**As can be seen, as the concentration increases, the E_g value decreases(see **Table V.12**),this is can be explained by the increase in electrical conductivity.

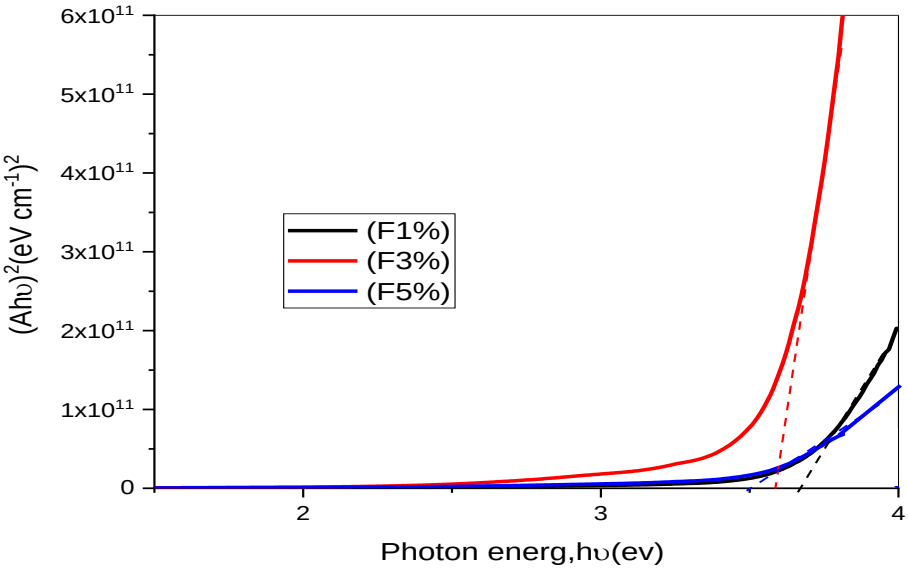

FigureV.12:*The variation of $(Ah\upsilon)^2$ as a function of hυ for Cu and F co-doped thin films at different doping concentrations.*

V-4-1-3-Urbach energy:

Figure V.13 displays the variation of *LnA* as a function of photon energy *hυ*, where the Urbach energy was derived from the inverse of the slope of the curve. The E_u values obtained are listed in **Table V.12**.

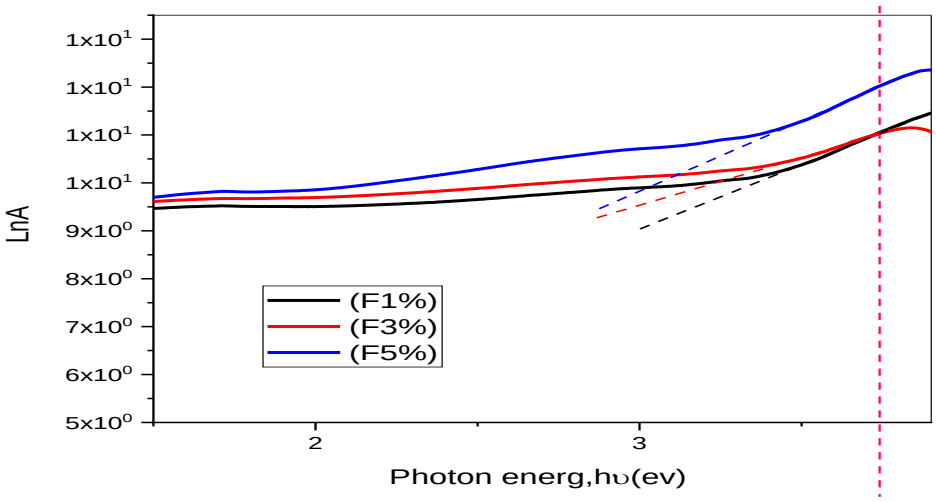

Figure V.13:*The variation of LnA as a function of hυ for Cu and F co-doped thin films at different doping concentrations.*

Figure V.14 shows the variation of the band gap energy and the Urbach energy of Cu and F co-doped thin films at different doping concentrations. From this figure we observe, as the concentrations increases, the variation of optical energy shows an inverse correlation with the Urbach energy (see **Table V.12**) they can be explained by the enhancement the electrical properties of NiO thin films.

TableV.12 *Shows the variation of optical band gap energy and Urbach energy of Cu and F co-doped NiO thin films at different doping concentrations.*

Samples	Optical gap energy E_g (eV)	Urbach energy E_U (eV)
NiO:1%F	3.69	0.346
NiO:3%F	3.63	0.381
NiO:5%F	3.5	0.5

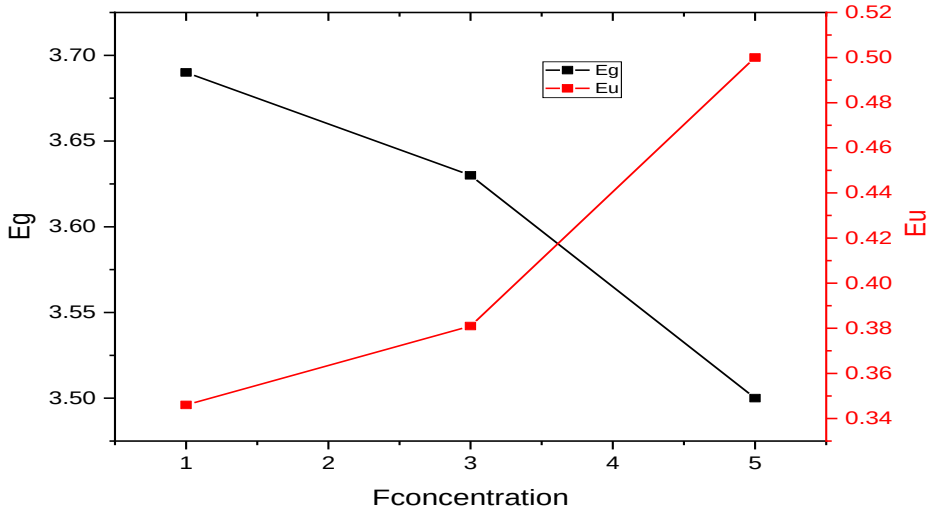

Figure V.14*: The variation of the band gap energy and the Urbach energy of Cu and F co-doped thin films at different doping concentrations.*

V-4-2-Electrical properties:

We used the same previous technique: four- point probe technique to determine the electrical conductivity of the prepared Cu and F co-doped thin films at different doping concentrations, using the equation(V.4)and(V.5),and the results were as shown in the **TableV.13.** Where, the Cu and F co-doped NiO thin film with F5% exhibits a minimum electrical resistivity of146.7 Ω.cm (see **Table V.13**).

Table V-13:*Shows the variation of sheet resistance and Electrical resistivity of Cu and F co-doped thin films at different doping concentrations.*

Samples	R_{sh} (Ω)	ρ (Ω.cm)
NiO: 1%F	1.74 x10^8	2.001 x10^3
NiO: 3%F	1.64 x10^8	2.132 x10^3
NiO: 5%F	9 x10^6	146.7

V-5-Conclusion:

In this chapter, we analyzed the properties of F and Cu co-doped NiO and Al and F co-doped NiO and Cu and F co-doped NiO thin films thin films, which were doped at various levels (1%, 3%, and 5%). The thin films were deposited on glass substrate by spray technique at a substrate temperature of 450 ° C.

F and Cu co-doped NiO thin films

- The maximum crystallite size is 17.84 nm obtained for 1%Cu and 5%F.
- All the F and Cu co-doped NiO thin films prepared exhibit good transmittance, approximately 80%in the visible region.
- The F and Cu co-doped NiO thin films deposited with 5% Cu and 5% F exhibit a minimum optical gap energy of 3.59 eV, with the biggest value of Urbach energy is 0.533 eV.
- The thin film prepared with 5%Cu and 5%Fexhibits a minimum electrical resistivity of 19.7 Ω.cm.

Al and F co-doped NiO thin films

- We can observe that all samples have a good transmittance (T %), where the average transmission in the visible range about 80%.
- The Al and F co-doped NiO thin films deposited with 3%Al and 1% F exhibit lowest optical gap energy of 3.43 eV, with the maximum Urbach energy value recorded at 0. 52eV.

Cu and F co-doped NiO thin films

- All of the Cu and F co-doped NiO thin films have a good transmittance, was varied from 67 to 84 % within the visible region.
- The Cu and F co-doped NiO thin films prepared with 5%F and 3%Cu exhibit a minimum optical gap energy of 3.5 eV, with the highest value of Urbach energy is 0.5 meV.
- The Cu and F co-doped NiO thin films prepared with 5%F and 3%Cu exhibits a minimum electrical resistivity of 146.7 Ω.cm.

References

[1]Sasaki, S., Fujino, K., &Takéuchi, Y. X-ray determination of electron-density distributions in oxides, MgO, MnO, CoO, and NiO, and atomic scattering factors of their constituent atoms. *Proceedings of the Japan Academy, Series B*, *55*(2), 43-48, 1979.

[2]Wang, J., Yang, P., Wei, X., & Zhou, Z. Preparation of NiO two-dimensional grainy films and their high-performance gas sensors for ammonia detection. *Nanoscale research letters*, *10*, 1-6, 2015.

[3]Chen, H. L., Lu, Y. M., & Hwang, W. S. Effect of film thickness on structural and electrical properties of sputter-deposited nickel oxide films. *Materials transactions*, *46*(4), 872-879, 2005.

[4]Cullity .B, Elements of XRD, USA Edison-Wesley P Inc,1978.

[5]Yang, M., Shi, Z., Feng, J., Pu, H., Li, G., Zhou, J., & Zhang, Q. Copper doped nickel oxide transparent p-type conductive thin films deposited by pulsed plasma deposition. *Thin Solid Films*, *519*(10), 3021-3025, 2011.

[6]Moghe, S., Acharya, A. D., Panda, R., Shrivastava, S. B., Gangrade, M., Shripathi, T., & Ganesan, V. Effect of copper doping on the change in the optical absorption behaviour in NiO thin films. *Renewable Energy*, *46*, 43-48, 2012.

[7]Liu, Z., Li, W., Topa, S., Xu, X., Zeng, X., Zhao, Z., ... & He, H. Fine tuning of fluorene-based dye structures for high-efficiency p-type dye-sensitized solar cells. *ACS Applied Materials & Interfaces*, *6*(13), 10614-10622, 2014.

[8]Lamastra, F. R., Nanni, F., Menchini, F., Nunziante, P., &Grilli, M. L. Transparent nanostructured electrodes: Electrospun NiO nanofibers/NiO films. *Thin Solid Films*, *601*, 54-58, 2016.

[9]Talebian, N., &Kheiri, M. Sol–gel derived nanostructured nickel oxide films: effect of solvent on crystallographic orientations. *Solid state sciences*, *27*, 79-83, 2014.

[10] Nalage, S. R., Chougule, M. A., Sen, S., Joshi, P. B., & Patil, V. B. Sol–gel synthesis of nickel oxide thin films and their characterization. *Thin solid films*, *520*(15), 4835-4840, 2012.

[11] Mahmoud, S. A., Shereen, A., &Mou'ad, A. T. Structural and optical dispersion characterisation of sprayed nickel oxide thin films. *Journal of modern Physics*, 1178-1186, 2011.

[12] Daranfed, W., Aida, M. S., Hafdallah, A., &Lekiket, H. Substrate temperature influence on ZnS thin films prepared by ultrasonic spray. *Thin Solid Films*, *518*(4), 1082-1084, 2009.

[13] Amor, M. B., Boukhachem, A., Boubaker, K., &Amlouk, M. Structural, optical and electrical studies on Mg-doped NiO thin films for sensitivity applications. *Materials science in semiconductor processing*, *27*, 994-1006, 2014.

[14] Chen, H. L., Lu, Y. M., & Hwang, W. S. Thickness dependence of electrical and optical properties of sputtered nickel oxide films. *Thin Solid Films*, *498*(1-2), 266-270, 2006.

[15] Tauc, J. (Ed.). *Amorphous and liquid semiconductors*. Springer Science & Business Media, 2012.

General conclusion

General conclusion:

In this thesis work we have developed and characterized thin films of pure NiO for different volumes, and doped by Cu, Al and F as well as co-doped by the pyrolysis spray technique (pyrolysis) on glass blade substrates.

To gather comprehensive information about our samples, we conducted multiple characterizations. The structural analysis involved utilizing XRD to examine the layers. Additionally, optical and electrical assessments were performed using UV-Visible spectroscopy and the four-point method.

On the other hand, enhancing various physical attributes of NiO thin films such as transparency, conductivity, and defect structure can be achieved through the incorporation of metal elements via doping. This study aims to investigate the impact of doping with copper (Cu), aluminum (Al), and fluorine (F), as well as co-doping of these elements, on the structural, optical, and electrical properties of NiO thin films fabricated using the pyrolysis spray method.

NiO thin films:

- The X-ray diffraction analyses reveal that the NiO films possess a nanocrystalline structure, exhibiting a strong preferred orientation along the (111) plane.
- The minimum crystallite size, measuring 15.08 nm, was recorded for the film deposited with 20 ml.
- An average transmittance of approximately 70% was noted across all NiO thin films.
- These films exhibit a range of band gap energies, spanning from 3.59 to 3.76 eV, with the lowest value observed at 20 ml deposition.
- The NiO thin film prepared with 20 ml exhibited a maximum electrical conductivity of 0.06527 $(\Omega.cm)^{-1}$.

F doped NiO thin films

- A maximum crystal of 19.21 nm was achieved using a volume of 20 ml.
- All the prepared F-doped NiO thin films show good transmittance, around 80% in the visible region.
- The F-doped NiO thin films deposited with 20 ml exhibit a minimum optical band gap energy of 3.51 eV and the highest Urbach energy value of 0.689 meV.

- The thin film prepared with 5 ml shows a minimum electrical resistivity of 231 Ω.cm.

Al doped NiO thin films

- The largest crystallite size, which is 15.09 nmfor15 ml.
- The entire Al -doped NiO thin films prepared exhibit well transparency, reaching 60% in the visible region.
- The Al -doped NiO thin films deposited with 15 ml exhibit minimum optical gap energy of 3.5 eV, with the highest Urbach energy value recorded at 0.644meV.
- The minimum electrical resistivity of 7x104 Ω.cm for the thin film which was prepared using 15 ml.

Cu doped NiO thin films

- The maximum crystallite size is 15.91 nm obtained for 20 ml.
- All of the Cu-doped NiO thin films prepared demonstrate good transmittance, approximately 70% in the visible region.
- The Cu doped NiO thin films prepared with 20 ml have minimum optical gap energy of 3.49 eV and the highest value of Urbach energy is 0.535meV.
- The thin film deposited using 10 ml exhibits a minimum electrical resistivity of 442.7 Ω.cm.

F and Cu co-doped NiO thin films

- The maximum crystallite size is 17.84 nm obtained for 5%Cu and 5%F.
- All the prepared F and Cu co-doped NiO thin films exhibit good transmittance, approximately 80%, in the visible region.
- The F and Cu co-doped NiO thin films, deposited with 5% Cu and 5% F, demonstrate a minimum optical band gap energy of 3.7 eV, with the largest Urbach energy value being 0.395 meV.
- The thin film prepared with 5%Cu and 5%F has a minimum electrical resistivity of 19.7 Ω.cm.

Al and F co-doped NiO thin films

- We can observe that all samples have a good transmittance (T %), where the average transmission in the visible range about 80% in the range of (300- 360 nm)

- The Al and F co-doped NiO thin films deposited with 5%Al and 3%F exhibit maximum optical gap energy of 3.66 eV, with the lowest Urbach energy value recorded at 0.644 meV.
- The Al and F co-doped NiO thin films have a good electrical resistivity.

Cu and F co-doped NiO thin films

- All of the Cu and F co-doped NiO thin films have a good transmittance, was varied from 67 to 84 % within the visible region.
- The Cu and F co-doped NiO thin films prepared with 5%F and 3%Cu have minimum optical gap energy of 3.5 eV and the highest value of Urbach energy is 0.5 meV.
- The Cu and F co-doped NiO thin films prepared with 5%F and 3%Cu exhibits a minimum electrical resistivity of 146.7 Ω.cm.

ABSTRACT

Abstract:

This thesis aimed to elaborate and characterize Nickel Oxide (NiO) thin films through the spray pyrolysis technique, employing a 450°C heated glass substrate. To investigate and optimize the conditions for spray deposition, we examined the impact of preparative parameters such as the volume of the sprayed solution on the structural, optical, and electrical properties of undoped NiO thin film.

Moreover, to augment certain attributes of NiO materials, incorporating dopants is an effective method for altering various physical properties such as transparency and conductivity. In this research, thin films of nickel oxide doped with copper (Cu), aluminum (Al), and fluorine (F) were prepared, we also prepared thin films of nickel oxide co-doped slices using the former elements with different concentrations, using the spray pyrolysis technique.

In the last part, the results obtained were presented and discussed by studying the physical properties of NiO's prepared thin films. These films were analyzed by DRX, UV-Visible, 4-point method.

Keywords: NiO thin films; Cu; Al; F; Spray Pyrolysis; X-ray diffraction.

ملخـــــص

تهدف هذه الأطروحة إلى تفصيل وتوصيف أغشية أكسيد النيكل الرقيقة (NiO) من خلال طريقة الانحلال الحراري بالرش، باستخدام ركيزة زجاجية ساخنة 450 درجة مئوية. للتحقيق وتحسين ظروف ترسيب الرذاذ، قمنا بفحص تأثير المعلمات التحضيرية مثل حجم المحلول المرشوش على الخصائص الهيكلية والبصرية والكهربائية لغشاء NiO الرقيق غير المعالج.

علاوة على ذلك، لزيادة سمات معينة من مواد NiO، فإن دمج المنشطات هو طريقة فعالة لتغيير الخصائص الفيزيائية المختلفة مثل الشفافية والتوصيل. في هذا البحث، تم تحضير أغشية رقيقة من أكسيد النيكل مطعمة بالنحاس (Cu) والألمنيوم (Al) والفلور (F)، كما قمنا بتحضير شرائح رقيقة لاكسيد النيكل مزدوجة التطعيم باستعمال العناصر السابقة بتراكيز مختلفة ، باستعمال تقنية الانحلال الحراري بالرش.

في الجزء الأخير، تم تقديم النتائج المتحصل عليها ومناقشتها وذلك بدراسة الخصائص الفيزيائية للأفلام الرقيقة NiO المحضرة. تم تحليل هذه الأفلام بواسطة تقنية الانعراج الاشعة السينية ، والاشعة في المجال المرئي -وفوق البنفسجية، وطريقة المسابر الاربعة.

الكلمات المفتاحية: طبقات اكسيد النيكل، النحاس، الالمنيوم، الفلور، الرش الحراري، انعراج الاشعة السينية.

Iranian Journal of Physics Research, Vol. 23, No. 3, 2023
DOI: 10.47176/ijpr.23.3.11780

Synthesis of high transparency of F doped NiO monocrystalline thin films by spray deposition

M Mammi[1], S Benramache[2], Y Aoun[3], and A Sbaihi[2]
1Department of Physics, University of El-Oued, 39000, Algeria.
2 Laboratoire des Matériaux, des Énergies et de l'Environnement, University of Biskra 07000, Algeria,
3 Mechanical Department, Faculty of Technology, University of El-Oued, El-Oued 39000, Algeria

E-mail: s.benramache@univ-biskra.dz,

(Received 4 November 2023; in final form 9 December 2023)

Abstract
The main objective of this work is to investigate a new material based on fluorine doped NiO thin films by spray deposition technique. Nickel nitrate hexahydrate $Ni(NO_3)_2.6H_2O$ and ammonium fluoride (NHF4) with a ratio of F/Ni = 0.04 were used to prepare F doped NiO. The structural, optical and electrical properties of F doped NiO thin films were investigated with different NiO:F solution volumes of 5, 10, 15 and 20 ml using the spray technique. The prepared F doped NiO thin films have a monocrystalline nature with a cubic structure; the (111) diffraction peak is the preferred orientation; the maximum crystallite size is 19.21 nm obtained for 20 ml. The optical property shows that the all the prepared F doped NiO thin films have a good transmittance of about 80 % in the visible region. The F doped NiO thin films deposited with 20 ml have a minimum optical gap energy of 3.51 eV and the highest value of Urbach energy of 0,689 meV. However, the thin film prepared with 5 ml has a minimum electrical resistivity of 231 Ω.cm, which can be used as a gas sensing.

Keywords: F, NiO, thin films, spray deposition technique, monocrystalline structure.

1. Introduction

Recent research shows that semiconductor metal oxides are essential compounds for the development of ultrahigh frequency devices, photocatalysis, optoelectronics, gas sensors, lithium ion microbatteries and cathode materials for alkaline batteries [1-3]. However, nickel oxide (NiO) is a direct large-gap (3.6-4.0 eV), semi-transparent p-type semiconductor material with a wide range of applications, represented by gas sensors, ultraviolet photo detectors, dye-sensitizers, photocatalysis, photovoltaic coatings, and lightweighting [1-6], the structural components in aerospace, in ceramic structures, counter electrodes and the anode layer of solid electrode oxide fuel cells [2–9]. On the other hand, nickel oxide has a cubic structure and NiO has a good transparency in the thin film [10-12].
NiO has recently focused on doping NiO with transition metals (TMs) such as Cu [2], Na [3], Zn [4], V [6], Mn [10], Al, Ga, In [12], Li [13], Ag [14], Mg [15], Co [16], and Mo [17] in cooperation with Ni to increase electrical conductivity. However, there is a new doping effect on optical properties; which is fluorine doped NiO thin films. The F doping can be used to increase the transmission and to increase the movement of F in the NiO:F.

The aim of this work is to study F doped NiO thin films with the help of organic solar cells for electrical energy harvesting. The organic solar cells consisted of an inner mirror layer inside (ITO glass) and a substrate holder. F doped NiO thin films can be deposited on a glass substrate by the spray pneumatic method with different volumes of 5, 10, 15 and 20 ml of the NiO:F mixture. The F doped NiO thin films were characterised by various methods, including X-ray diffraction, UV-vis spectrophotometry, and four-point techniques.

2. Experiments

The prepared solution of NiO was dissolved by 0.10 $mol.l^{-1}$ of nickel nitrate hexahydrate $Ni(NO_3)_2.6H_2O$ (industrial powder with 99 purity) and ammonium fluoride (NHF_4) (industrial powder with 97 purity) with the ratio of F/Ni = 0.04, the mixture powder was dissolved in the same volumes absolute of water H_2O, we have added drops of HCl solution for stabilisation.

Figure 1. A photograph of the experimental setup for the deposition of F-doped NiO thin films.

The mixture solution was stirred and heated at 45°C until a time of 4 h to transparent solution. F doped NiO thin films were sprayed onto the heated glass substrates at 450 °C with different solution volumes using the organic solar cells, and the volumetric spray rate was 0.1 ml/s. The structure of the spray deposition system and the fabricated organic solar cells are shown in figure1. In this work, we used a digital display thermocouple (C100FK02 - M*AN) to determine the temperature, which it determined between 400 and 600 °C. However, the direct calcinations of $Ni(NO_3)_2$ $6H_2O$ follows the reaction as:

$$2Ni(NO_3), 6H_2O = 2Ni + 4NiO_2 + 4\,NO_2 + O_2 + 12H_2O, \quad (1)$$

The thin films of F doped NiO were characterised by different techniques to find the crystalline structure, optical transmission and electrical conductivity, which it are the respectively the X-ray diffraction (XRD Bruker AXS-8D with λ = 0.15406 nm), spectrophotometer (UV-Lambda 35 with 300–900 nm of wavelength), and the four point techniques of the instrument Keithley Model 2400 Low Voltage Source Meter instrument.

3. Results and discussion

Figure 2 shows the crystal structure of F-doped NiO thin films prepared at different NiO:F solution volumes of 5, 10,15 and 20 ml and NiO at 10 ml.

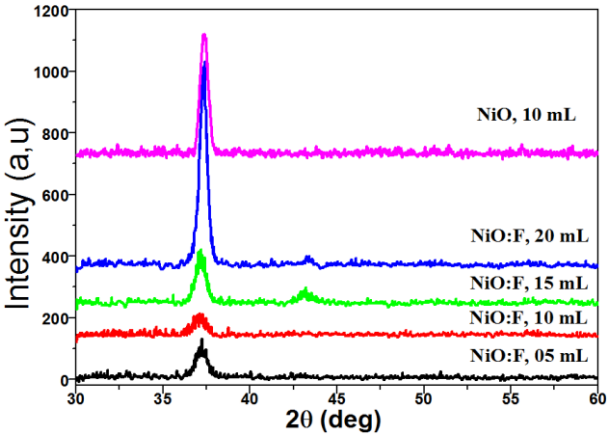

Figure 2. The results of X-ray diffraction spectra of undoped and F-doped NiO thin films at different NiO:F volumes.

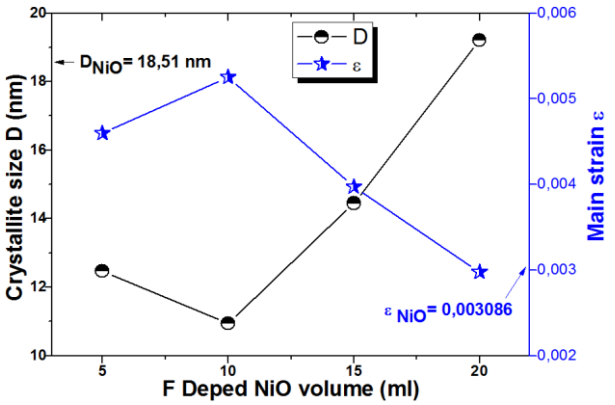

Figure 3. The results of crystallite size D (111) and main strain ε of F undoped and doped NiO thin films at different NiO:F volumes.

As a first result, we have found that all the films exhibited a diffraction peak at 2θ = 37 related to the (111) plane of the NiO phase, which is a single crystal cubic structure. It can be seen that the thin film of F doped NiO deposited with 20 ml has a good crystal structure showed for a highest and strong peak, which confirm that the increase in the deposition volume can be improve the crystalline quality of F doped NiO thin films.

The crystal structure of F-doped NiO thin films represented by crystallite size D (111) and main strain ε was calculated using the following equations [16-18]:

$$D = \frac{0.9\lambda}{\beta \cos\theta}, \quad (2)$$

$$\varepsilon = \frac{\beta}{4\tan\theta}, \quad (3)$$

where D is the crystallite size, λ is the X-ray wavelength (λ = 1.5406 A°), β is the full width at half-maximum (FWHM), and θ is the angle of diffraction peak and ε is the main strain.

Figure 3 shows the variation of the crystallite size and the main strain of F doped NiO thin films at different volumes. As can be seen, as the volumes increases, the variation of the crystallite size is inversely with to the main strain (see Table 1), which is can be explained by the variation of the FWHM.

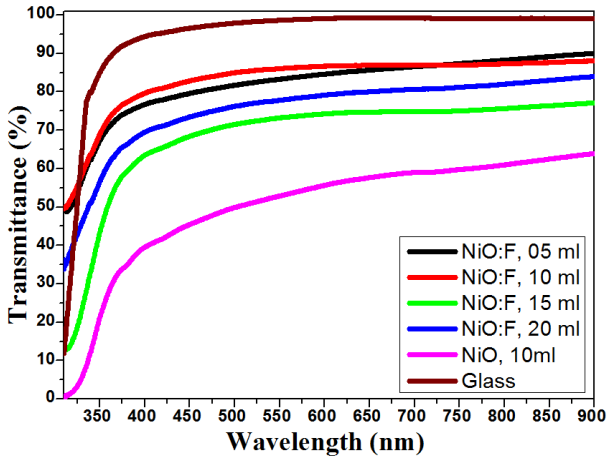

Figure 4. The results of the transmission spectra's of undoped and F doped NiO thin films at different NiO:F volumes.

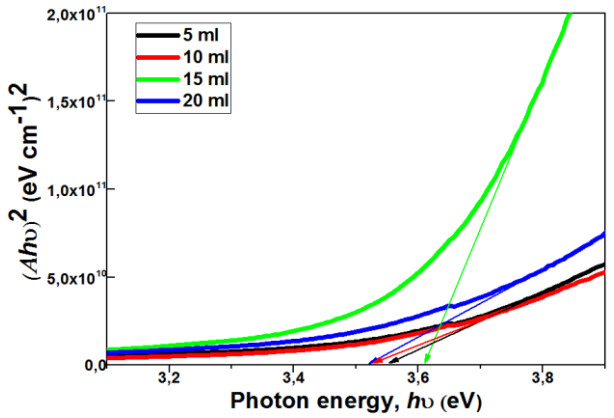

Figure 5a. The typical variation of values $(Ah\nu)^2$ as a function of photon energy $h\nu$ of F doped NiO thin films deposited at different NiO:F volumes, used to determine the optical band gap energy.

Table 1 Shows the crystal structure of F doped NiO thin films representing of the diffraction angle, FWHM, the crystallite sizes, the lattice parameter a and main strain of the (111) plane of undoped and F doped NiO thin films as a function of NiO:F volume.

Samples	Diffraction angle 2θ (°)	FWHM β (°)	Crystallite size D (nm)	Lattice parameter a (nm)	Main strain ε
NiO, 10 ml	37.37	0.54	18.51	0,44144	0.00308
NiO:F, 05 ml	37,21	0,80	12.47	0,442662	0,00459
NiO:F, 10 ml	37,09	0,91	10.94	0,44205	0,00525
NiO:F, 15 ml	37,15	0,69	14.45	0,44032	0,00397
NiO:F, 20 ml	37,32	0,52	19.21	0,43982	0,00298

Table 2 Shows the average transmittance and Film thickness of undoped and F doped NiO thin films as a function of NiO:F volume.

Samples	NiO, 10 ml	NiO:F, 05 ml	NiO:F, 10 ml	NiO:F, 15 ml	NiO:F, 20 ml	Glass
Average Transmittance (%) 400-800 nm	53.6	83.9	85.6	73.8	78.0	98
Film thickness (nm)	160	110	112	134	140	/

Where, the maximum crystallite size is 19.21 nm obtained for 20 ml, this is can be explained by the homogeneous in the surface and coalescence, which it's corresponded in the minimum value of lain strain (see table 1). However, the undoped NiO thin film has a main strain of 0.00308 and a crystallite size of 18.51 nm.

The optical properties of undoped and F doped NiO thin films were represented by the transmission spectra in the range of 300 to 900 nm of wavelength. Figure 4 shows the variation of the transmission of the deposited thin films at different NiO and NiO:F volumes. As the NiO:F volume increased, the transmission was decreased due to the increase in the film thickness. However, the prepared F doped NiO thin films have a good transmission is about 80 % in the visible region due to the fluorine doping (see table 2). The transmittance of 20 ml (78%) high then the 15 ml (73.8%) due to the crystallinity of the film .The region exist between 300 and 400 nm, it is the region of strong absorption, heir the transmission of F doped NiO decreased due to the excitation and the migration of the electrons from the conduction band to the valence band.

The optical band gap energy of the thin films of undoped and F doped NiO was calculated from transmission spectra, which it was applied the following equations [18-20].

$$A = \alpha d = -\ln T, \tag{4}$$

$$(Ah\upsilon)^2 = B(h\upsilon - E_g), \tag{5}$$

where E_g the optical band gap energy; A is the absorbance, d is the film thickness; T is the transmission spectra of thin films; α is the absorption coefficient values; B is a constant and $h\upsilon$ is the photon energy. It was found by the extrapolating the curve of $(Ah\upsilon)^2$ vs $h\upsilon$ at A = 0 [21], which the variation was indicated in figure 5a, show the drawn of the $(Ah\upsilon)^2$ as a function of $h\upsilon$ of F doped NiO thin films. However, the Urbach energy of F doped NiO thin films has been determined by the following expression [21,22]:

$$A = A_0 \exp(\frac{h\upsilon}{E_u}), \tag{6}$$

where A_0 is a constant and E_u is the Urbach energy, Figure 5b shows the variation of the drawn of LnA as a function of the photon energy $h\upsilon$, where the Urbach energy was deduced by the inverse of the slope of the curve.

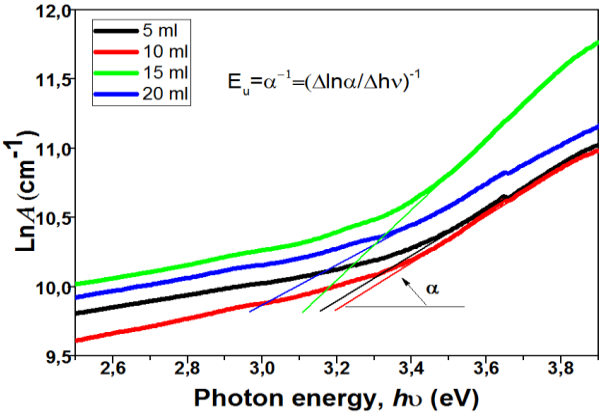

Figure 5b. The typical variation of values LnA as a function of photon energy $h\nu$ of F doped NiO thin films deposited at different NiO:F volumes, used to determine the Urbach energy.

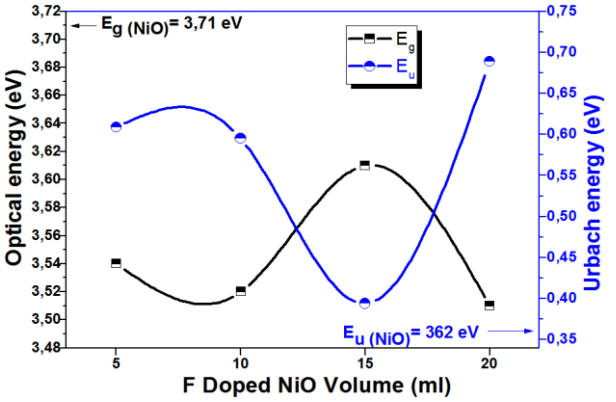

Figure 6. The results of optical band gap E_g and Urbach energy E_u of F doped NiO thin films at different NiO:F volumes.

Table 3. Shows the optical properties such as the variation of optical band gap energy and Urbach energy of undoped and F doped NiO thin films as a function of NiO:F volume.

Samples	Optical gap energy E_g (eV)	Urbach energy E_u (eV)
NiO, 10 ml	3.71	0.362
NiO:F, 05 ml	3,54	0,609
NiO:F, 10 ml	3,52	0,595
NiO:F, 15 ml	3,61	0,394
NiO:F, 20 ml	3,51	0,689

Table 4. Shows the electrical characterisations such as the variation of measured current and voltage and the sheet resistance of F doped NiO thin films as a function of the NiO:F volume.

Samples	Measured Current I (nA)	Measured voltage V (mV)	Sheet resistance R_{sh} (Ω)	Electrical resistivity ρ (Ω.cm)
NiO, 10 ml	0.011	5	$1.1x10^{10}$	$1.5x10^5$ Ω.cm
NiO:F, 05 ml	١٠,٨٠		$2.1x10^7$	231 Ω.cm
NiO:F, 10 ml	٠,١٣		$1.7x10^9$	$1.9x10^3$ Ω.cm
NiO:F, 15 ml	٠,٠٨٠		$2.8x10^9$	$3.8x10^3$ Ω.cm
NiO:F, 20 ml	٠,٠٨٧		$2.6x10^9$	$3.6x10^3$ Ω.cm

Table 5. The comparative study of the structural, optical and electrical properties of undoped and F doped NiO thin films.

Thin films	*Experiments*	*Film thickness (nm)*	*Crystallite size G (nm)*	*Transmittance (%)*	*Optical Band Gap Eg (eV)*	*Sheet resistance or electrical resistivity*	*Ref.*
NiO NiO: 1F% NiO: 5F% NiO: 10F%	- Spray deposition - ST=400 °C - 0.1M - 0.3 mL/s		25 35 21.9 13.5	75 75+1 75+2 75+2	3.67 3.72 3,71 3.72	18 Ωcm 2 Ωcm 14 Ωcm 18 Ωcm	[23]
NiO NiO: 1Li% NiO: 2Li% NiO: 3Li% NiO: 4Li% NiO: 5Li%	- Spray deposition - ST= 500 °C -0.1M -13 mL	197 236 221 374 435 421	41 59 31 45 44 36	59 32 48 37 50 47	3.865 3.744 3.697 3.738 3.714 3.716	- $2.403x10^9$ Ω $1.195x10^7$ Ω $7.984x10^6$ Ω $1.386x10^7$ Ω $1.694x10^7$ Ω	[24]
NiO NiO: 1Cu% NiO: 2Cu% NiO: 3Cu% NiO: 4Cu% NiO: 5Cu%	- Spray deposition - ST= 410 °C -0.2 M	-	64 37 51 38 51 57	about 50	3.572 3.519 3.536 3.461 3.473 3.467	2712 Ωcm 589 Ωcm 490 Ωcm 1106 Ωcm 545 Ωcm 669 Ωcm	[25]
NiO, 10ml NiO:F, 05ml NiO:F, 10ml NiO:F, 15ml NiO:F, 20ml	- Spray deposition - ST=400 °C - 0.1M - F/Ni = 4%	160 110 112 134 140	18.51 12.47 10.94 14.45 19.21	53.6 83.9 85.6 73.8 78.0	3.71 3,54 3,52 3,61 3,51	$1.5x10^5$ Ω.cm 231 Ω.cm $1.9x10^3$ Ω.cm $3.8x10^3$ Ω.cm $3.6x10^3$ Ω.cm	This Work

Figure 6 shows the variation of the band gap energy and the Urbach energy of newly deposited F doped NiO thin films at different volumes. As can be seen, as the volumes increases, the variation of the optical energy is inversely with the Urbach energy (see table 3). The film deposited with 20 ml has a minimum optical energy and maximum Urbach energy, this is can be explained by the increased movement of F in the NiO:F, and the corporation between F and O and thus there is an increase in the substitutional site. However, the undoped NiO thin film has a highest the optical energy of 3.71 eV and a minimum the Urbach energy of 0.362 eV (see Table 3).

The electrical conductivity of F doped NiO thin films was determined by four- point probe technique, it is based on the measured voltage, current and sheet resistance expressed by:

$$R_{sh} = \frac{1}{d}\left(\frac{\pi}{\ln 2} * \frac{V}{I}\right), \quad (7)$$

$$\sigma = \frac{1}{\rho} = \frac{1}{dR_{sh}}, \quad (8)$$

where R_{sh} is the electrical resistivity; d is the film thickness; σ is the conductivity; ρ is the resistivity; V is the applied voltage =5V and I is the measurement current (see Table 4). As can be seen, as the volume increases, the electrical resistivity increases from 5 to 15 ml (see table 4), this increase can be explained by the decrease in the number of electrons and mobility, leading to a p-type semiconductor. However, the undoped NiO thin film has a highest electrical resistivity of 1.5×10^5 Ω.cm and the F doped NiO thin film with 5 ml has a minimum the electrical resistivity of 231 Ω.cm (see Table 3).

The comparative study of the structural, optical and electrical properties of undoped and F doped NiO thin films are presented in Table 5**,** as can be seen, we have a lowest crystallite size, good transmittance and good electrical property.

4. Conclusion

In the conclusion, the structural, optical and electrical properties of undoped F doped NiO thin films were investigated. The thin films of F doped NiO were deposited by spray technique at substrate temperature of 450 °C with different NiO:F solution volumes of 5, 10, 15 and 20 ml. The prepared F doped NiO thin films have a monocrystalline nature with a cubic structure, the (111) diffraction peak is the preferred orientation, the maximum crystallite size is 19.21 nm obtained for 20 ml. The optical property shows that the all the prepared F doped NiO thin films have a good transmittance which is about 80 % in the visible region. The F doped NiO thin films deposited with 20 ml have minimum optical gap energy of 3.51 eV and the highest value of Urbach energy is 0,689 meV. However, the thin film prepared with 5 ml has a minimum electrical resistivity of 231 Ω.cm, which can be used as a gas sensing.

References

1. M H Raza, K Movlaee, Y Wu, S M El-Refaei, M Karg, S G Leonardi, G Neri, and N Pinna, *Chem. Electro. Chem* **6** (2019) 383.
2. S H Wang, S R Jian, G J Chen, H Z Cheng, J Y Juang, *Coatings* **9** (2019) 107.
3. Y Aoun, M Marrakchi, S Benramache, B Benhaoua, S Lakel, and A Cheraf, *Materials Research* **21** (2018) e20170681.
4. C Zaouche, A Gahtar, S Benramache *et al*. *Digest Journal of Nanomaterials & Biostructures (DJNB)* **17** (2022) 1453
5. R S Kate, S C Bulakhe, and R J Deokate, *Journal of Electronic Materials* **48** (2019) 3220.
6. V Panneerselvam, K K Chinnakutti, S T Salammal, A K Soman, K Parasuraman, V Vishwakarma, and V Kanagasabai, *Applied Nanoscience* **8** (2018) 1299.
7. M Z Muzamil Aftab, A Dilawar, F Bashir, and Z H Aftab, *Ceramics International* **46** (2020) 5037.
8. M Sh Abdel-wahab, H K El Emam and W M A El Rouby, *RSC Advances* **13** (2023) 10818.
9. K Sato, S Kim, S Komuro and X Zhao, *Japanese Journal of Applied Physics* **55** (2016) 06GJ10.
10. N R Aswathy, J J Varghese, Sh Ranjini Nair, and R Vinod Kumar, *Materials Chemistry and Physics* **282** (2022) 125916.
11. H S Rasheed, H I Abdulgafour, F M Hassan *et al. Journal of Materials Science: Materials in Electronics* **33** (2022) 18187.
12. I L P Raj, S Valanarasu, A Asuntha *et al. Journal of Materials Science: Materials in Electronics* **33** (2022) 11753.
13. X Chu, J Leng, J Liu *et al*. *Journal of Materials Science: Materials in Electronics* **27** (2016) 6408.
14. M S Abdel-wahab, H K El Emam. & W M A El Rouby, *Journal of Materials Science: Materials in Electronics* **34** (2023) 1637.
15. Y Zhao, J Yan, Y Huang et al. *Journal of Materials Science: Materials in Electronics* **29** (2018) 11498.
16. R S Kate, S C Bulakhe and R J Deokate, *Opt. Quant. Electron.* **51** (2019) 319.
17. H H Abdelhalium, M S Abdel-wahab, M T Tamm and W Z Tawfik, *Appl. Phys. A,* **129** (2023) 459.
18. A Diha, S Benramache and L Fellah, *J. Nano- Electron. Phys.* **11** (2019) 03002.
19. A Kumar and P P Sahay, *Appl. Phys. A,* **127** (2021) 286.
20. A Gahtar, S Benramache, A Ammari, A Boukhachem and A Ziouche, *Inorg. Nano-Metal Chem.* **52** (2022) 112.
21. U Alver, H Yaykaşlı, S Kerli and A Tanrıverdi, *Int. J. Min. Met. Mater.* **20** (2013) 1097.
22. H Aydin, Sh A. Mansour, C Aydin, A A Al-Ghamdi, O A. Al-Hartomy, F El-Tantawy and F Yakuphanoglu, *J. Sol-Gel Sci. Techn.* **64** (2012) 728.

23. S Kerli, and U Alver, *Crystallogr. Rep.* **59** (2014) 1103.
24. D P Joseph, M Saravanan, B Muthuraaman, P Renugambal, S Sambasivam, S P Raja, P Maruthamuthu and C Venkateswaran, *Nanotechnology* **19** (2008) 485707.
25. M Aftab, M Z Butt, D Ali, F Bashir and T M Khan, *Opt. Mater.* **119** (2021) 111369.